

AGB / CARBON MAPPING USING AIRBORNE LIDAR DATA AND GEOEYE SATELLITE IMAGES IN TROPICAL FOREST OF CHITWAN-NEPAL: A COMPARISON OF COMMUNITY AND GOVERNMENT MANAGED FORESTS

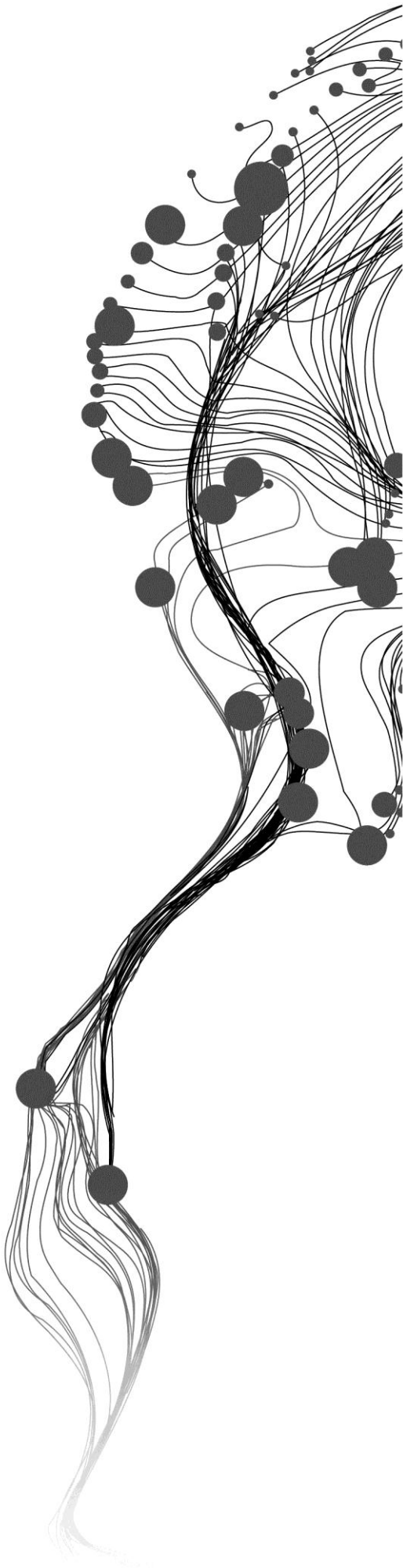
PURITY RIMA MBAABU

February, 2012

SUPERVISORS:

Dr, Y.A, (Yousif) Hussin

Dr, M.J.C, (Michael) Weir



AGB / CARBON MAPPING USING AIRBORNE LIDAR DATA AND GEOEYE SATELLITE IMAGES IN TROPICAL FOREST OF CHITWAN-NEPAL: A COMPARISON OF COMMUNITY AND GOVERNMENT MANAGED FORESTS

PURITY RIMA MBAABU

Enschede, The Netherlands, February, 2012

Thesis submitted to the Faculty of Geo-Information Science and Earth Observation of the University of Twente in partial fulfilment of the requirements for the degree of Master of Science in Geo-information Science and Earth Observation.

Specialization: Natural Resource Management

SUPERVISORS:

Dr, Y.A, (Yousif) Hussin

Dr, M.J.C, (Michael) Weir

THESIS ASSESSMENT BOARD:

Dr, Alexey, Voinov (Chair)

Dr, T, Kauranne (External Examiner, Arbonaut Oy Ltd, and Department of Mathematics and Physics - Lappeenranta University of Technology, Finland)

DISCLAIMER

This document describes work undertaken as part of a programme of study at the Faculty of Geo-Information Science and Earth Observation of the University of Twente. All views and opinions expressed therein remain the sole responsibility of the author, and do not necessarily represent those of the Faculty.

ABSTRACT

Forests reduce impacts of climate change and its consequences by sequestering CO₂ from the atmosphere and storing carbon in different parts of them which include above ground biomass, belowground biomass, forest understory and soil. This storage depends on forest ecosystem management, disturbances, forest succession and climate variation among others. The impact of forest management activities on the ability of forest ecosystems to sequester and store atmospheric carbon is of increasing scientific and social concern. A quantitative understanding of how forest management enhances carbon storage is lacking for most forest types because few studies have been conducted. Therefore, this study endeavours to estimate and compare the above ground biomass (AGB)/carbon stock of two forest types under different forest management regimes.

Very high resolution Geoeye satellite images and airborne LiDAR data were used for this study. Both images have 0.5 m spatial resolution with Geoeye having a 2D view while airborne LiDAR has a 3D view of the forest canopy. Individual tree crowns were generated using multiresolution segmentation which was followed by species classification in eCognition Developer. Total AGB was estimated by allometric equation using DBH and tree height measured in the field. The total AGB was used to predict the AGB for the entire study area by regressing it with crown projection area (CPA) and height from the LiDAR canopy height model (CHM). Non-linear interactive models are used for two species classes (*Shorea robusta* and others).

Segmentation accuracy for community forest was 70% ("D" value = 0.3 or 30% error) and 77% 1:1 correspondence, while that for government forest was 70% ("D" value =0.3) and 78% 1:1 correspondence. The image objects generated are classified per species and result in 70% and 82% accuracy for community and government forests respectively. Modeling of the relationship between CPA, height and AGB result in accuracies of R² = 0.81, RMSE=10% for *Shorea robusta* and R² = 0.62, RMSE=13% for other species in community forest and R² = 0.69, RMSE=25% for *Shorea robusta* and R² = 0.73, RMSE=13% for other species in government forest.

The average carbon stock was found to be 244 t C/ha and 140 t C/ha for community and government forest respectively. These results of carbon stock obtained agree with those in other studies for the same area and confirm the results of other researchers. Based on the findings of this study, we conclude that forest management significantly affects the carbon stock of a forest.

Keywords: Forest management, LiDAR, Object Based Image Analysis, Multiresolution segmentation, Classification, Allometric equation, Regression, Carbon Stock

ACKNOWLEDGEMENTS

It is my pleasure to express sincere gratitude to a number of persons, groups and organizations whose efforts and contribution has enabled the completion of my study in the Faculty of Geo-Information and Earth Observation (ITC), University of Twente.

To begin with, I am grateful to the Netherlands Government and the Netherlands Fellowship Program (NFP) for granting me a scholarship to study at ITC.

I also appreciate the Faculty of ITC for facilitating my study and research. I extend my special gratitude to all the NRM staff whose support gave me a good learning atmosphere for new skills and techniques of GIS, Remote Sensing, modelling and presentations among others.

In a very special way, I pass my heartfelt gratitude to my first supervisor, Dr. Yousif Hussin for his support, guidance, comments and suggestions during the entire thesis period. You were really like a dad to me. Special thanks also to my second supervisor, Dr. Michael Weir for his invaluable contribution and support both before and during the research period. Thanks also to Dr. Alexey Voinov who chaired my proposal and mid-term defence and for his critical and helpful suggestions and comments.

I also thank the International Centre for Integrated Mountain Development (ICIMOD), Asia Network for Sustainable Agriculture and Bio-resources (ANSAB), Forest Resources Assessment (FRA), Federation of Community Forest Users' Nepal (FECOFUN) and Arbonaut of Finland for their support. Special thanks to ICIMOD for the data, financial support and hosting a workshop that helped expand and improve this work. Many thanks also to FRA for providing me with the LiDAR data used in this study.

In a special way, I thank Hammad Gilani and Him Lal Shrestha from ICIMOD who worked tirelessly during my fieldwork which enabled me collect all the required data. I am also grateful to Basanta Gautam of Arbonaut and Khamarrul Azahari of ITC, who gave me invaluable information regarding LiDAR data and the processing software.

I extend my sincere gratitude to my academic mentors; Dr. Gilbert Nduru (Moi University), Peter Ndunda (Green Belt Movement) and Dr. Jeniffer Kinoti (CETRAD) for their priceless support during my study period.

Special thanks also go to my Kenyan friends especially; George Okwaro, Francis Muthoni and Vincent Omondi for their constructive criticism and suggestions. Many thanks also to Cyprian Ogut and Kamina Chororoka for helping me with relevant literature for part of my work. I do appreciate my fellow NRM students for their moral support and encouragement and most especially the carbon team for their cooperation during our fieldwork in Nepal. It has been a pleasure studying with you all and I wish you a prosperous life, now and in the future.

Finally, I extend my deepest appreciation to my family and friends; Sophia Wambui, Wairimu Ndungu, Christabel Maguma, Elmano Kinoti, Clare Kerubo, Judy Ndichu, Victor Obwocha, Martin Bunyasi and Victor Odipo who kept encouraging me especially during my difficult moments at ITC.

Purity Rima Mbaabu
ITC Enschede, The Netherlands
February, 2012

".....dedicated to my parents, brother John Kiogora, and dad Gilbert Nduru. You have all added value to my life in a very special way. May God richly bless you!"

TABLE OF CONTENTS

1.	INTRODUCTION.....	1
1.1.	Background.....	1
1.2.	Overview of forest Biomass and carbon estimations	2
1.3.	Application of Remote Sensing measurements for Biomass/Carbon stock mapping	3
1.4.	Forest management and carbon.....	4
1.5.	Forests and Forest management in Nepal	4
1.6.	Problem statement and Justification	6
1.7.	Research Objectives, Questions and Hypotheses.....	8
1.7.1.	General objectives.....	8
1.7.2.	Specific objectives	8
1.7.3.	Research Questions and Hypotheses.....	9
1.8.	Theoretical framework of research	9
2.	STUDY AREA	11
2.1.	Study Area selection.....	11
2.2.	Background of the carbon project	11
2.3.	Study Area Description	12
2.3.1.	Geographic Location.....	12
2.3.2.	Climate	13
2.3.3.	Vegetation / Forest types	13
2.3.4.	Land cover / Land use.....	13
2.3.5.	Social, economic and demographic.....	13
2.4.	Management Interventions	13
3.	MATERIALS AND METHODS	15
3.1.	Material Description	15
3.1.1.	Data set.....	15
3.1.2.	Other Materials.....	16
3.2.	Fieldwork	17
3.2.1.	Pre-fieldwork	18
3.2.2.	Design of sampling and measurement techniques	18
3.2.3.	Training local field assistants.....	18
3.2.4.	Delineation of Government forest boundary	19
3.2.5.	Field data collection.....	19
3.3.	Research Methods	19
3.4.	Data preparation and Image Pre-processing	20
3.4.1.	Geometric correction	20
3.4.2.	Image Fusion	21
3.4.3.	Image filtering/ Convolution filter	22
3.4.4.	Image masking.....	22
3.4.5.	Tree Identification and Manual crown delineation	22
3.4.6.	Lidar Data analysis.....	23
	Data Component of point clouds	23
3.4.7.	Canopy Height Model (CHM) generation from Lidar point clouds	23
3.5.	Forest condition assessment.....	24
3.5.1.	Stand density and Basal area estimation	25
3.5.2.	Canopy density modeling and Validation	25
3.6.	Object-Based Image Analysis (OBIA).....	27

3.6.1.	Image segmentation.....	27
3.6.2.	Tree crown delineation in eCognition	27
3.7.	Classification and accuracy assessment	30
3.7.1.	Classification.....	30
3.7.2.	Accuracy assessment	30
3.8.	Above Ground Biomass and carbon stock calculation	30
3.9.	Regression analysis	31
3.10.	Carbon stock Mapping.....	32
4.	RESULTS	33
4.1.	Forest condition assessment.....	33
4.1.1.	Canopy density modeling.....	33
4.1.2.	Canopy density model validation (CDM)	36
4.2.	Canopy Height Modeling (CHM).....	36
4.2.1.	CHM Validation.....	37
4.3.	Image segmentation	38
4.3.1.	Multi-resolution segmentation.....	38
4.4.	Image classification	39
4.5.	Descriptive Statistics	43
4.6.	Model development and Validation.....	45
4.6.1.	Model Validation.....	48
4.7.	Carbon stock mapping	49
5.	DISCUSSION.....	53
5.1.	Forest Condition Assessment	53
5.1.1.	Comparison of forest management activities in the two forest management types	53
5.1.2.	Site statistics	54
5.1.3.	Canopy Density Modeling.....	56
5.2.	Canopy Height modeling and accuracy assessment	57
5.2.1.	Canopy Height Modeling (CHM).....	57
5.2.2.	Validation of the CHM	57
5.3.	Image segmentation and accuracy Assessment.....	58
5.3.1.	Delineation of tree crowns in eCognition.....	58
5.4.	Object based Image classification and accuracy assessment	59
5.5.	Modeling Height, CPA and Carbon stock	61
5.5.1.	Model development and validation.....	61
5.5.2.	Biomass and carbon stock estimation	62
5.5.3.	Carbon stock comparison for the two forest types.....	62
5.5.4.	Relationship between forest management and AGB /carbon stock.....	62
5.6.	Sources of error in biomass estimation	63
5.6.1.	Data characteristics.....	63
5.6.2.	Processing and analysis	65
5.7.	Magnitude of errors	68
5.8.	Strengths and Limitations of this study.....	69
6.	CONCLUSIONS AND RECOMMENDATIONS	71
6.1.	Conclusions	71
6.2.	Recommendations.....	72

LIST OF FIGURES

Figure 1-1: Theoretical Framework of research	10
Figure 2-1: Map of the location of study area.....	12
Figure 3-1: Flowchart of research methods.....	20
Figure 3-2: Missing data areas in the DSM (left) and DTM (right).....	22
Figure 3-3: LiDAR laser file (left) LiDAR point clouds in vector (centre) and LiDAR points in Raster (right)	23
Figure 3-4: flowchart for generating a canopy height model.....	23
Figure 3-5: DTM (Source: Terrainmap.com) (left) and DSM of Bezmiechowa airfield, S. East Poland (right)	24
Figure 3-6: The procedure for modelling canopy density	26
Figure 3-7: ESP Tool for Geoeye and LiDAR CHM.....	28
Figure 3-8: Rule-set and the segmentation procedure	29
Figure 4-1: Canopy density model for CF forest.....	34
Figure 4-2: Canopy density model for GMF forest	35
Figure 4-3: Scatter plots of observed canopy density and estimated canopy density from LiDAR for government (left) and community (right) forests.	36
Figure 4-4: An example of 3D and 2D perspective of DTM (left) and (Centre), and 2D DSM (right).....	36
Figure 4-5: 2D (left) and 3D (right) views the generated of canopy height models	37
Figure 4-6: Scatter-plots of relationship between LiDAR-derived canopy height and observed height in CF and GMF forests.....	37
Figure 4-7: An example of individual tree crowns with height values from multi-resolution segmentation.....	38
Figure 4-8: Overlap between the image objects and reference crowns	39
Figure 4-9: Species map of government forest	40
Figure 4-10: Species map of community forest	41
Figure 4-11: Species distribution in the GMF forest	43
Figure 4-12: Species distribution in the community forest	44
Figure 4-13: Box plots of DBH and height of <i>Shorea robusta</i> and other species for the two forests	45
Figure 4-14: Scatter plots of model validation for <i>Shorea robusta</i> and other species in CF forests.....	48
Figure 4-15: Scatter-plots of the model validation for <i>Shorea robusta</i> and other species for GMF forest.....	49
Figure 4-16: Carbon stock map for CF forest	51
Figure 4-17: Carbon stock map for GMF forest.....	52
Figure 5-1: Photographs showing sample trees from community (left) and government forest (right).	54
Figure 5-2: An example of well delineated crowns and poorly delineated crowns.....	59
Figure 5-3: Photographs of trenches and fence in the Government forest.....	63
Figure 5-4: Examples of irregularly shaped crowns and templates	65
Figure 5-5: Three possible cases that tree crowns are mis-segmented.....	66

LIST OF TABLES

Table 1-1: Research objectives, questions and hypotheses	9
Table 2-1: Summary of land cover in Kayarkhola watershed.....	13
Table 3-1: Geoeye Satellite Images characteristics	15
Table 3-2: Summary of Airborne LiDAR sensor characteristics	16
Table 3-3: List of instruments used for field work.....	17
Table 3-4: List of software used in this research	17
Table 3-5: Summary of area (ha) and no. of samples collected from each forest.	19
Table 4-1: Stand density and basal area for the forest management types.....	33
Table 4-2: The average error of height estimation from LiDAR data for the two forest types	38
Table 4-3: Accuracy assessment of the segmentation process using D and 1:1 methods	39
Table 4-4: Accuracy report for community forest species classification	42
Table 4-5: Accuracy report for government forest species classification.....	42
Table 4-6: Distribution of sample plots and sample trees inventoried in the study sites.	43
Table 4-7: Average DBH and Height for <i>Shorea robusta</i> and other species.....	44
Table 4-8: Regression analysis for <i>Shorea robusta</i> in the community managed forest.....	46
Table 4-9: ANOVA test results for <i>Shorea robusta</i> in the community forest	46
Table 4-10: Regression analysis for other species in the CF forest	46
Table 4-11: ANOVA test results for other species in the CF forest.....	46
Table 4-12: Regression analysis for <i>Shorea robusta</i> in the GMF forest.....	47
Table 4-13: ANOVA test results for <i>Shorea robusta</i> in GMF forest	47
Table 4-14: Regression analysis for other species in the GMF forest.....	47
Table 4-15: ANOVA test results for other species in the GMF forest	47
Table 4-16: Various accuracy measures for the models 1-4	49
Table 4-17: T-test for Carbon stocks from the two forests.....	50
Table 5-1: Summary of forest management activities in the two forest types.....	53
Table 5-2: Source of errors and their influence on different steps in this research.....	68

LIST OF APPENDICES

Appendix 1: Data collection Sheet	80
Appendix 2: Sample plot location for community and government managed forests.....	81
Appendix 3: An example of sample individual tree basal area from CF and GMF forests	82
Appendix 4: Map of sample plot used for tree identification in the field	83
Appendix 5: Data distribution and Models comparison	84
Appendix 6: Slope correction table for the radius of the plot (Plot size = 500m ²).....	85

LIST OF ACRONYMS

AGB	Above Ground Biomass
ALS	Airborne Laser Scanning
ALTM	Airborne Laser Terrain Mapper
ANSAB	Asia Network for Sustainable Agriculture and Bio-resources
AOL	Airborne Oceanographic Laser
AVHRR	Advanced Very High Resolution Radiometer
CASI	Compact Airborne Spectrographic Imager
CDM	Canopy Density Model
CF	Community Forest
CFUGs	Community Forest User Groups
CHM	Canopy Height Model
CPA	Crown Projection Area
DBH	Diameter at Breast Height
DSM	Digital Surface Model
DTM	Digital Terrain Model
EPA	Environmental Protection Agency
ESP	Estimation of Scale Parameter
FAO	Food and Agricultural Organization of the United Nations
FRA	Forest Resources Assessment of Nepal
GMF	Government Managed Forests
HPF	High Pass Filter
ICIMOD	International Centre for Integrated Mountain Development
IPCC	Inter-Governmental Panel on Climate Change
LiDAR	Light Detection and Ranging
LoG	Laplacian of Gaussian
LV	Local Variance
NDVI	Normalized Difference Vegetation Index
NECB	Net Ecosystem Carbon Balance
OBIA	Object Based Image Analysis
REDD	Reducing Emissions from Deforestation and Degradation
RMSE	Root Mean Square Error
ROC	Rate of Change
TAGB	Total Above Ground Biomass
UNFCCC	United Nations Framework Convention on Climate Change
VHR	Very High Resolution

1. INTRODUCTION

1.1. Background

Forests cover approximately 30% of the global land area and account for almost half of the terrestrial carbon pool. A growing forest sequesters and stores more carbon than any other terrestrial ecosystem (IPCC, 2007; Kauppi *et al.*, 1992; Dixon *et al.*, 1994; USAID, 2009) and is an important natural ‘brake’ on climate change. It is estimated that, global vegetation and soils removed carbon from the atmosphere at a rate of 4.7 ± 1.2 Gt (Giga tones) y^{-1} in 2008, compared to carbon emissions from fossil fuels and deforestation of 8.7 ± 0.5 Gt y^{-1} and 1.2 ± 0.7 Gt y^{-1} respectively (IPCC, 2007). When forests are cleared or degraded, their stored carbon is released into the atmosphere as carbon dioxide (CO₂) (Gibbs *et al.*, 2007). On the other hand however, timber harvesting from forests has enabled substantial storage of carbon in wood products and structures (Miner & Perez-Garcia, 2007; USAID, 2009) and allowed more carbon storage from forest regrowth. FAO (2010) reported that a significant fraction of the carbon in industrial round wood is stored in products for periods ranging from months to centuries.

The largest source of greenhouse gas emissions in most tropical countries is deforestation and forest degradation (Gibbs *et al.*, 2007). In Africa, for instance, it accounts for nearly 70% of the total CO₂ emissions (FAO, 2005). Increase in CO₂ concentration and other greenhouse gases have raised concerns about global warming and climatic changes (IPCC, 2007; Malhi & Grace, 2000). According to the Intergovernmental Panel on Climate Change (IPCC, 2007) report, CO₂ in the atmosphere is increasing by 1.4 parts per million (ppm) per year and this will contribute to the increase in temperature by 1.5^o C to 4^o C by the end of the century. These increases have resulted to global warming which in turn is changing the earth’s climatic conditions. This changing of the earth’s climate (climate change), has far reaching effects on the social, environmental and economic facets of the planet Earth (EPA, 2011).

As a response to these effects, various international agreements on climate change such as UNFCCC of 1992 and Kyoto Protocol of 1997 (Patenaude *et al.*, 2005), have come together to address the problem through mitigation and adaptation mechanisms (USAID, 2009). UNFCCC particularly, has considered the need for reducing carbon emissions from deforestation and forest degradation (REDD) as one of the central efforts to combat climate change. REDD has gained major attention in international climate negotiations (ANSAB, 2010). It creates financial value for the carbon stored in forests, and offers incentives for developing countries to reduce emissions from forested lands and invest in low-carbon paths to sustainable development (UN - REDD, 2009). These incentives are based on quantification of

the carbon cycle components. Effective measurement of this carbon, in both space and time is therefore a crucial activity in order to secure this financial compensation.

Carbon estimation plays a key role in national carbon management schemes, - such as the national reporting of emissions and sinks under the UNFCCC and in carbon trading (USAID, 2009) as well as meeting Kyoto obligations by signatory countries. The process should meet international standards and, at the same time, be manageable in a cost-effective manner within the local context (ANSAB, 2010). REDD programmes require reliable, accurate, and cost-effective methods for measurement and monitoring of forest carbon storage (ANSAB, 2010).

1.2. Overview of forest Biomass and carbon estimations

Carbon is approximately 47% of the Above Ground Biomass (AGB) which is defined as “all biomass of living vegetation, both woody and herbaceous, above the soil including stems, stumps, branches, bark, seeds, and foliage” (IPCC, 2007b). The carbon stored in the aboveground living biomass of trees is typically the largest pool and the most directly impacted by deforestation and degradation. Thus, estimating aboveground forest biomass / carbon is the most critical step in quantifying carbon stocks and fluxes especially from tropical forests (Gibbs *et al.*, 2007).

To understand the planetary carbon budget, it is necessary to generate accurate and reliable estimates of global forest cover and the amount of biomass and carbon harboured by the planet’s forests (Skole *et al.*, 1994; Treuhaft *et al.*, 2010; Fagan & DeFries, 2009), yet widespread uncertainties in forest measurements have hampered efforts to obtain this basic scientific data (Fagan & DeFries, 2009; Myneni *et al.*, 1997 & Smith *et al.*, 1993). Large-scale estimates of terrestrial carbon stocks and fluxes are uncertain, particularly over regions where measurements are sparse (Hurtt *et al.*, 2004).

Greenhouse gases inventories and emissions reduction programs require robust methods to quantify carbon sequestration in forests (Gonzalez *et al.*, 2010). Forest inventories and remote sensing (RS) are the two principal data sources used to estimate AGB (Krankina *et al.*, 2004). This estimation is based on measurement of forest attributes that are highly correlated with biomass such as diameter at breast height (DBH), basal area, height and crown volume (Husch *et al.*, 1982; Smith & Brand, 1983). For worldwide forest biomass or carbon stock measurements, satellite imagery is essential. Aerial observations are expensive at present and only cover small areas at a time. Ground measurements, such as destructive sampling of carbon stocks, are expensive (Fagan & DeFries, 2009; Gonzalez *et al.*, 2010), while indirect estimates, such as NDVI, are often inaccurate (Anderson *et al.*, 1993; Brown, 1997; Smith & Brand, 1983).

1.3. Application of Remote Sensing measurements for Biomass/Carbon stock mapping

Remote sensing, the process of imaging the interactions between electromagnetic energy and matter at selected wavelengths, has the ability to monitor terrestrial ecosystems at various temporal and spatial scales and has been widely tested for land cover mapping and forestry applications (Patenaude *et al.*, 2005). Forest carbon stocks can be evaluated using remote sensors mounted on satellites or airborne platforms, but substantial refinements are needed before routine assessments can be made at national or regional scales (Baccini *et al.*, 2004; DeFries *et al.*, 2007). The three main RS sensor systems are optical, Light Detection and Ranging (LiDAR) and Radar (Goetz *et al.*, 2009).

Optical remote sensing, i.e., passive sensing of visible, near-infrared and middle infrared reflectance from the earth, forms the basis for much of the current global scale mapping (Gibbs *et al.*, 2007). Optical measurements have been widely used in studies that link AGB measurements from the field to satellite observations, based on sensitivity of the optical reflectance to variations in canopy structure. These measurements, however, have not proven to be consistent over large areas because surface conditions may change more rapidly than the repeat time of the cloud-free satellite observations, producing artefacts in the derived maps (Goetz *et al.*, 2009). Attempts have been made to estimate forest carbon stocks indirectly by developing statistical relationships between ground-based measurements and satellite-observed vegetation indices (e.g. Foody *et al.*, 2003; Lu, 2005). This method however, tends to underestimate carbon stocks in tropical forests where optical satellites are less effective due to dense canopy closure, and has been unsuccessful in generating broad or transferable relationships (Waring *et al.*, 1995).

Whereas remote-sensing systems relying on optical data (visible and infrared light) are limited in the tropics by cloud cover, new technologies, such as radar systems, can penetrate clouds, haze and smoke, while providing data day and night (Asner, 2001). Radar transmits microwave energy that penetrates into forest tree canopies, with the amount of backscattered energy largely dependent on the size and orientation of canopy structural elements, such as leaves, branches and stems. The radar signals returned from the ground and tops of trees are used to estimate tree heights (Hyde *et al.*, 2007), which are then converted to forest carbon stock estimates using allometry. One major limitation of satellite Radar data is that the signal tends to saturate at fairly low biomass levels (~50-100 t C/ha) when used to quantify carbon stocks in homogenous or young forests (Patenaude *et al.*, 2004; Le Toan *et al.*, 2004). Saturation here refers to the biomass level where radar backscatter no longer increases with biomass for C band (Imhoff, 1995).

LiDAR (Light Detection and Ranging) is based on the concept of actively sensing the vegetation using a pulse of energy from a laser operating at optical wavelengths. LiDAR systems send out pulses of laser light and measure the signal return time to directly estimate the height and vertical structure of forests

(Dubayah & Drake, 2000; Patenaude *et al.*, 2004), which is highly correlated with biomass (Hyde *et al.*, 2007). Forest carbon stocks are estimated by applying allometric height–carbon relationships (Hese *et al.*, 2005). However, this can introduce some challenges in tropical forests that reach their maximum height relatively quickly but continue to accumulate carbon for many decades (Gibbs *et al.*, 2007). LiDAR has been used for more than a decade and has revolutionized biomass estimations from satellites (Herold and Johns, 2007). Large-footprint LiDAR remote sensing far exceeds the capabilities of radar and optical sensors to estimate carbon stocks for all forest types (Drake *et al.*, 2003). However, airborne LiDAR is currently very expensive for use over large areas (Gibbs *et al.*, 2007).

1.4. Forest management and carbon

Forest management can be defined as management practices in forests used for production of wood or non-wood forest products (IPCC, 2007b). Forests reduce impacts of climate change and its consequences by sequestering CO₂ from the atmosphere and storing carbon in different parts of them which include above ground biomass, belowground biomass, forest understory and soil. According to (FAO, 2010), forests and their carbon sequestration potential are affected by management practices, climate and the rise in atmospheric CO₂ among others. One of the aspects of Kyoto Protocol is the possibility of compensating part of the emission reduction in the “Land Use, Land Use Change and Forestry” sector (LULUCF). Articles 3.3 and 3.4 of Kyoto Protocol refer to how signatory countries must report net emissions from the following activities; afforestation, reforestation, deforestation and forest management.

Klaus *et al.* (2010) highlight that, to fully account for the CO₂ sequestration potential of forests, the temporal changes in forest structure and function at the stand and landscape level, and their effects on the net primary productivity (NPP) and the net ecosystem carbon balance (NECB) must be assessed. Changes in forest management practices can improve the quality of forests for carbon sequestration (Jandl *et al.*, 2007; Bravo *et al.*, 2008). In a study by Gonzalo *et al.*, (2007) forest thinning regimes have been found to result in an increase in carbon (C) stock by up to 12% from various tree species in boreal forests. Davis *et al.* (2009) and Karjalainen *et al.*, (2003) also demonstrated that actively managed forests sequester substantial amounts of carbon. Net carbon loss due to poor management practices has also been reported by (Leighty *et al.*, 2006; Gough *et al.*, 2008). Janssens *et al.*, (1999) emphasized the effect of forest management techniques on forest growth and biomass.

1.5. Forests and Forest management in Nepal

According to Nepal’s Department of Forest, Nepal’s forests area is estimated to be about 5.83 million hectares or 39.6% of the total geographical area of the country. Agencies responsible for forests in Nepal are: the Department of Forests of the Ministry of Forest and Soil Conservation, the National Planning Commission, District Forest Offices, non-governmental organizations (NGOs) and local communities

(user groups). Forestry laws make provision for handing over forests to an industry, institution or the community after signature of an agreement between the government and the concerned party. Nepal's current forest policy and legislation classify forests mainly based on their tenure or control to the following categories: government-managed forests, community forests, leasehold forest and religious forest. In the government forests, scientific forest management plans are applied to large areas of forests, away from settlements, to fulfill timber and the fuel wood demands, principally of urban areas, and to contribute to national income. For community forests, use rights and management responsibilities are officially handed over to a group of people who depend on the forest resource for their day to day use. Approximately 30% of Nepal's forest, although officially owned by the government, is under the *de facto* use of local communities which for generations have depended on the forests to meet their subsistence requirements for fuel wood, forage and timber.

The Department of Forests is responsible for the management, demarcation, control and conservation of national forests, as well as conservation and utilization responsibilities for private and community managed forests. All types of national forests are required to be managed under a management plan. The management plans for government managed forests are prepared by the department of forests while those for community forests are prepared by Forest User Groups with assistance from District Forest Office staff. Most of the Forest User Groups are implementing silvicultural interventions and when appropriate they undertake selective felling, planting, thinning, and pruning operations known as *Ban Godne* silviculture. These activities are generally geared towards providing products and services to meet users' current needs such as fuel wood.

The Community Forestry programme is regarded to be successful in Nepal, not only in restoring the degraded sites, biodiversity and improving the supply of forest products to rural people, but also in forming local level institutions for resource management and in improving the environmental situation in the hills of Nepal (Acharya, 2002). However, approximately 70% of Nepal's forests remain under government jurisdiction, and most of these receive inadequate scientific silvicultural management due to lack of a proper forest management policy while the planned and active forest management is poor and forests are under-utilized or not utilized within the legal framework. The exceptions are valuable lowland production forests, particularly in the Terai region which has trees of high economic value. These forests comprise of high proportions of Sal tree species (*Shorea robusta*) and are managed under scientific coppice with standards regimes, although encroachment by migrants has regularly compromised management efforts (FAO, 2010) both in Terai and other government managed forests. This has been attributed to conflicts between the forest guards (Royal Nepal Army) and the people, conversion of part of protected areas into buffer zone community forest, restriction of community forestry to mid-hills that produce trees of lower economic value, proximity to timber market across the border in India, as well as deployment of the Royal Nepali Army for counter – insurgency duty (to the Maoist rebels). The latter activity reduces the presence of the guards in the forest, giving the illegal loggers a free hand in cutting trees for timber (ForestMonitor, 2006). In view of this context, the aim of this study is to estimate and compare

biomass/carbon stock between community managed forests and government managed forests. To do this, high resolution optical GeoEye satellite imagery in combination with airborne LiDAR data were used.

1.6. Problem statement and Justification

There are no practical methods to directly measure all forest carbon stocks, both ground-based and remote-sensing estimation of forest attributes have been used (Gibbs *et al.*, 2007). However, these methods have some level of uncertainty (Drake *et al.*, 2002; Hajnsek *et al.*, 2009; Treuhaft *et al.*, 2009). How to overcome these uncertainties still remains a challenge for researchers today. Use of ground based methods would be the most direct and accurate technique. However, it is expensive, time consuming and impractical for large areas (Gibbs *et al.*, 2007). The present suite of optical satellite sensors, such as Landsat, AVHRR and MODIS, cannot yet be used to estimate carbon stocks of tropical forests with certainty (Thenkabail *et al.*, 2004), because they have limited ability to develop good models for tropical forests while spectral indices saturate at relatively low C stocks (Gibbs *et al.*, 2007).

Very High resolution airborne and optical sensors have been used with low to medium uncertainty. With spatial resolution of less than 5m (Lu, 2006), it is possible to recognize, identify and delineate individual tree crown (Gougeon & Leckie, 2006). However, they are expensive and technically demanding. They relate biomass estimated using allometric equations with crown projection area (CPA) delineated from satellite imagery. There are no allometric equations related to CPA available currently and delineation of heights is impossible with 2D optical data. Tree height and diameter at breast height (DBH) are highly correlated with biomass. DBH has been widely used because it is easy to measure and explains 95% of tree biomass while accurate estimations of tree height in the field remain a challenge. LiDAR data has the capability of measuring 3D vertical structure of vegetation in great detail (Dubayah and Drake 2000; Patenaude *et al.*, 2004). With LiDAR, biomass is estimated by applying allometric height-carbon relationships (Hese *et al.*, 2005), which can introduce some challenges in tropical forests that reach their maximum height relatively quickly but continue to accumulate carbon for many decades (Gibbs *et al.*, 2007). For this reason, DBH, CPA and Height information need to be integrated for any meaningful biomass estimation. This study therefore seeks to enhance the capability of GeoEye images in estimating biomass by incorporating LiDAR data (height information) to improve the accuracy of carbon stock estimation.

Forest carbon storage depends on disturbances, forest succession, and climate variation (Gough *et al.*, 2008) as well as forest ecosystem management (Ryan *et al.*, 2010). The impact of forest management activities on the ability of forest ecosystems to sequester and store atmospheric carbon is of increasing scientific and social concern (Swanson, 2009). The nature of these impacts varies among forest ecosystems (Swanson, 2009). Different forest management regimes for instance have been found to have an effect on carbon sequestration and storage (Karjalainen *et al.*, 2003; Leighty *et al.*, 2006; Gonzalo *et al.*, 2007). Stand

conditions and density are impacted by management and other growing conditions, which determine the carbon content. Forest thinning regimes have been found to result in an increase in carbon (C) stock by up to 12% (Gonzalo *et al.*, 2007). Net carbon loss has also been reported by Leighty *et al.*, (2006) which contradicts the results of many studies which have reported that forest management increase carbon stock e.g. (Gonzalo *et al.*, 2007; Davis *et al.*, 2009; Heath *et al.*, 2010). However, there are few studies on the effect of forest management practices on the condition of the forest such as deforestation and tree density. Gibbs *et al.* (2007) emphasized on appropriate sampling design that accounts for both forest type and condition in order to improve the understanding of carbon stocks and fluxes. FAO (2010) also noted that connections between sustainable forest management and carbon are not explicit. Gough *et al.*, (2008) highlights that a quantitative understanding of how forest management enhance C sequestration is lacking for most forest types because few whole-ecosystem C storage studies have been conducted in managed forests. Moreover, many questions remain unanswered about how whole-ecosystem C storage responds to contemporary forest management practices and to treatments that may enhance C sequestration (Gough *et al.*, 2008). For this reason, this study endeavors to find out if there is a difference in carbon stock of the two management regimes.

Nepal is a signatory country to the Kyoto Protocol and implementing the REDD pilot project for developing countries initiated by UNFCCC. As a result, it is required to report on its CO₂ reductions through conservation and enhancement of carbon stored in forest (Patenaude *et al.*, 2005). For this reason, carbon stock estimations are obligatory to Nepal.

Nepal's forests are under different forest management regimes mainly government managed forest (GMF) forests and community managed forest (CF). According to (FAO, 2010), forests and their carbon sequestration potential are affected by management practices. They can improve the quality of forests for carbon sequestration (Jandl *et al.*, 2007; Bravo *et al.*, 2008; Natural Resources Canada, 2010) or contribute to net carbon loss (Leighty *et al.*, 2006). According to USAID (2009), any carbon accounting system must measure and monitor two variables: the area of forest and the changes in the area due to deforestation or afforestation, carbon stock density and its changes due to degradation, reforestation and forest management. This makes the focus on forest management an important aspect in this study.

Estimating AGB with certainty is still a challenge today due to the complicated biophysical environments especially in the tropics and the uncertainties in accuracy of the available data. For this reason, various biomass studies have sought for better approaches to estimate AGB with higher certainty. Presently, the focus is on integrating multi-sensor data. In this context, (Goetz *et al.*, 2009; Lu, 2006; Koch, 2010) highlights that use of ground based data in a synergistic fashion can potentially overcome the limitations of the previous methods. Therefore, the essence of incorporating Airborne LiDAR data in this study is to

find out if the biomass estimations can be obtained with improved accuracy than in previous studies through additional height information provided by LiDAR data.

1.7. Research Objectives, Questions and Hypotheses

1.7.1. General objectives

1. To model and map carbon stock using very high resolution GeoEye satellite images, airborne LiDAR data and object oriented classification.
2. To compare the forest management regimes in community managed forests and government managed forests and investigate if, and how, they affect the above ground biomass (AGB)/carbon stock.

1.7.2. Specific objectives

- 1 To estimate AGB/carbon stock of subtropical forest using a combination of airborne LiDAR data and High Resolution optical Geoeeye satellite images and assess the accuracy of the estimation.
- 2 To map AGB/carbon stock in the two managed forest types, to compare and analyze the results
- 3 To assess and compare forest management practices in relation to AGB/carbon between GMF and CF forests.

1.7.3. Research Questions and Hypotheses

Table 1-1: Research objectives, questions and hypotheses

<i>Objectives</i>	<i>Research Questions</i>	<i>Research Hypothesis</i>
1.	1. What is the accuracy of biomass estimation for the two forest management types?	
2.	2. What is the AGB/carbon stock in the two forest management types? 3. Is there a significant difference in AGB/carbon stock from the two forests? 4. Is there a relationship between the management practices and AGB /carbon?	H₀ : There is a significant difference in AGB/carbon stock from the two forests. H₁ : There is no significant difference in the AGB/carbon stock from the two forests H₀ : There is a relationship between forest management practices and AGB/ carbon H₁ : There is no relationship between the forest management and AGB /carbon
3.	5. What are the management types/activities for each forest? 6. Is there evidence of deforestation in the forest units? 7. What is the tree density in each management unit? Is there a significant difference in tree density between the two units?	H₀ : There is a significant difference in tree density between the two units H₁ : There is no significant difference in tree density between the two units

Assumptions: That the respective forest management plans are followed in both cases.

1.8. Theoretical framework of research

This study started with the reviewing of literatures and identification of research problem, which was then used to formulate research objectives and questions. Data needs were identified and field work was carried out. This was followed by data processing and analysis and finally discussions and conclusions. This process is shown in Figure 1-1.

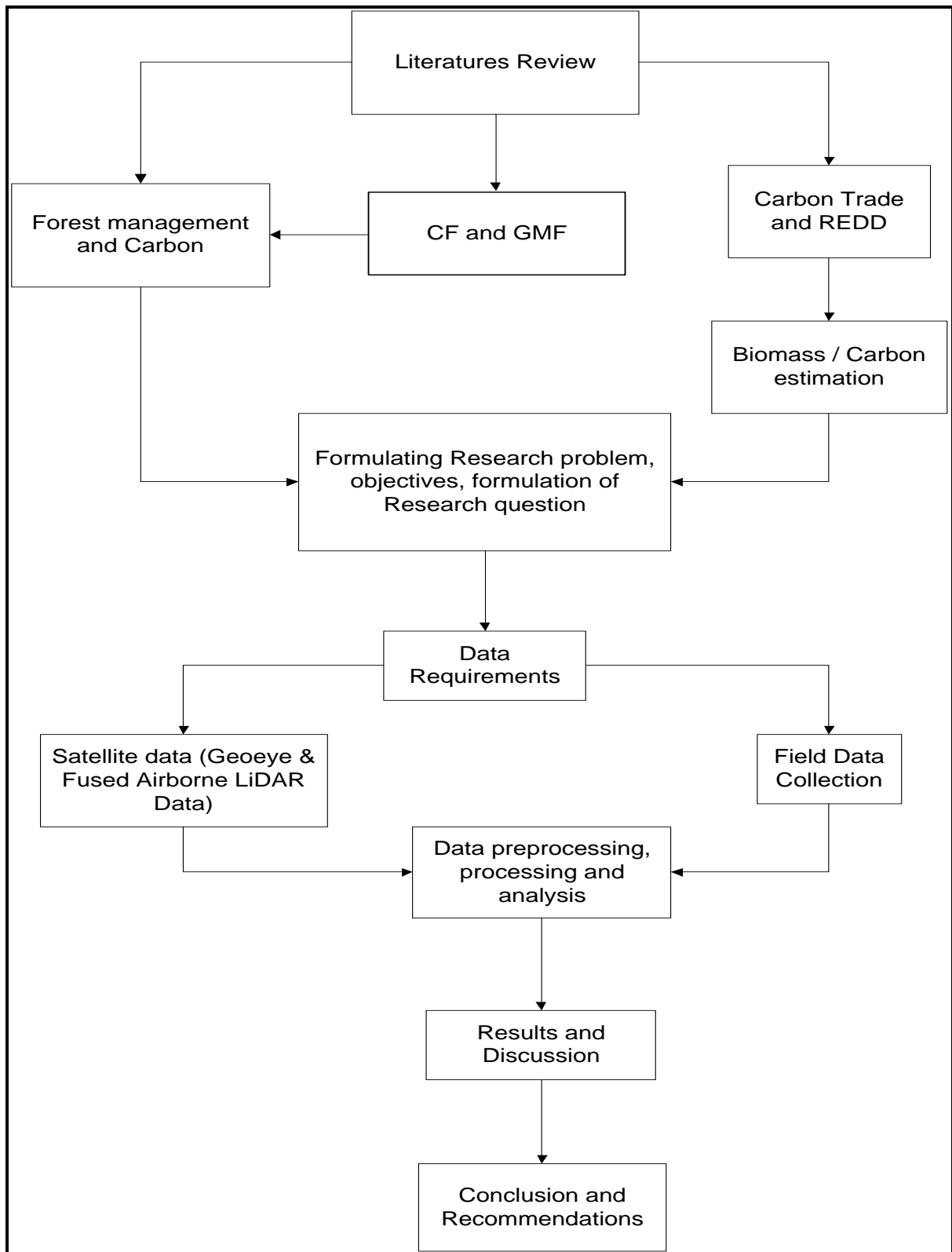


Figure 1-1: Theoretical Framework of research

2. STUDY AREA

2.1. Study Area selection

Nepal's forests are classified into three namely protection, conservation and production forests. Chitwan district, specifically Kayarkhola Watershed was selected for this study because it is a major forest area in Nepal.

The study area was selected based on the following criteria.

- 1) Accessibility: Most of Nepal is characterized by very rugged terrain/steep slopes. Due to the limited time for fieldwork, this site was preferred because it is relatively accessible in comparison to other forested sites.
- 2) Data availability: Both optical satellite data and Airborne Lidar data that were proposed for use in this study were available for this area.
- 3) REDD implementation: Kayarkhola watershed is amongst the three watersheds in Nepal under REDD pilot programme being implemented by Asia Network for Sustainable Agriculture and Bioresources (ANSAB), International Centre for Integrated Mountain Development (ICIMOD) and Federation of Community Forest Users' Nepal (FECOFUN).
- 4) Existence of various forest management regimes: This study aims to investigate if different management regimes have impact on carbon stock. The site has a range of forest management regimes such as community, government, leasehold and religious forests.

2.2. Background of the carbon project

ANSAB, ICIMOD, and FECOFUN, are implementing the project "Design and setting up of a governance and payment system for Nepal's Community Forest Management under Reducing Emissions from Deforestation and Forest Degradation (REDD)" in three watershed areas of Nepal, namely, Kayarkhola of Chitwan district, Charnawati of Dolakha district and Ludhikhola of Gorkha district with financial support from The Norwegian Agency for Development Cooperation (NORAD). This REDD pilot project aims to demonstrate the feasibility of REDD payment mechanism in Community Forest (CF) by involving local communities including marginalized groups so that deforestation and forest degradation can be reduced by linking sustainable forest management practices with economic incentives (ICIMOD, 2010). For this reason, estimation of carbon stock in Kayarkhola watershed holds a lot of significance to REDD mechanism.

2.3. Study Area Description

2.3.1. Geographic Location

Chitwan District is one of the seventy-five districts of Nepal, located in the Central lowland area at approximately 150 km southwest of Kathmandu, the Capital City (Figure 2-1). It is located between 27°40'07" to 27°46'37" northern latitude and 84°33'25" to 84°41'48" eastern longitude. It covers an area of 2,218 km² and bordered by Dhading, Gorkha and Tanahum districts in the north, Parsa district and India to the South.

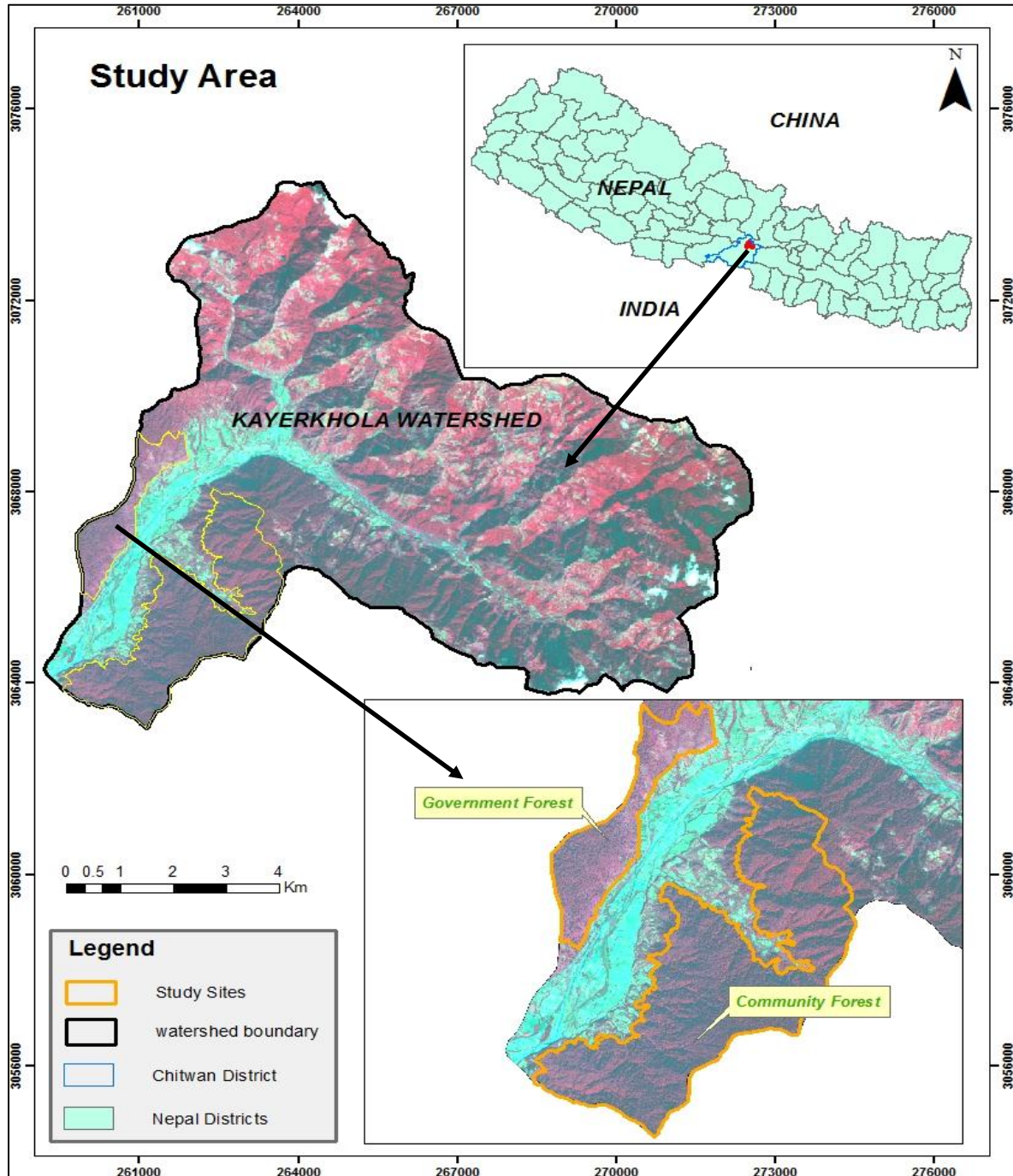


Figure 2-1: Map of the location of study area

2.3.2. Climate

The Kayarkhola watershed represents tropical and sub-tropical with huge altitudinal variation, which ranges from 245 m to 1944 m. The average temperatures are between 16°C to 19°C minimum and 29°C to 32°C maximum (Land Cover analysis, 2010). The average rainfall is about 1500mm (Panta, 2003). July is the onset of monsoon and therefore the study area receives summer rain while the winters are relatively dry

2.3.3. Vegetation / Forest types

Although most of Nepal lies within the subtropical monsoon climatic region, the wide range of topographic conditions allows for a variety of forest types. The distribution of natural forests generally follows altitudinal zones. According to broader climatological categorization of forests, forests in Kayarkhola fall under tropical broadleaved forests. Dominant forest tree species range from the hilly *Shorea robusta* (Sal) forest to *Schima-Castanopsis* to *Rhododendron*.

2.3.4. Land cover / Land use

Conservation areas are the dominant land use with forest covering about 60% of the total land area (128500 ha). Agriculture and urban area account for 40% (89500ha). Chitwan National Park which covers an area of 970km² and part of Parsa Wildlife Reserve are found in this district. Table 2-1 gives a summary of the land cover/land use in the watershed.

Table 2-1: Summary of land cover in Kayarkhola watershed

Land cover type	Area in Ha	Percentage
Forest	5821	73%
Natural water bodies	31	0.39%
Bare soil	30	0.38%
Agricultural land and Built up areas	2038	25%

(ICIMOD Report, 2010)

2.3.5. Social, economic and demographic

Kayarkhola watershed has a population of approximately 22,090 people, all from diverse ethnic backgrounds. The area has good population of Chepang community, one of the most vulnerable communities in Nepal. These people mostly depend on forest for their livelihoods. Additionally, shifting cultivation, a traditional rotational agriculture system, is being practiced.

2.4. Management Interventions

Generally, the entire watershed covers an area of 8,002 ha and hosting over 15 community forests. Although the watershed site represents community forest management systems, there are many different interventions such as government, private and leasehold forests. Community forests in this area cover an

area of 2381ha. These community forests were originally under government management but were later handed over to the forest adjacent communities for management since 1970s. Forest management systems in Kayerkhola are very diverse. This watershed area hosts large Chepang populations who mostly depend on forest for their livelihoods. Additionally, shifting cultivation, as a traditional rotational agriculture system, is being practiced by this community that are believed to be deteriorating the status of forest continuously. As a management strategy for the government forests, the forest area is fenced round and deep trenches dug to curb any illegal extraction of timber from the forest (Figure 5-3).

Almost all the Community Forest User Groups (CF) have approved constitutions and operations plans. The government forests are under the jurisdiction of Chitwan District Forest Office.

The focus of this study is the community and government forest regimes (Figure 2-1). Five out of the 15 CFUGs covering an area of 764 ha, and a government forest of 213 ha, were considered for sampling plots.

3. MATERIALS AND METHODS

3.1. Material Description

3.1.1. Data set

Remote Sensing Data

Two different datasets for Kayerkhola watershed were used for this study namely GeoEye (MSS and Panchromatic) images and Airborne LiDAR data.

Geoeye1 satellite images

Geo-eye1 satellite was launched by Geo Eye on the 6th September 2008 by the U.S Air force. It has the highest resolution of any commercial imaging system. The GeoEye used in this study was obtained on 2nd November 2009. GeoEye Multispectral Image consists of 4 bands (3 in visible and 1 in NIR (GeoEye, 2010). The MSS image at time of acquisition has 1.65m spatial resolution but is resampled to 2m resolution. The Panchromatic GeoEye image has one band (450 -800nm), also obtained on the same date has 0.41m resolution and is resampled to 0.5m. The images are resampled from their actual resolution at time of acquisition (1.65m and 0.41m) because Geo-Eye’s operating license from the U.S Government requires this to be done for all customers who are not explicitly granted a waiver by the U.S Government. The image specifications are shown in Table 1-1.

Table 3-1: Geoeye Satellite Images characteristics

Spatial Resolution	Panchromatic: 0.5 m Multispectral: 2 m
Dynamic Range	11 bits
Band wavelength (nm)	Blue (450 – 510nm) Green (510 – 580nm) Red (655 – 690nm) NIR (780 – 920nm) PAN (450- 800nm)
Orbit height	684 km
Orbit type	Sun – synchronous
Swath width	15.2 km
Processing Level	Geometric and Radiometric correction
Projection	Universal Transverse Mercator UTM Specific Parameters Hemisphere: N Zone Number: 45
Datum	WGS84
Acquisition time	05:12 GMT; 10:57 Kathmandu

Airborne LiDAR Data

Airborne laser scanning, LiDAR data of average point density ranging from 0.5 to 2.0 return pulses/m² for both first and last Lidar echoes, is normally suitable for forest mapping (Arbonaut, 2011). LIDAR

technology provides horizontal and vertical information 3D point clouds (Gautam & Kandel, 2010) at high spatial resolution and vertical accuracies. Forest attributes such as canopy height can be directly retrieved from LiDAR data through modelling process. LiDAR data has great advantage over optical data because it is not affected by saturation and penetrates through spaces of dense canopy and helps to detect height and density. It allows mapping in inaccessible terrain conditions.

The LiDAR data used for this project of average (0.8 points/m²) was acquired by Arbonaut in March 2011 and supplied for our use by the Forest Resources Assessment (FRA) of Nepal funded by Finish Government. The LiDAR system used was mounted on a Helicopter (9N-AIW)-platform with a sensor pulse rate and sensor scan speed of 52.9 KHz and 20.4 lines/second respectively. The flying altitude and speed of the sensor were 2200 m AGL and 80 knots respectively. More sensor details are summarized in (Table 3-2).

Table 3-2: Summary of Airborne LiDAR sensor characteristics

Aerial Platform	Helicopter (9N-AIW)
Flying altitude	2200 m AGL
Flying speed	80 knots
Sensor pulse rate	52.9 KHz
Sensor Scan speed	20.4 lines/second
Nominal outgoing pulse density @ground level	Average: 0.8 points/m ²
Scan FOW half-angle	20 degrees
Swath @ ground level	1601.47 m
Point spacing	max 1.88 m across, max 2.02 m down
Beam footprint @ ground level	50 cm

Maps

Other reference data provided by FRA were used in this study which includes:

- ❖ Topographic maps at a scale of 1:25000 (source: Survey Department of Government of Nepal)
- ❖ RGB Airborne Digital Ortho-photo image of 0.45 m resolution of Kayerkhola watershed.

3.1.2. Other Materials

In addition to the dataset, other materials were used for the study which includes: instruments used for fieldwork (Table 3-3) and Software for data analysis and thesis writing (Table 3-4).

Table 3-3: List of instruments used for field work

Equipment Name	Purpose
Garmin GPS & IPAQ	Navigation and marking sample plots
Haga altimeter and Laser range finder	Measuring tree height
Measuring Tape (30m)	Measuring the plot radius
Diameter tape (3m)	Measuring DBH & crown diameter
Clipboard and pencil	Recording data
Data sheets	Recording field data
Print out plot maps	Identifying and marking the trees
Spherical densiometer	Canopy cover measurement
Clinometer Haga	Slope measurement
Compass	Navigation
Slope correction sheet	Slope correction
Chalk	Marking all trees within the plot
Digital camera	Taking photographs

Software

Table 3-4: List of software used in this research

Software	Usage
ArcGIS10	GIS Analysis Canopy density modelling (from LiDAR data)
Erdas Imagine 10, 11	Image pre-processing and processing
eCognition 8	Tree crown delineation and classification
R statistical Software SPSS Microsoft Excel	Statistical analysis
Lastools	LiDAR analysis
Adobe Acrobat Professional Microsoft word End note	Thesis writing, editing
Microsoft Visio	Diagrammatic representations
Microsoft Powerpoint	Powerpoint preparation
Intersector	Assessing segmentation accuracy (D-Value test)
QT Modeller	3D Visualisation of the LiDAR output/images

3.2. Fieldwork

Fieldwork was carried out for this study to identify the trees and measure their parameters for AGB estimation. This data was also used as ground truth data for individual tree crown delineation, species classification and validation of the models for the relationship between the CPA, height and carbon stock

of trees. Since some forest stand parameters such as volume and biomass are impossible to measure directly in the field, relationships between directly measurable stand parameters (e.g. DBH, height) and biomass have to be established (Husch *et al.*, 2003). Thus, forest stand parameters DBH and height were measured and used for biomass estimation by applying allometric equations.

3.2.1. Pre-fieldwork

Navigation facilities (IPAQ and GPS), measuring tools for forest stand parameter measurements as well as the data sheets were prepared ahead of the fieldwork. Reference data were prepared based on secondary data provided by ICIMOD, Nepal. For the identification of recognizable tree on the map in the field, large scale Geo-Eye map of every sample plot with its surrounding areas were printed before fieldwork.

3.2.2. Design of sampling and measurement techniques

Stratified random sampling

Stratified random sampling (SRS) was used to find the location of sampling plots in the study area as well as basing the data collection and filed measurements on the SRS. The study site was divided into two strata depending on management type namely community forest and government forest. The community forest comprised of five CFUGs or substrata (Kankali, Satkanya, Kalika, Dharapani and Davidhunga) covering a total area of 764 ha while the government forest was one block with a total area of 213 ha. The formula below was used to determine the sample size.

$$n = \frac{t^2 \sum_{j=1}^M P_j S_j^2}{E^2} \dots\dots\dots \text{eqn 3-1}$$

Where n = minimum number of samples required

- t= t value associated with specified probability
- Sj2 = Variance of X for jth stratum
- E= allowable standard error in units of X (Husch *et al.*, 2003)
- Pj= proportion of total forest area in jth stratum =Nj /N
- M= Number of strata in population
- Nj= total area of sampling units in jth stratum
- N= total area of sampling units in population

The sample size for CF was 86 plots while that for government forest was 23 plots. This was based on the proportion of the area of each forest.

3.2.3. Training local field assistants

With the aims of ensuring consistency in collection of data and field measurement, two local persons were hired and taken through a short introductory training on the data collection exercise prior to the commencement of the work.

3.2.4. Delineation of Government forest boundary

Owing to the unavailability of the government forest boundary shapefiles, the boundary was digitized with the help of local community experts' knowledge of the area and use of topographic maps for the area.

3.2.5. Field data collection

Circular plots of 12.62m (500m²) radius (Husch *et al.*, 2003; ANSAB, 2010) were established in the field. Circular plots are used because they are relatively easy to establish (ANSAB, 2010). A base map was used to produce locations of random sample plots. Print outs of each sample plot (appendix 4) made prior to fieldwork were used for tree identification in the plot. IPAQ and GPS were used to navigate to the plot centre. A slope correction factor was applied for every plot depending on the slope percentage (%) (appendix 6), which in turn was used to determine the plot radius. All trees measured in the field were also marked on the image print outs. It is generally assumed that the trees with diameter less than 10 cm have little contribution to the total biomass/ carbon of a forest and thus they are often not measured (Brown, 2002). In this study, tree parameters (DBH, height, crown diameter, species) were measured and recorded for trees with DBH ≥ 10 cm. Canopy density, slope, elevation, aspect and photographs were taken for each plot.

Sampling plots

This study considered two strata for analysis namely government managed forests and community managed forests. Tree parameters were measured in 86 plots in five community forests and 23 plots in the government forest as shown in Table 3-5. The location of the sample plots is shown in (Appendix 2)

Table 3-5: Summary of area (ha) and no. of samples collected from each forest.

Stratum Name	Substratum name	Total area (Ha)	No. of Plots
Community Forest (CFUGs)	Kankali	92	86 plots
	Satkanya	58	
	Kalika	214	
	Davidhunga	254	
	Dharapani	147	
Government Forest	One block	213	23 plots

3.3. Research Methods

Figure 3-1 shows the steps that were followed to achieve this study's objectives. The methods are divided into three parts: Fieldwork, image/data analysis and statistical analysis. Tree parameters (DBH, height and crown diameter) were obtained through fieldwork. LiDAR data processing and image analysis was also carried out to obtain canopy height model (CHM), and crown projection area (CPA). CPA refers to the proportion of the forest floor that is covered by the vertical projection of the tree crowns (Jennings *et al.*, 1999). It is calculated from the average crown diameter assuming a circular crown projection

(Kuuluvainen, 1991). Statistical analysis was done through allometry relating DBH and height to calculate the AGB/ carbon for the measured trees. Further, regression modelling relating CPA, height and biomass was done to estimate the carbon stock for the entire study area (Figure 3-1).

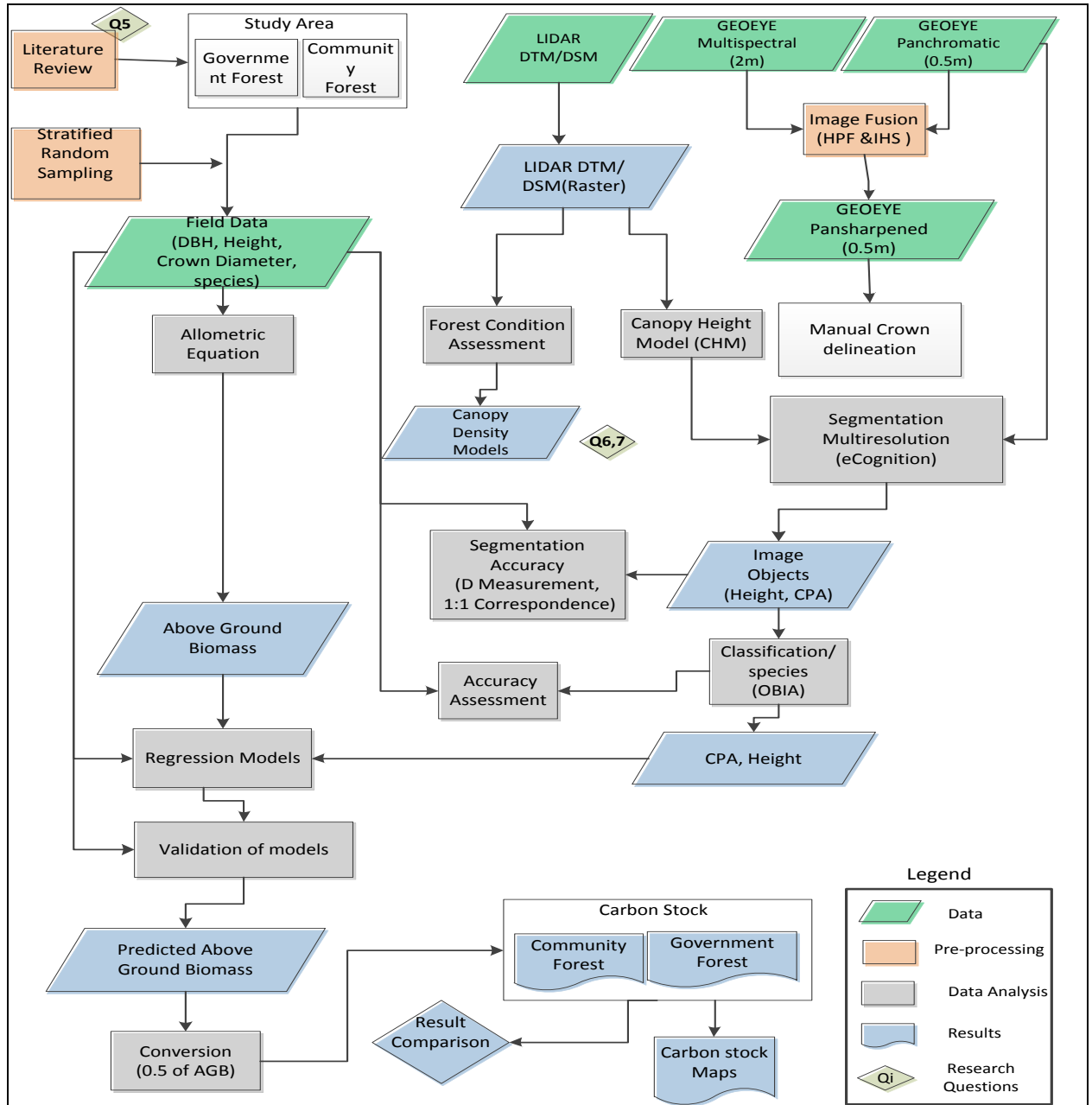


Figure 3-1: Flowchart of research methods

3.4. Data preparation and Image Pre-processing

3.4.1. Geometric correction

Geometric correction is done to correct the sensor and platform-specific radiometric and geometric distortion of the raw data and aims to correct the distorted or degradation of the image generated at the

time of acquisition. The satellite images used in this study were ortho-rectified basing on the Ortho-photo of 0.45m resolution before fusing them for further analysis. Geoeye MSS 2m was ortho-rectified with an accuracy of 0.9m RMSE while Geoeye panchromatic image 0.5m was corrected at RMSE of 0.36m.

3.4.2. Image Fusion

Image fusion of Multispectral Geoeye 2m resolution and Panchromatic Geoeye 0.5m resolution was done to improve the spatial resolution of the image as well as to maintain the spectral characteristics. This technique can be implemented using data from the same sensor or different sensors. Image fusion normally can be done at three different processing levels: signal, feature and decision (Petrovic, 2003). Signal level image fusion, also known as pixel-level image fusion, represents fusion at the lowest level, where a number of raw input image signals are combined to produce a single fused image signal (Petrovic, 2001). Specifically, image pan-sharpening (e.g. fusion technique) was used in this case to enhance MSS images with high radiometric resolution geometrically by merging it with a panchromatic image (Neteler & Mitasova, 2008).

When a panchromatic image (PAN) 0.5m, is fused with multispectral imagery (MSS) 2m, the result is an image with the spatial resolution and quality of PAN imagery and the spectral resolution and quality of the MSS imagery (Amolins *et al.*, 2007). This technique of fusing high resolution PAN image with a low resolution MSS to produce a high resolution multispectral image is known as pan-sharpening (Amro & Mateos, 2010).

There are various image fusion techniques such as high pass filter (HPF), Intensity, Hue and Saturation (IHS), principal components (PC) and wavelet transformation that are commonly used for image fusion. The HPF resolution merge function allows the combination of high-resolution panchromatic data with lower resolution multispectral data, resulting in an output with both excellent detail and a realistic representation of original multispectral scene colours. The low spatial resolution image is resampled to the pixel size of the high resolution image. The resulting HPF image will, therefore, have the same pixel size as the high resolution image (Erdas, 2010). This HPF resolution-merge has proven useful in spectral analysis, especially spectral classifications (Ahmad & Singh, 2002). IHS method processes three bands at a time and it follows three steps. First, MSS bands are transformed from RGB to IHS space. Secondly, intensity of low resolution MSS image is replaced by intensity of high spatial resolution image (PAN), then the original hue and saturation and new intensity images are transformed back to RGB display for visualization. More than three bands also can be produced by doing multiple iterations for RGB combinations.

Geoeye MSS image with 2m resolution was fused with Geoeye PAN image 0.5m resolution and a pan-sharpened image with spatial resolution of 0.5m was obtained. Both IHS and HPF were used. IHS gave better visual appearance while HPF was spectrally appealing. The IHS output was used for tree identification and manual delineation of tree crowns after applying a 3x3 convolution filter.

3.4.3. Image filtering/ Convolution filter

Image filtering is an image enhancement technique which improves the visual interpretability of an image by increasing the distinction between the scenes. Spatial filters work on a number of adjacent cells to smooth data, enhance edges, or remove or decrease noise patterns in images. Spatial filters can be divided into three categories: low pass, high pass and edge detection filters. Low pass filters are used to remove small random spatial variations, typically noise, through averaging a smoothing process (Neteler & Mitasova, 2004). High pass filters emphasize high frequency detail to enhance or sharpen linear features such as roads, faults, and land/water boundaries. Edge detection filters emphasize edges surrounding objects or features in an image to make them easier to analyze.

Prior to segmentation, a low pass filter is applied to smoothen the image and to avoid over segmentation (Platt & Schoennagel, 2009). This filter produces more homogenous image segments and may reduce the amount of convolutions in the final segmented polygons (Mora *et al.*, 2010). Depending on homogeneity of the images, researchers have used different kernel sizes, e.g. median filters for individual crown delineation, but kernel of 3-by-3, 5-by-5, and 7-by-7 are the most commonly used (Erikson and Olofsson, 2005; Gougeon and Leckie, 2006; Mora *et al.*, 2010)

3.4.4. Image masking

Geoeye image obtained covered the entire Kayerkhola watershed area. Image subset was done in ArcGIS 2011 to extract the study area from the whole image. This was done for the two study sites (government managed and community managed forests). The image areas with “missing data” in the LiDAR data were masked out both in the CHM and the Geoeye image. Figure 3-2 shows an example of areas of missing data on the DSM and DTM respectively.

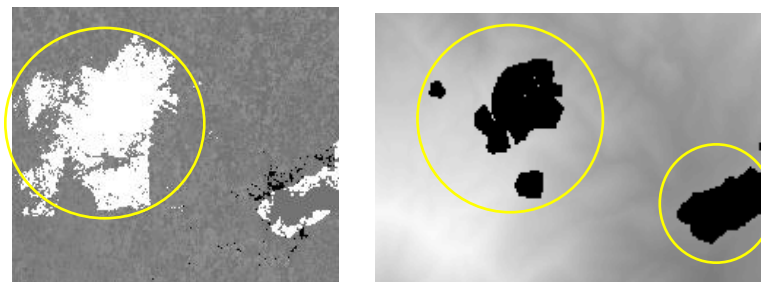


Figure 3-2: Missing data areas in the DSM (left) and DTM (right).

3.4.5. Tree Identification and Manual crown delineation

After fieldwork, the trees marked on the plot sheet were identified on the images. A total of 341 and 111 trees were identified for community and government forests respectively. Image objects or tree crowns generated in eCognition are usually validated using manually delineated tree crowns. Manual crown delineation for the identified trees was done on a 3*3 filtered image so that the tree crowns would be smooth. Delineation of the individual tree crowns was carried out with the following rules in consideration 1) use of crown width measured in the field as reference for delineation of the trees 2) carried out only on the trees that were actually recognized in the field 3) the same trees are clearly visible in the LiDAR canopy height model (CHM) 4) a comparison of the field measured height and LiDAR

height. A total of 228 and 103 tree crowns were delineated for community and government forests respectively.

3.4.6. Lidar Data analysis

Data Component of point clouds

LiDAR field data set is usually supplied in point format as a laser file (.las) hence the name point clouds. With some software such as Lastools, Terrascan and TerraMoulder, the las file can be changed into a text file containing X, Y, Z and *intensity* information. Here, *coordinate_X*, *coordinate_Y*, *height vale_Z* indicate the geometry of a certain point while *intensity* indicates the optical information of the echo (Wu *et al.*, 2008). Figure 3-3 shows airborne LiDAR data in laser format, points (vector) and raster.

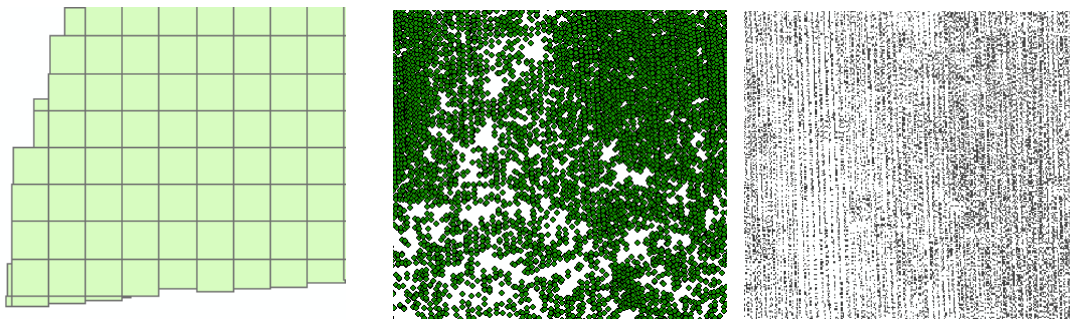


Figure 3-3: LiDAR laser file (left) LiDAR point clouds in vector (centre) and LiDAR points in Raster (right)

3.4.7. Canopy Height Model (CHM) generation from Lidar point clouds

Light detection and ranging (LiDAR) technology provides horizontal and vertical information at high spatial resolutions and vertical accuracies. Forest attributes such as canopy height can be directly retrieved from LiDAR data. Direct retrieval of canopy height provides opportunities to model above ground biomass and canopy volume (Lim *et al.*, 2003). A CHM model is generated through three distinct processing steps as shown in the simple flowchart (Figure 3-4).

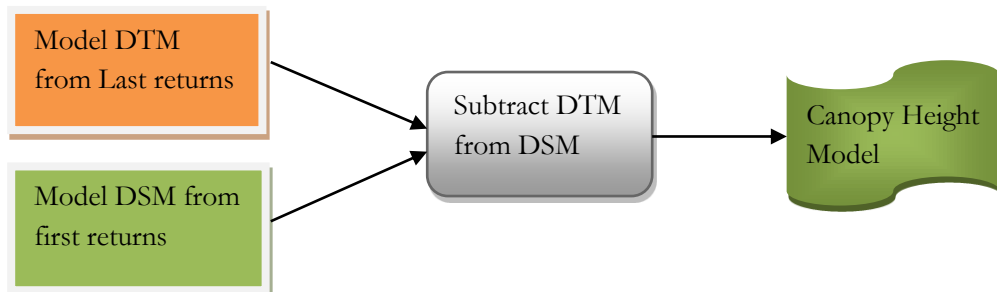


Figure 3-4: flowchart for generating a canopy height model.

A DTM is a topographic model of the bare earth – terrain relief. It represents the spatial elevation of the terrain. A DSM on the other hand, contains all the features on the terrain such as vegetation and buildings. An example of a DTM and DSM are shown in Figure 3-5.

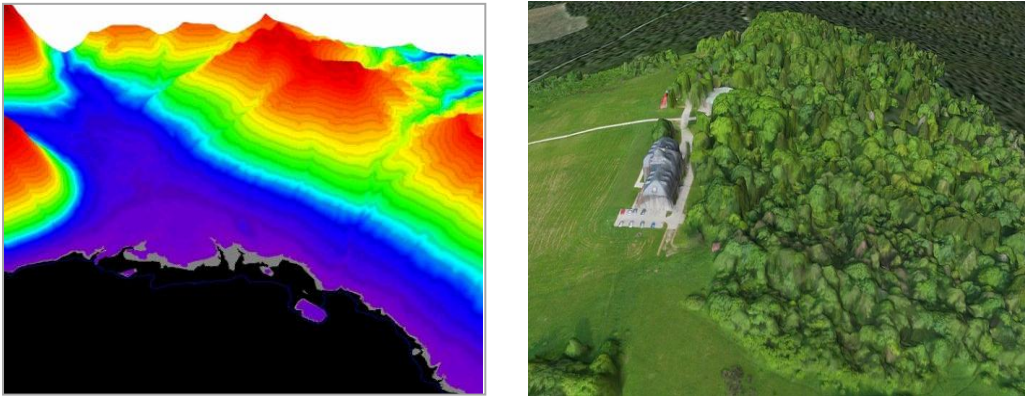


Figure 3-5: DTM (Source: Terrainmap.com) (left) and DSM of Bezmiechowa airfield, S. East Poland (right)

A height difference between the DSM and DTM represents the absolute height of the trees normally referred to as normalized Digital Surface model (nDSM or CHM) which represents the tree height of the forest canopy (Ali *et al.*, 2008). The tree heights for CHM in this study were limited to a minimum of 5m and a maximum of 40m with reference to the field data. Trees with heights below 5m were assumed to be small and contributing insignificantly to biomass. Additionally, this helped in masking out the shrubs and other understory vegetation from the image. This analysis was carried out in lastools software and command prompt. Leftsky *et al.*, (1999a), also modelled canopy height and limited CHM height values to between 4m and 40m for deciduous forests of eastern Maryland, USA. The steps below show the command lines for the processing procedure. Before undertaking the steps, las files (blocks) for the area of interest were selected and merged as one .las file in the lastools software.

Step 1: Generating a DTM (blast2dem tool)

Command

- ❖ blast2dem -i Study_sites2.las -o Study_sites2dem.tif -v -step 0.5 -keep_class 2

Step 2: Generating a DSM (lasgrid tool)

- ❖ lasgrid -i Study_sites2.las -o Study_sites2_dsm.TIF -first_only -highest -step 0.5 -fill 5 -mem 2000

Step3: Generate Canopy Height Model (CHM)

Subtract function in Raster Calculator in ArcGIS 10 was used.

The commands for steps 1 and 2 above were implemented in the command prompt.

3.5. Forest condition assessment

Tropical forest communities are among the world's most threatened systems and urgent measures are required to protect and restore them in degraded landscapes (Sagar & Singh, 2006). For planning conservation or management strategies, there is a need to determine the essential measurable properties, such as species distribution, stand density, basal area and canopy density that describe the forest vegetation and also influence the forest biomass/carbon stocks. For this reason, these parameters were estimated in this study as described in the following section.

3.5.1. Stand density and Basal area estimation

Stand density estimation

Stand density is a quantitative measure of tree cover in an area or number of trees per unit area or space. It is useful in analysis and estimation of forest growth and yield. Stand density is important in forestry because, within limits, the more growing space made available to a tree, the less competition it will face and the faster it will grow (Fennerschool, 1996). Stand density monitoring has been used as an indicator of the level of deforestation and forest degradation as well as the contribution of stand to forest carbon stocks. Estimates of stand density are made to express the degree to which the growing space available for tree growth is utilized hence it is a function of number of trees, tree size and spatial distribution on the ground. In this study, density was determined by summing up all the trees measured in the field. The mean stand density per plot (0.05ha) was estimated which was then converted to density per ha.

Basal area estimation

Basal area (BA) is a term used in forest management that defines the cross-sectional area of a tree at DBH, inside the bark (Hedl *et al.*, 2009). Measurements are usually made for 1 hectare of land for comparison purposes to examine a forest's productivity and growth rate or the stocking of trees in a unit area. It is a useful parameter for forest inventory because it is relatively easy to estimate and can be related to many other parameters of interest e.g. site density and stand volume. The internationally accepted symbol for basal area is G (m²/ha) and for tree basal area, g(m²). G values commonly range from 10 to 60m²/ha in both coniferous and hardwood forests. G values of 150m²/ha may be reached on exceptionally good sites. To estimate a tree's basal area, the tree's diameter at breast height (DBH) is used. The basal area of a forest stand (G) is found by adding the basal areas of all the living trees in an area and dividing by the area of land in which the trees were measured. G is usually expressed as ft²/acre or m²/ha.

In this study, the formula in eqn 3-2 was used for calculating the basal area for the trees in the two forest management types.

$$\text{Basal area} = 0.00007854 * \text{dbh}^2 \dots \dots \dots \text{eqn 3-2}$$

The result will be in m²

NB: The equation is only applicable if the DBH is cm units (Hedl *et al.*, 2009). 0.0007854 = ($\pi/40000$). The division by 40000 corrects for the difference in units (cm and m) and diameter to radius (Fennerschool, 1997).

3.5.2. Canopy density modeling and Validation

Deforestation and forest degradation is a major threat to vast forested areas particularly in the tropical forests where currently it contributes to more than 70% of CO₂ emissions (FAO, 2005). The anthropogenic intervention in the natural forest reduces the number of trees per unit area and canopy closure (Jamalabad & Abkar, *No date*).

Due to the interaction of numerous bio-physical and socio-economic factors, the dynamics of deforestation and degradation is rendered more complex and difficult to analyse. Therefore modelling

approaches hold a high potential for analysis of such complex phenomena (Namaalwa *et al.*, 2007). In addition, satellite remote sensing has played a pivotal role in generating information about forest cover, vegetation type and land use changes. Jamalabad and Abkar, (*no date*), note that, for better management of forest, changes in stand density should be considered.

Canopy density is the ratio of vegetation to ground as seen from the air or space. Canopy density models are unique in capturing the forest systems behaviour by assessing deforestation and degradation, which is approximated through changes in forest area and stand density (Namaalwa, 2007), which have direct impacts on forest carbon stocks. It is one of the most useful parameters to consider in the planning and implementation of rehabilitation program (Jamalabad and Abkar, *no date*). Conventional methods for forest density estimation include 1) Measurement with instruments (ground survey) 2) Aerial photo and satellite image interpretation and 3) satellite based methods.

In this study, a remote sensing approach utilizing fused airborne Lidar data of 0.8 points/m² density (resampled to 3m spatial resolution) was used to model canopy densities for the two forest management sites. Lidar was preferred to satellite data because it has the capability of measuring 3D vertical structure of vegetation in great detail (Drake *et al.*, 2002; Patenaude *et al.*, 2005). Forest canopy density is used in this study to assess the forest condition in the two study sites under investigation, with the aim of explaining the variations in carbon stocks due to implementation of different management regimes. Figure 3-6 represents a flowchart for procedure of modelling canopy density.

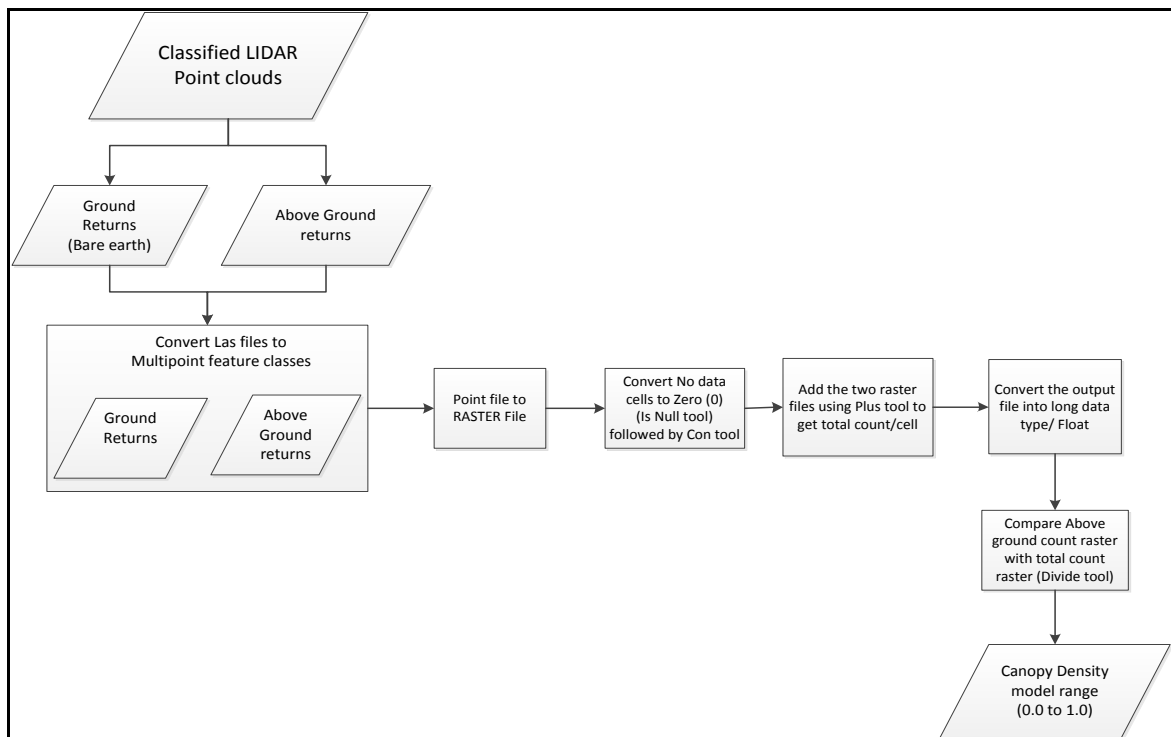


Figure 3-6: The procedure for modelling canopy density

Canopy density models are relevant in many forestry applications such as quantifying crown fuel layer development (Falkowski *et al.*, 2005), biomass estimation (Muukkonen and Heiskanen, 2005) and mapping invasive plant species (Joshi *et al.*, 2006).

Canopy density model validation

The canopy density models generated were validated using the canopy density data collected from the field. This involved fitting a scatterplot of the generated canopy densities per plot against the field estimated canopy cover (%). The validation was done in Erdas imagine 2010.

3.6. Object-Based Image Analysis (OBIA)

Pixel-based classifications have difficulties in adequately or conveniently exploiting expert knowledge or contextual information in the image. Object-based image processing techniques overcome these difficulties by first segmenting the image into multi-pixel objects of various sizes, based on both spectral and spatial characteristics of groups of pixels (Flanders *et al.*, 2003).

3.6.1. Image segmentation

Image segmentation procedures are used to generate image objects by partitioning an image into non-intersecting or non-overlapping regions (Blaschke, 2010; Moller *et al.*, 2007). Similarly, for the delineation of individual tree crowns, OBIA is used to create objects that are rough approximations of the size and shape of the individual tree crown area (Kim *et al.*, 2009). There are various segmentation techniques currently in use, the major ones being edge based and region based. In this study, region based type of segmentation (multi-resolution) was used.

Multi-resolution segmentation is the most commonly used method. It uses the multi-resolution segmentation algorithm, which merges pixels or existing image objects. It is a bottom-up segmentation based on a pairwise region merging technique. It is an optimization procedure which for a given number of image objects, minimizes the average heterogeneity and maximizes their respective homogeneity (Definiens, 2011).

3.6.2. Tree crown delineation in eCognition

Estimation of Scale Parameter (ESP)

Currently, there is no tool available to objectively guide the selection of appropriate scales for segmentation (Dragut *et al.*, (2010). Scale in image segmentation plays a vital role in determining the size of image objects generated. The degree of heterogeneity within an image-object is controlled by a subjective measure called 'scale parameter' as implemented in eCognition Developer software. ESP tool builds on the idea of local variance (LV) of object heterogeneity within a scene. This tool iteratively generates image-objects at multiple scale levels in a bottom-up approach and calculates the LV plotted against the corresponding scale. The thresholds in rates of change (ROC) of LV (ROC-LV) indicate the scale levels at

which the image can be segmented in the most appropriate manner, relative to the data properties at the scene level.

During the segmentation process, higher values for the scale parameter result in larger image objects and smaller values in small objects. Estimation of Scale Parameter (ESP) tool in eCognition was used to determine the most appropriate scale for multi-resolution segmentation. Figure 3-7 shows the estimation of scale parameter graph for the Geoeye Panchromatic image and LiDAR CHM loaded in eCognition Developer, which shows that scale parameter of 18 or 24 among others, are the appropriate scales to segment the images. Scale of 18 was used because the objects of interest in the study area are trees whose average crown diameter was 6 m. Higher scale parameter is used when the objects of interest are large for example in the detection of buildings.

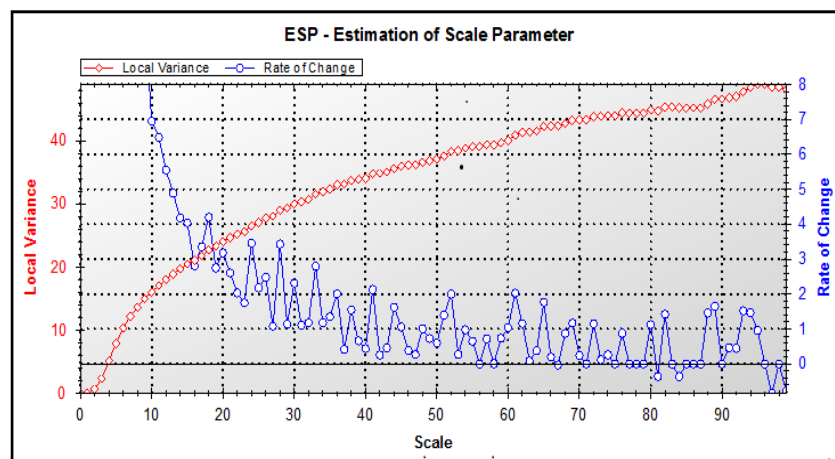


Figure 3-7: ESP Tool for Geoeye and LiDAR CHM

Multi-resolution Segmentation

Different image segmentation techniques of OBIA are being used for forest inventory, especially for individual tree crown delineation. For instance, image segmentation for tree crown delineation can be done using Individual Tree Crown delineation suite (ITC), an extension of the image processing software PCI Geomatica and OBIA software eCognition (Kim *et al.*, 2009).

For this study, multi-resolution segmentation was carried out in eCognition. Multi-resolution means that the algorithm is able to segment images at any given resolution. This segmentation is based on Region Growing approach starting at the level of pixel and neighbouring pixels having similar spectral values are grouped into the same objects (Platt & Schoennagel, 2009). The procedure identifies single image objects of one pixel in size and merges them with their neighbours, based on relative homogeneity criteria. This homogeneity criterion is a combination of spectral and shape criteria.

Unlike the Region Growing from local maxima (tree top), Multi-resolution segmentation uses user specified parameters such as the scale parameter, from which size and shape of resulting object is determined (Hay *et al.*, 2005; Kim *et al.*, 2009). From 3-7, Estimation of scale parameter was carried out

and a scale of 18 was used for the segmentation. Figure 3-8 shows the segmentation procedure and the rule-set developed for object based image analysis in this study.

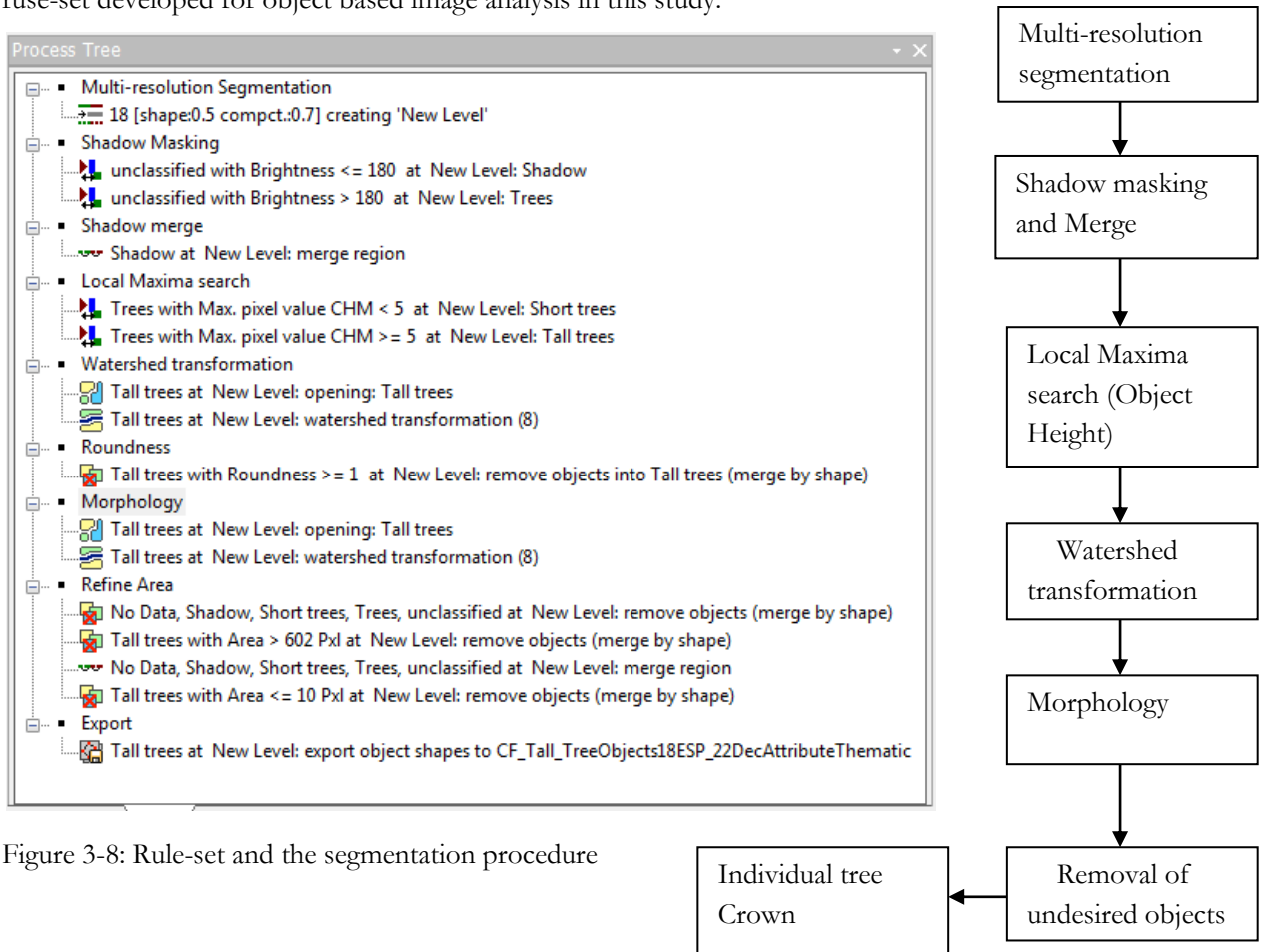


Figure 3-8: Rule-set and the segmentation procedure

Validation of tree crown delineation

The quality of segmentation is related to quality of data (spatial and spectral resolution, noise) as well as data integration procedures and the optimization of scale parameter settings, which enables the adaptation of segmentation results on the target objects (Moller *et al.*, 2007). The image objects generated were validated using the manually delineated tree crowns as the reference crowns. Two accuracy measures for goodness of image segmentation were carried out namely, “D” value and one to one (1:1) matching of crowns. “D” measure is used to obtain the over-segmentation and under-segmentation ratio which helps to decide on the parameter to be used. The “D” value ranges from 0-1 and value closer to 0 is the best with the objects (reference and segmented) exactly overlapping each other.

1:1 matching of reference crowns versus the segmented crowns for the same trees was done. It is based on the visual interpretation. Accuracy is determined by comparing the objects overlap with the reference. Objects with 50% overlap with the reference are considered to be matching. Figure 4-8 shows the reference crowns (purple) versus the segmented objects in green colour (tree crowns) from eCognition.

3.7. Classification and accuracy assessment

3.7.1. Classification

Object-oriented classification techniques based on image segmentation are being actively studied in the high-resolution image process and interpretation to extract a variety of thematic information. Different from the pixel-based image analysis, the processing of the object-oriented method is based on image segment, not single pixel. The object-oriented classification includes two consecutive processes. An image is subdivided into separated regions according to the spectral and spatial heterogeneity in the image segmentation process. Then the objects are assigned to a specific class according to the class's description in the image classification process (Zhao *et al.*, 2007).

Before assigning classes in eCognition, image-object primitives are created. These objects are polygons of roughly equal size exhibiting interior homogeneity (within-object variance is small compared to between-object variance) (Flanders *et al.*, 2003). The segmented objects were classified according to species composition in the study areas. Two classes were taken which are *Shorea robusta* (Sal) (dominant species) and all others subdominant species were grouped into a class called others. These species include *Caeseria graveolens* (Barkaule), *Cassia fistula* (Raj Brikshya), *Holarrbena pubescens* (Khirra), *Lagerstromia parviflora* (Bot Dhayero) and *Cleistocalyx operculatus* (Kyamuna). Classification was carried out using the panchromatic Geoeye image and the nearest neighbour approach. The eCognition Developer version 8.64 software was used for object-based classification analysis. Classification results were exported as a raster file for accuracy assessment in Erdas Imagine.

3.7.2. Accuracy assessment

To assess which classes may contain membership ambiguities, eCognition provides a fuzzy membership value and stability values for each object. The fuzzy logic that forms the basis for classification assigns a membership value to each object between zero (totally ambiguous) and one (unambiguous) for each potential class. In this study, accuracy assessment was done in Erdas Imagine 2010. The species information from field data was used as reference for the accuracy assessment. An independent validation dataset comprising of 30% of field data which was 67 and 38 tree samples for community and government forest respectively was used.

3.8. Above Ground Biomass and carbon stock calculation

Forest biomass is commonly estimated using allometric equations (Ketterings *et al.*, 2001). Allometric equations are used to extrapolate both in situ and remotely sampled data to a larger area and to derive biomass from other variables. Allometry relates the size of one structure in an organism to the size or amount of another structure in the same organism. Therefore, it is possible to estimate biomass from tree diameter, height, etc., and extend the datum to a larger area with the same characteristics (Bombelli *et al.*, 2009).

In this study, species wise allometric equation relating both DBH and height to biomass were not available hence a generalized equation recommended by (Chave *et al.*, 2005) for tropical moist hardwood forests was used. Moist tropical forest is considered to be area receiving an average annual rainfall of between 1500mm to 3500mm/yr. The sites under investigation in this study receive an average annual rainfall of 2250mm/yr hence the allometric equation was considered applicable for the carbon stock analysis in these areas. Secondly, all the species in the study area were hardwoods. The equation made use of species specific wood specific gravity. Wood specific gravities of 0.88 and 0.72 (ICIMOD, 2010) were used for *Shorea robusta* other species respectively.

Equations

$$AGTB = 0.0509 * \rho D^2 H \dots\dots\dots eqn 3-3$$

Where;

- AGTB = above ground tree biomass (kg)
- ρ = Wood specific gravity (kg/m³)
- D = Tree Diameter at Breast Height (DBH cm)
- H = Tree Height (m)

(ICIMOD *et al.*, 2010, Chave *et al.*, 2005)

3.9. Regression analysis

Regression analysis is aimed at quantifying the relationship between a response variable and one or more explanatory variables. Quantitative relationship is expressed by an equation and its graphic representation (Husch *et al.*, 2003). Coefficient of determination (R²) shows the percentage of variation in one variable that is associated with other variable(s) which is explained by the given equation. R² value ranges from 0-1, a model with a value closer to 1 and with a low RMSE is considered to be a good model. Generally, for biomass estimations, models with a R² of above 0.5 are considered to be good for prediction.

Regression models are used for biomass estimation because of their relative simplicity and ease for converting inventory data into a biomass estimate (Baishya & Barik, 2011). Although it is difficult and tedious at the initial stage to develop the best-fit models, tree dimension values as the input data requirement for subsequent estimations have made the regression-based biomass estimation method extremely popular (Brown, 1997). Several regression models have been developed to estimate biomass or biomass-related parameters (Brown *et al.*, 1989; Schmitt *et al.*, 2009), which are being used to prepare volume tables for several forestry species (Li & Weiskittel, 2010) and to estimate carbon in a variety of forest types (Schroeder *et al.*, 1997). The total biomass data obtained from such models are then converted into carbon content for estimating carbon by applying a conversion factor of 0.5 or 0.47 (Kale *et al.*, 2009; Somogyi *et al.*, 2008) on the assumption that a tree contains 50% or 47% carbon of the dry biomass.

In this study, non-linear interactive regression models were used to model the statistical relationship between biomass, CPA and Lidar derived canopy height. Non-linear regression was preferred to linear

regression because changes in above ground biomass over time are non-linear and vary among ecoregions (Scheller & Mladenoff, 2005). Before the models were fitted, scatter plots were used to check the general trend of the data (Appendix 5). This guided in the choice of the model since they show that the relationship between the predictor or independent variables (CPA and height) and response or dependent variable (AGB) is non-linear. Interactive modelling was preferred to other models because of the interaction between parameters height, tree density and CPA. With higher tree density, trees tend to grow more vertically than laterally hence limiting the crown expansion, thus have interaction effect. Additionally, in a dense forest, the growth of tree crown is not directly proportional to height; rather it is constrained by height.

The individual trees which were identified, correctly classified and had 1:1 matching of the segments were used for model development and validation. Outliers were also removed to ensure a robust model. Model calibration was done using 70% of the field data set. The models for these sites were developed basing on the species classification. Therefore, four models were developed for the two forests types. *Shorea robusta* and other species were modelled and validated independently in each of the forest management types.

The fitted models were validated using 30% of the test data from the field. This involved comparing the amount of biomass calculated from field data (observed carbon) with the carbon predicted by the model. Coefficient of Determination (R²) and Root Mean Square Error (RMSE) were calculated to assess the *goodness of fit* and to determine amount of error in the models.

$$RMSE = \sqrt{\frac{\sum (Cp - Co)^2}{N}} \dots\dots\dots eqn 3-4$$

Where, RMSE = Root Mean Square Error,

Cp – Carbon predicted by the model

Co – Observed carbon (Calculated from field data)

N – Number of observations

3.10. Carbon stock Mapping

After the models were developed and validated, AGB /carbon stock was calculated and visualized in carbon stock maps.

4. RESULTS

4.1. Forest condition assessment

4.1.1. Canopy density modeling

An assessment of the condition of each forest through canopy modelling, stand density and basal area analysis was carried out and results shown in (Table 4-1). The output of canopy density models prepared for CF and GMF are shown in Figure 4-1 and Figure 4-2 respectively. The green areas show dense forest cover (areas where a few LiDAR shots could reach the ground surface) while the blue areas show areas with little or no vegetation cover (areas where higher LiDAR shots could reach the ground surface). Also, the basal area for the CF is higher (20 m²/ha) than GMF which has (15m²/ha). Table 4-1 shows the average stand density distribution per plot (0.05 ha) and per hectare as well as the basal area per hectare for the two sites.

Table 4-1: Stand density and basal area for the forest management types

Site Name	Average Stand density (trees/plot)	Stand density (trees/Ha)	Basal area (m ² /Ha)
Community Forest	19	397	20
Government Forest	6	120	15

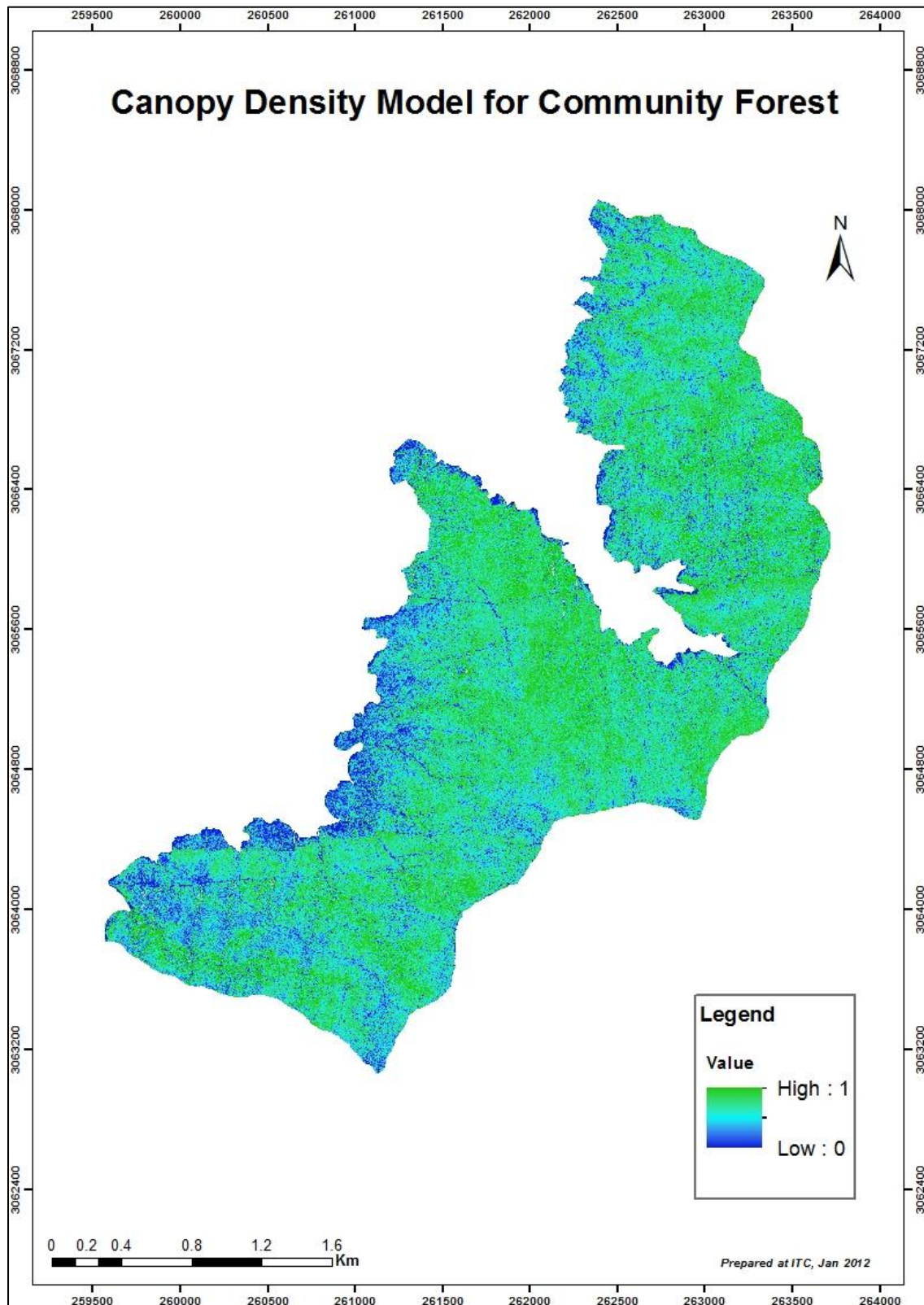


Figure 4-1: Canopy density model for CF forest

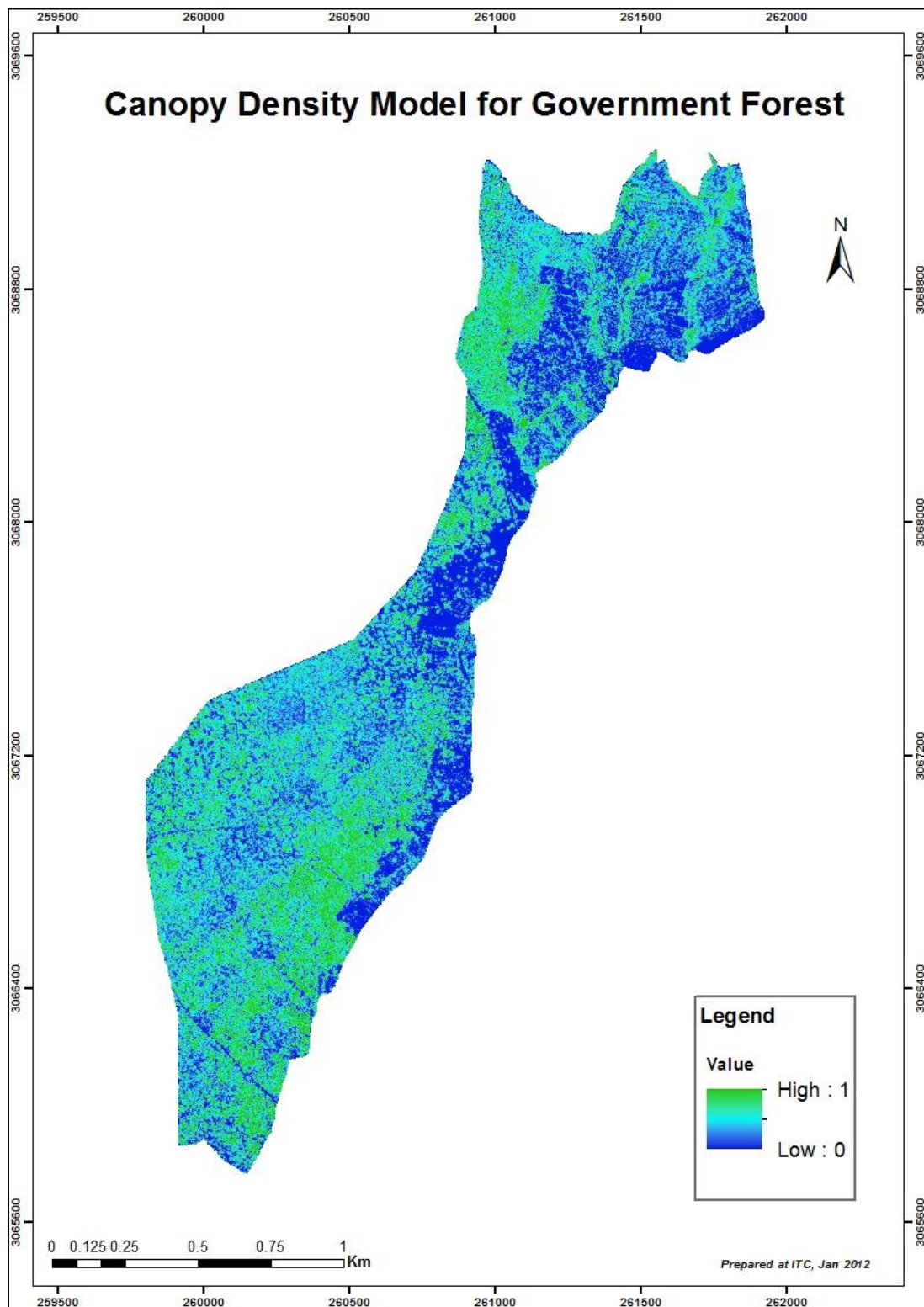


Figure 4-2: Canopy density model for GMF forest

4.1.2. Canopy density model validation (CDM)

Figure 4-1 and Figure 4-2 show the CDMs derived from LiDAR data and were validated using the canopy cover percentage (%) from the field data. Figure 4-3 shows that there is 89% and 77% agreement between the field canopy cover and LiDAR derived canopy cover (%) for GMF and CF forests respectively.

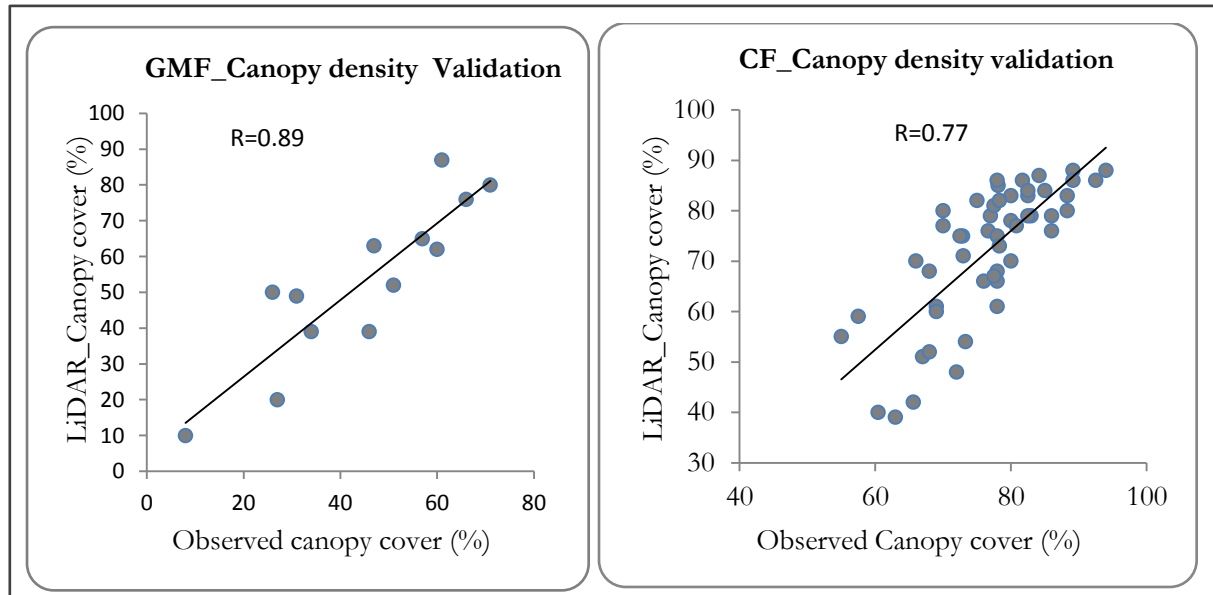


Figure 4-3: Scatter plots of observed canopy density and estimated canopy density from LiDAR for government (left) and community (right) forests.

4.2. Canopy Height Modeling (CHM)

CHMs for both GMF and CF forests were generated (Figure 4-5) from airborne LiDAR data point clouds. To come up with a CHM, a Digital Terrain Model (DTM) and Digital Surface Model (DSM) are first generated from the last and first LiDAR returns respectively (Figure 4-4) as described in section 3.5.3.

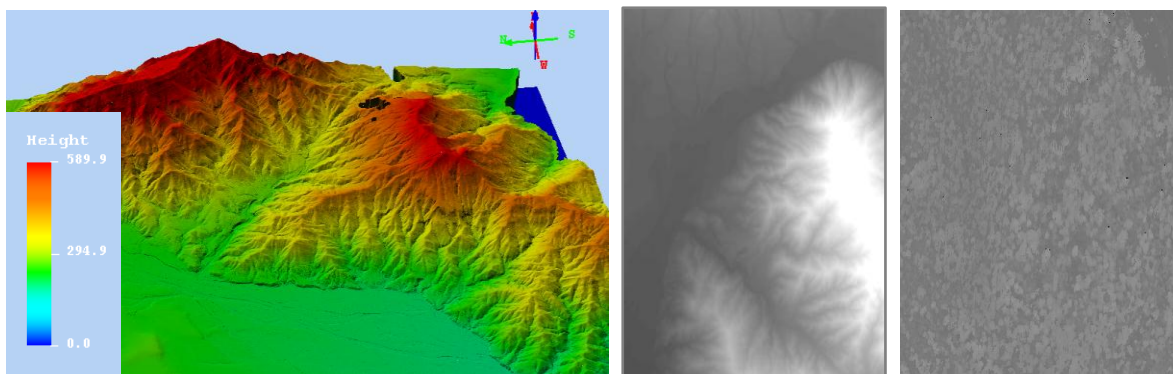


Figure 4-4: An example of 3D and 2D perspective of DTM (left) and (Centre), and 2D DSM (right).

In the DTM (bright areas show high elevation and darker areas show low elevation), in the DSM, bright areas show the terrain features (trees) while darker areas show the ground surface. In the 3D DTM, areas in red show highest elevation while blue show the lowest elevation.

A height difference between the DSM and DTM represents the absolute height of the trees normally referred to as normalized surface model (nDSM or CHM) which represents the height of the tree canopies of the forest Figure 4-5.

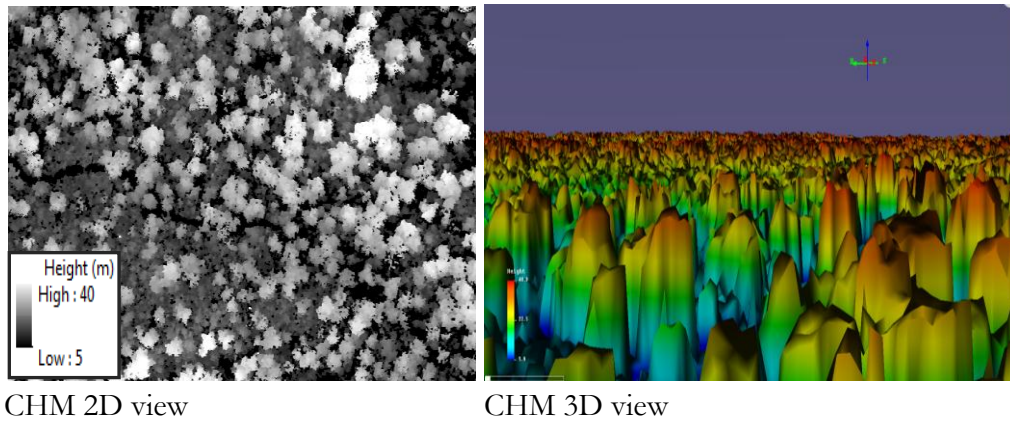


Figure 4-5: 2D (left) and 3D (right) views the generated of canopy height models

The brighter areas on the image show high values of canopy height while the darker areas represent lower canopy height

4.2.1. CHM Validation

The CHM generated was assessed for accuracy by relating the LiDAR-derived height with the real height measured in the field. The scatter plots in Figure 4-6 show the relationship between the CHM and the real height, which shows that there is 88% and 90% agreement between the two heights ($r=0.88$; 0.90) from CF and GMF forests respectively. The mean error of height estimation was calculated and results shown in Table 4-2. GMF forest trees showed a low error (RMSE=12%) than the CF forest trees (RMSE=19%)

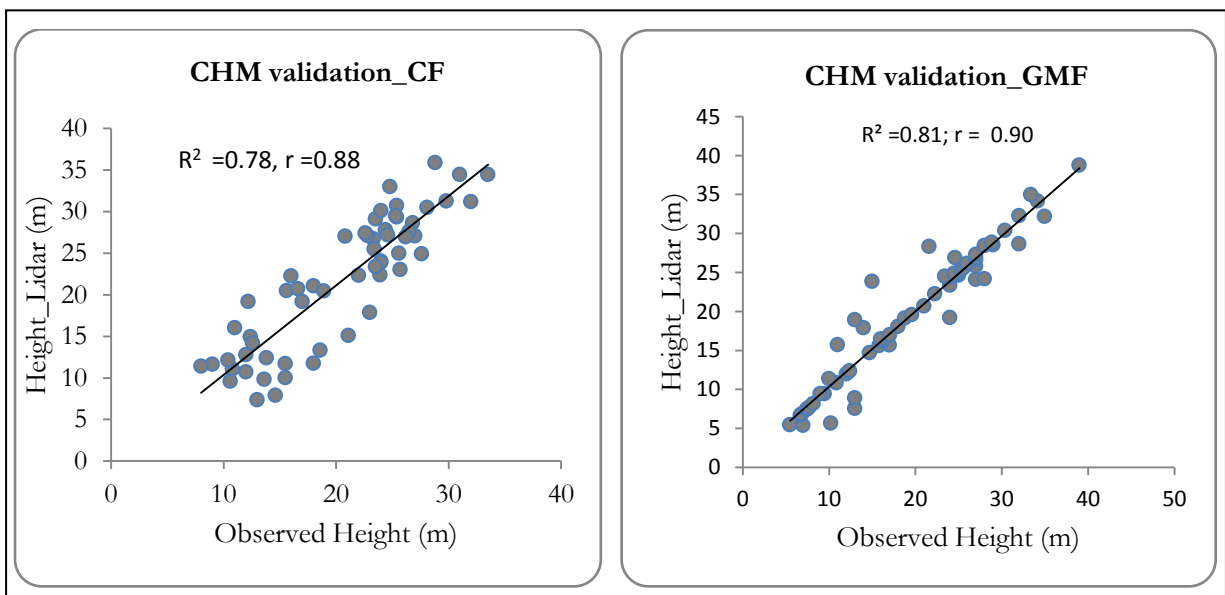


Figure 4-6: Scatter-plots of relationship between LiDAR-derived canopy height and observed height in CF and GMF forests.

Table 4-2: The average error of height estimation from LiDAR data for the two forest types

site	RMSE	Mean error of height
CF	19%	3.8m
GMF	12%	2.4m

4.3. Image segmentation

Image segmentation was done on Lidar CHM (0.5m) and the Geoeye panchromatic image (0.5m). Before image segmentation was undertaken, estimation of scale parameter was carried out to determine the appropriate scale. Multi-resolution segmentation was then carried out to group the pixels into homogenous area to form an image object. Shadow areas were masked out from the image before segmentation process so as to avoid overestimation of the crown projection area. Canopy height was also limited to a range of 5m to 40m to avoid inclusion of shrubs and small trees (below 5m). Image objects with a height greater than 40m were excluded based on the fact that the maximum height recorded in the field was 38m.

4.3.1. Multi-resolution segmentation

LiDAR CHM and Geoeye Panchromatic Image were segmented. During the segmentation, there was search for local maxima which represents the tree height. Therefore, each of the resulting image objects has a height attribute in addition to the geometry and spectral information. Figure 4-7, shows part of the output image objects from multi-resolution segmentation.

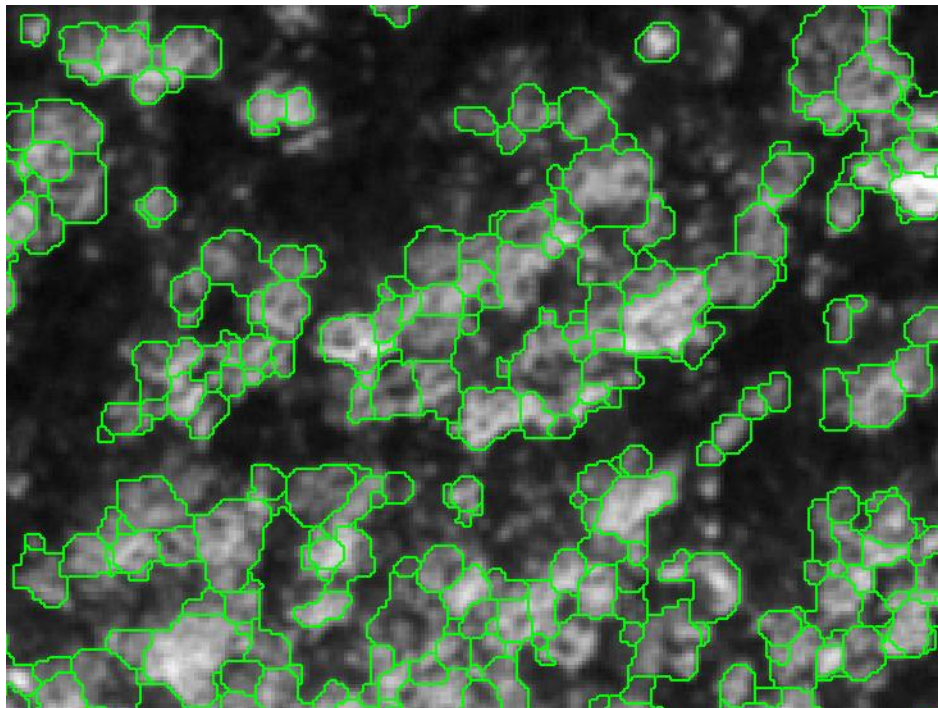


Figure 4-7: An example of individual tree crowns with height values from multi-resolution segmentation

Segmentation accuracy

Image objects, (i.e. tree crowns) generated were validated using two accuracy measures namely 1:1 matching and “D” value. “D”, is a measure of “goodness of fit” which is used to obtain the over-segmentation and under-segmentation ratio. The “D” value measure ranges from 0-1 and values closer to 0 are best which indicate that the objects (reference and segmented) are overlapping each other hence no problem of over or under-segmentation. The 1:1 matching of manually delineated crowns against the segmented image objects based on the visual interpretation was also carried out. The accuracy for the GMF forest site was 78% with a “D” value of 0.30 (70% accurate, 30% error) while that for CF forest was 77% with a “D” value of 0.30 as shown in table 4-3. Figure 4-8 shows the overlay of the image objects and reference crowns for the 1:1 method of accuracy assessment of segmentation process.

Table 4-3: Accuracy assessment of the segmentation process using D and 1:1 methods

	Total no. 1:1 match	Total reference	Accuracy	“D” value
GMF Forest	80	103	78%	0.30
CF Forest	175	228	77%	0.30

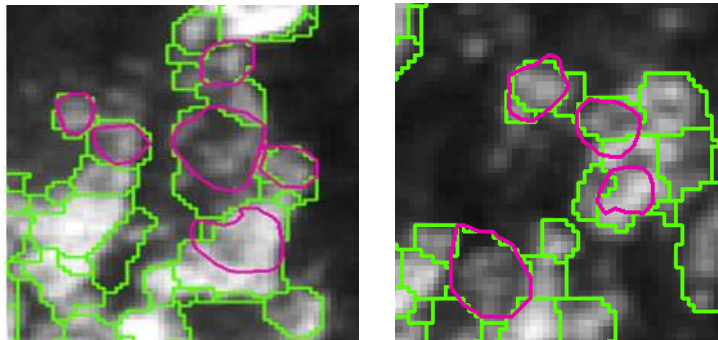


Figure 4-8: Overlap between the image objects and reference crowns

The purple objects represent the manually delineated crowns for the identified trees while the green objects are the output of multi-resolution segmentation.

4.4. Image classification

Object based classification is a type of supervised classification technique. The delineated crowns were classified into two classes namely: *Shorea robusta* (dominant species) and all the other tree species were grouped into one class (others). Figure 4-9 and Figure 4-10 show the classified maps for the two forest management study sites (government and community respectively).

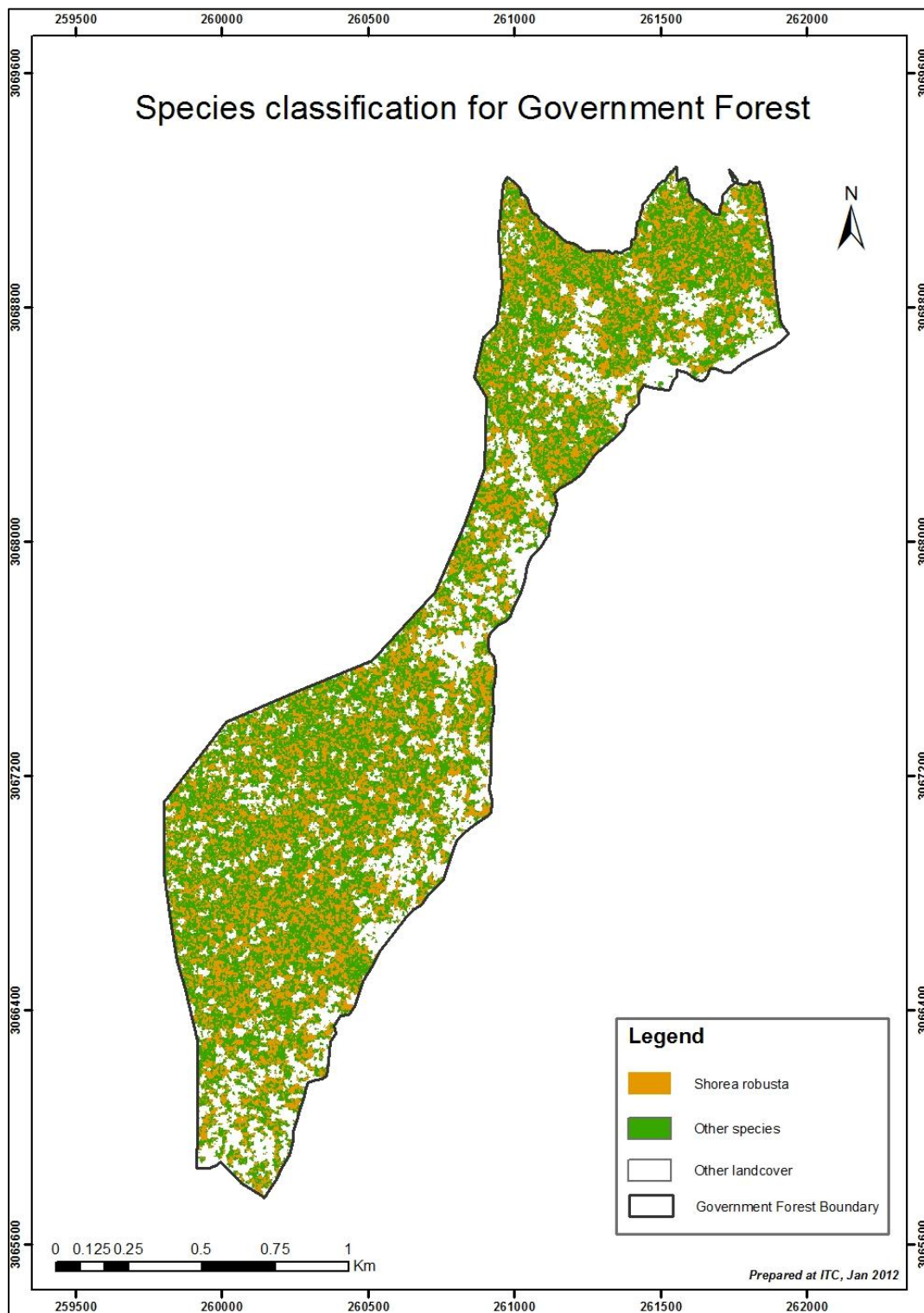


Figure 4-9: Species map of government forest.

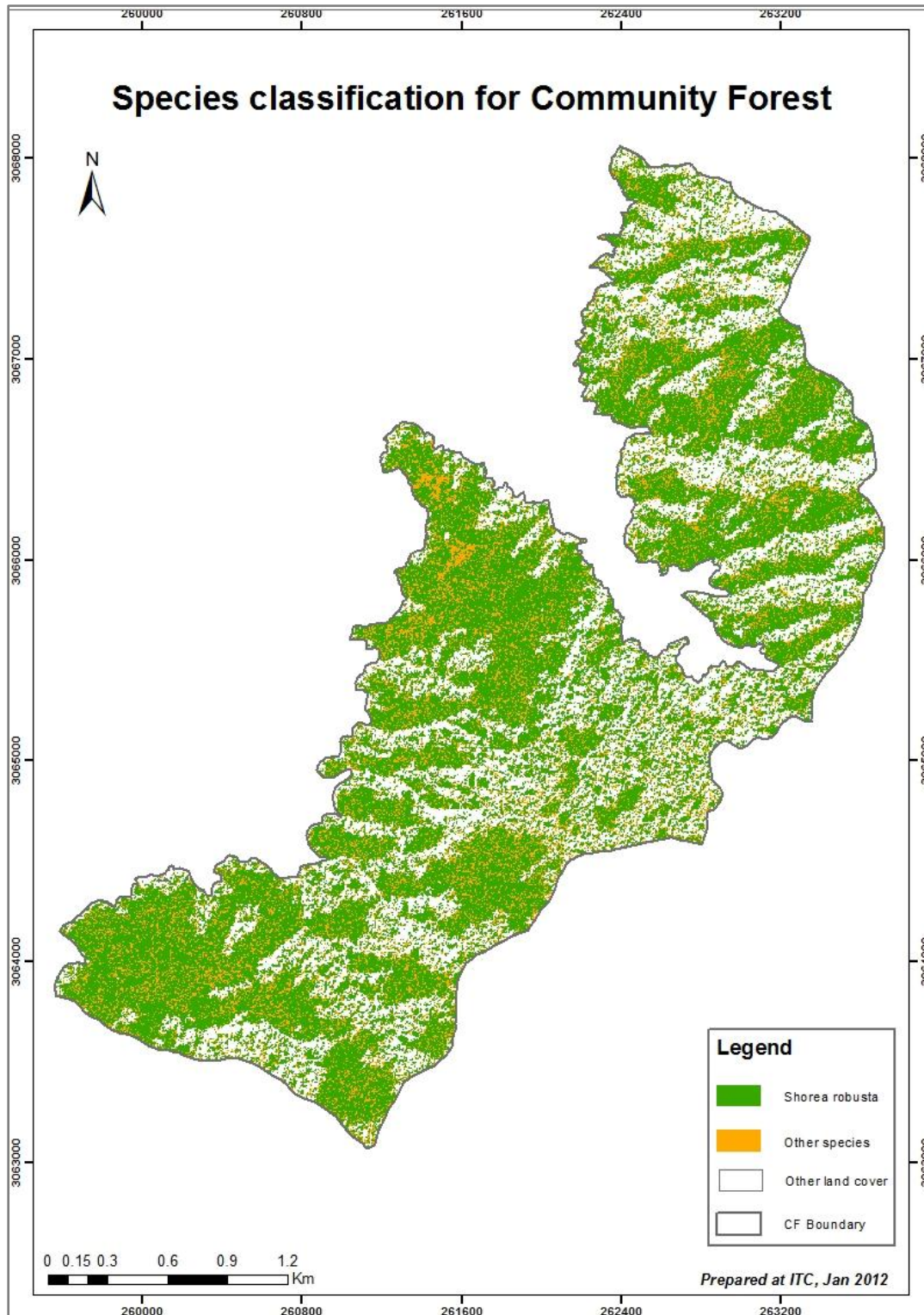


Figure 4-10: Species map of community forest

The training dataset for classification comprised of 70% of the identified trees which were randomly selected from the field dataset while 30% was used to assess the classification accuracy. In total, 67 and 38 sample trees and were used to validate CF forest and GMF forest classifications respectively.

Accuracy Assessment

The accuracy was assessed based on the overall accuracy, users' accuracy and producer's accuracy as shown in Table 4-4 and Table 4-5 for community and government forest respectively. Users' accuracy corresponds to error of commission (inclusion). For example, for *Shorea robusta* class, if samples from class 'other' are included, then it is error of commission, while producer's accuracy corresponds to the error of omission (exclusion). For example, if for *Shorea robusta* class, some samples are classified as 'other species', then it is an error of omission. In other words, users' accuracy tells from the perspective of the user of the classified map, how accurate the map is while producer's accuracy tells from the perspective of the maker of the classified map, how accurate the map is.

Table 4-4: Accuracy report for community forest species classification

Class Name	Reference Total	Classification Total	Correct Total	Producer's Accuracy	Users' Accuracy
<i>Shorea robusta</i>	43	45	34	79%	76%
Others	24	22	13	54%	59%
Totals	67	67	47		
Overall classification accuracy = 70%					

Table 4-5: Accuracy report for government forest species classification

Class Name	Reference Total	Classification Total	Correct Total	Producer's Accuracy	Users' Accuracy
<i>Shorea robusta</i>	9	12	7	78%	58%
Others	29	26	24	83%	92%
Totals	38	38	31		
Overall classification accuracy = 82%					

The overall accuracy was higher in GMF forest (82%) than in the CF forest (70%). The accuracy of *Shorea robusta* species was higher (79%) in CF forest compared to that of GMF forest (78%). On the other hand, the accuracy of other species in GMF was significantly higher (83%) than in the CF forest (54%). The users' accuracy was highest (92%) in other species classification from GMF forest while also the lowest users' accuracy (58%) was for *Shorea robusta* classification for the same site.

Notably, the reference samples for *Shorea robusta* was relatively small (9 samples) for the GMF forest compared to the CF forest (43 samples)

4.5. Descriptive Statistics

During fieldwork, a total of 86 plots were sampled in the CF forest from which 1708 trees were recorded. A total of 23 plots were sampled in the GMF forest which had a total of 139 trees. Table 4-6 shows a summary of the distribution of the sampled plots in the sites.

Table 4-6: Distribution of sample plots and sample trees inventoried in the study sites.

Site Name	Strata Name	Total Plots	Total trees	Trees Identified	Species	
					<i>Shorea robusta</i>	Others
Government Forest	Government F	23	139	111	26	85
Community Forest	Kankali	86	1708	341	215	126
	Kalika					
	Davidhunga					
	Dharapani					
	Satkanya					

The study sites had diverse distribution of species. More than 17 different types of tree species were recorded in the CF forest, while over 22 species were recorded in the government forest. The dominant species in the GMF forest were *Shorea robusta* (28%), followed by *Lagerstromia parviflora* (22%) while *Careya arborea*, *Sphaeranthus indicus* L., *Albezia procera* and *Semecarpus anacardium* are among the least occurring species and are grouped into others (23%) as shown in Figure 4-11, while the other species in CF forest comprised of 17% of the total trees inventoried (Figure 4-12).

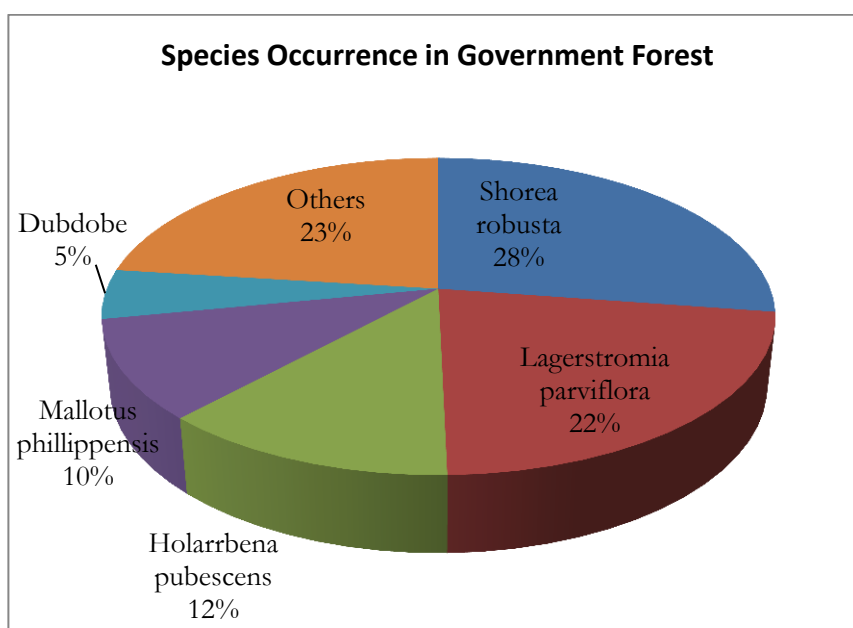


Figure 4-11: Species distribution in the GMF forest

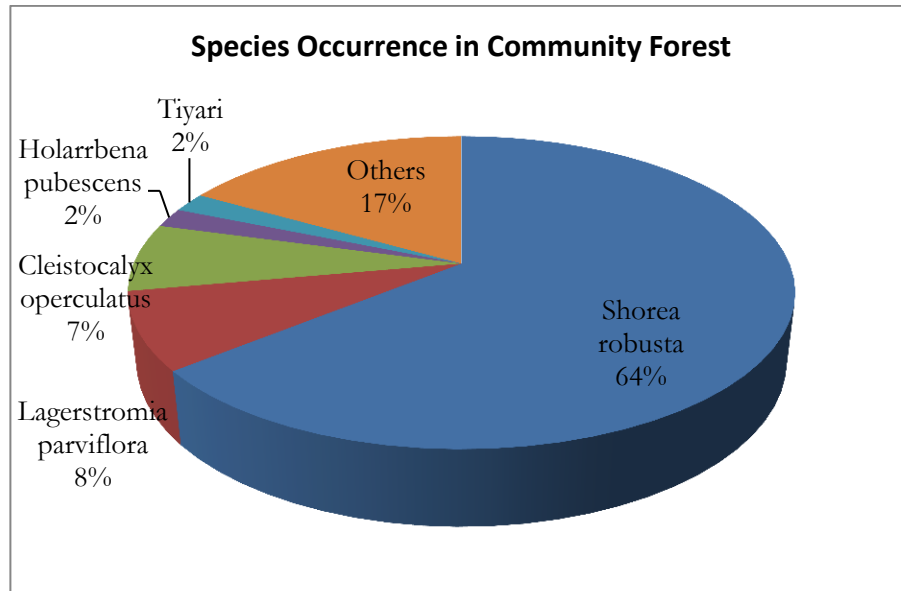


Figure 4-12: Species distribution in the community forest.

Shorea robusta and *Lagerstromia parviflora* were the most dominant species in the community forest just like in the government forest representing 64% and 8% of the total species respectively. Although *Shorea robusta* is the dominant species in the two areas as indicated on Figure 4-11 and Figure 4-12, there is a significant difference in the occurrence of the species in the two sites.

DBH and height were also measured in the field and are represented in box plots in Figure 4-13. The average DBH and height for *Shorea robusta* and other species in GMF and CF forest are shown in Table 4-7. Generally, trees from GMF forest were larger in terms of DBH and height compared to those in the CF forest (Figure 5-1).

Table 4-7: Average DBH and Height for *Shorea robusta* and other species

Forest type	Parameter	<i>Shorea robusta</i>	Others
CF	DBH (cm)	21	19
	Height (m)	22	18
GMF	DBH (cm)	42	31
	Height (m)	25	17

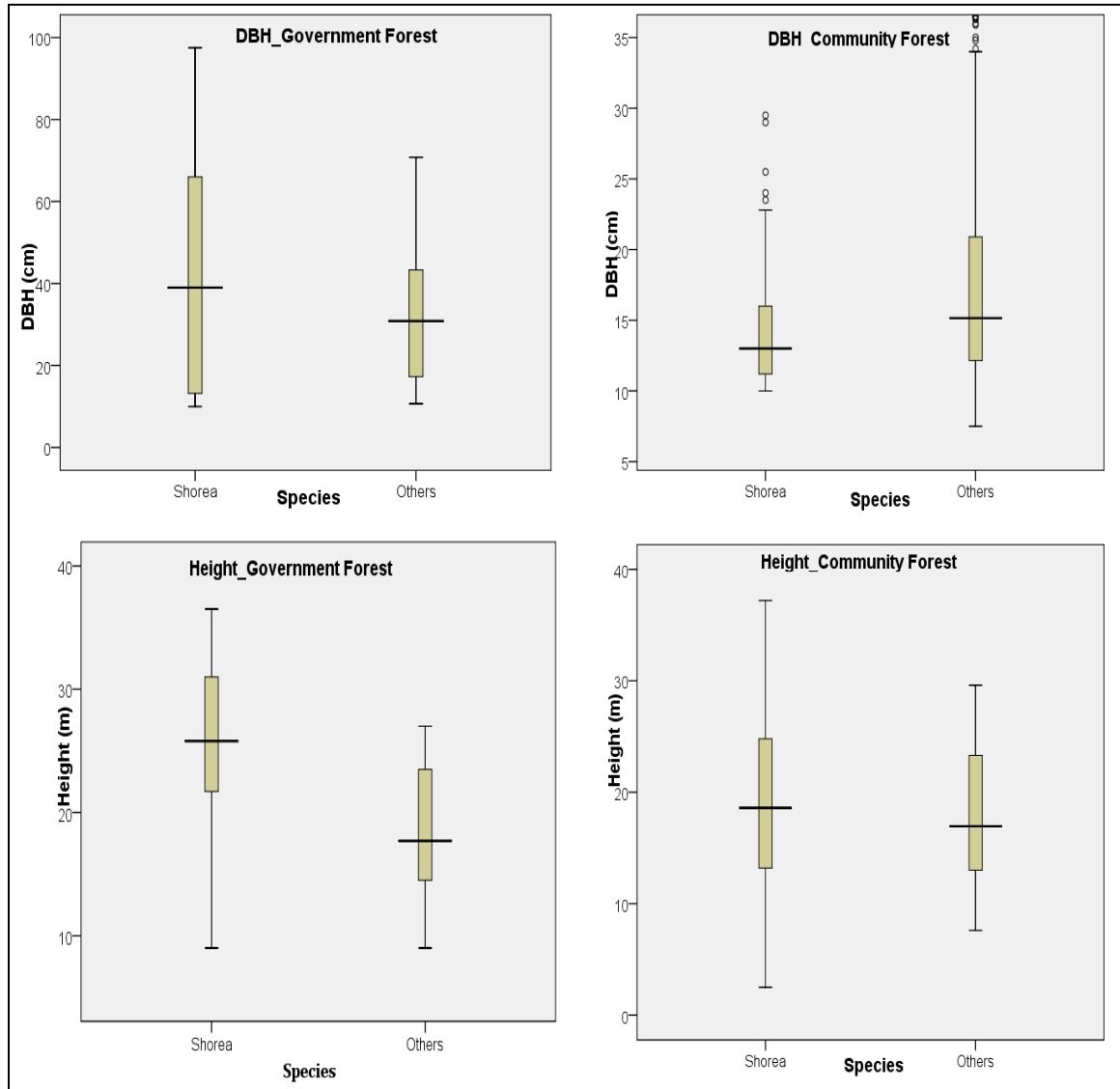


Figure 4-13: Box plots of DBH and height of *Shorea robusta* and other species for the two forests

4.6. Model development and Validation

Interactive models were used to model the statistical relationship between AGB, CPA and LiDAR-derived canopy height as described in section 3.9. Four interactive models (equation 4-1 to 4-4), (2 models for each forest management type), were developed based on the species classification, to estimate the AGB in the study area. *Shorea robusta* was modelled separately from other species as it was the dominant species. The models and the results showing the relationships between CPA, height and AGB of *Shorea robusta* and other species are shown in Table 4-8 to Table 4-15.

In all the models, AGB = above ground biomass (kg/tree), CPA = Crown Projection Area (m²), and H= LiDAR derived tree height.

Model 1: *Shorea robusta* – Community forest

$$AGB = -1087.14 + 67.83CPA + 10.67H + 3.0CPA*H \dots \dots \dots \text{eqn 4-1}$$

Table 4-8: Regression analysis for *Shorea robusta* in the community managed forest.

<i>Shorea robusta</i> Community managed Forest					
<i>Regression Statistics</i>		<i>Coefficients</i>		<i>t Stat</i>	<i>P-value</i>
Multiple R	0.91	Intercept	-1087.14	-1.02621263	0.311115
R Square	0.83	H	10.67	0.210231962	0.834581
Adjusted R Square	0.82	CPA	67.83	1.375055618	0.176963
Standard Error	1139.55	CPA*H	3.00	1.507918018	0.139634
Observations	43				

Table 4-9: ANOVA test results for *Shorea robusta* in the community forest

ANOVA – <i>Shorea robusta</i> Community managed Forest					
	<i>df</i>	<i>SS</i>	<i>MS</i>	<i>F</i>	<i>Significance F</i>
Regression	3	253266879.1	84422293	65.01049	3.11254E-15
Residual	39	50645205.39	1298595		
Total	42	303912084.5			

Model 2: Other species – CF forest

$$AGB = -733.55 + 50.87CPA + 5.63H + 0.29CPA*H \dots \dots \dots \text{eqn 4-2}$$

Table 4-10: Regression analysis for other species in the CF forest

Other Species Community managed Forest					
<i>Regression Statistics</i>		<i>Coefficients</i>		<i>t Stat</i>	<i>P-value</i>
Multiple R	0.84	Intercept	-733.55	-0.51457391	0.611038
R Square	0.71	H	5.63	0.116261631	0.908306
Adjusted R Square	0.67	CPA	50.87	0.728834943	0.472378
Standard Error	546.78	CPA*H	0.29	0.12685353	0.899996
Observations	31				

Table 4-11: ANOVA test results for other species in the CF forest

ANOVA Other Species - Community managed Forest					
	<i>df</i>	<i>SS</i>	<i>MS</i>	<i>F</i>	<i>Significance F</i>
Regression	3	19409564	6469854.542	21.64028	2.38401E-07
Residual	27	8072266	298972.831		
Total	30	27481830			

Model 3: *Shorea robusta* – GMF Forest

$$AGB = -2975.74 + 221CPA + 43.44H + 0.9CPA*H \dots \dots \dots \text{eqn 4-3}$$

Table 4-12: Regression analysis for *Shorea robusta* in the GMF forest

<i>Shorea robusta</i> - Government managed Forest					
Regression Statistics		Coefficients		<i>t Stat</i>	<i>P-value</i>
Multiple R	0.90	Intercept	-2975.73	-0.642456464	0.544329
R Square	0.80	H	43.43	0.17864954	0.864093
Adjusted R Square	0.70	CPA	221.00	1.086796431	0.318847
Standard Error	2457.43	CPA*H	0.91	0.090652807	0.930719
Observations	10				

Table 4-13: ANOVA test results for *Shorea robusta* in GMF forest

ANOVA <i>Shorea robusta</i> - Government managed Forest					
	<i>df</i>	<i>SS</i>	<i>MS</i>	<i>F</i>	<i>Significance F</i>
Regression	3	143581508.3	47860503	7.925256513	0.016486211
Residual	6	36233908.15	6038985		
Total	9	179815416.4			

Model 4: Other species Government Forest

$$AGB = 9.22 + 19.36CPA - 22.7H + 0.84CPA*H \dots \dots \dots \text{eqn4-4}$$

Table 4-14: Regression analysis for other species in the GMF forest

Other species Government managed Forest					
Regression Statistics		Coefficients		<i>t Stat</i>	<i>P-value</i>
Multiple R	0.81	Intercept	9.22	0.028580548	0.977335
R Square	0.66	H	-22.70	-1.416536751	0.163993
Adjusted R Square	0.63	CPA	19.36	1.2739042	0.209702
Standard Error	499.99	CPA*H	0.84	1.418727558	0.163357
Observations	46				

Table 4-15: ANOVA test results for other species in the GMF forest

ANOVA Other species Government Forest					
	<i>df</i>	<i>SS</i>	<i>MS</i>	<i>F</i>	<i>Significance F</i>
Regression	3	20301927	6767308.991	27.06986	6.61304E-10
Residual	42	10499758	249994.2271		
Total	45	30801685			

The model that explained the highest variation in AGB was that for *Shorea robusta* in the community forest with ($R^2 = 0.83$), while the model that explained the lowest variation was that for other species in the government forest with ($R^2 = 0.66$). Generally, the relationship between the predictor variables and AGB

was higher for single species (*Shorea robusta*) than in the case of clustered species (other species) for both forests.

One way ANOVA was employed to test the significance of coefficient of determination (R^2) and the results are displayed on Table 4-9, Table 4-11, Table 4-13 and Table 4-15. All the models were significant at 95% confidence level or ($\alpha = 0.05$) as shown in the ANOVA tables displayed above. This means that the explanation of AGB using CPA and LiDAR derived canopy height was significant.

4.6.1. Model Validation

The developed models were used to predict carbon for validation dataset, which was plotted against the observed carbon from the field as a way of testing the accuracy of the models. Independent datasets (30%) of the sample data was used for validating the four regression models. Coefficient of Determination (R^2) was calculated to measure the *goodness of fit* between the observed and predicted carbon. Root Mean Square Error (RMSE) was used to test for the amount of errors in each of the models. The model for *Shorea robusta* from the CF forest showed the best fit with ($R^2 = 0.81$) and the least error (RMSE = 10%), Table 4-16, while the model for same species from GMF forest had the highest amount of error (RMSE = 25%). The model also had the least RMSE of 13%. Figure 4-14 and Figure 4-15, show the scatter plots for models validation for CF and GMF forests respectively.

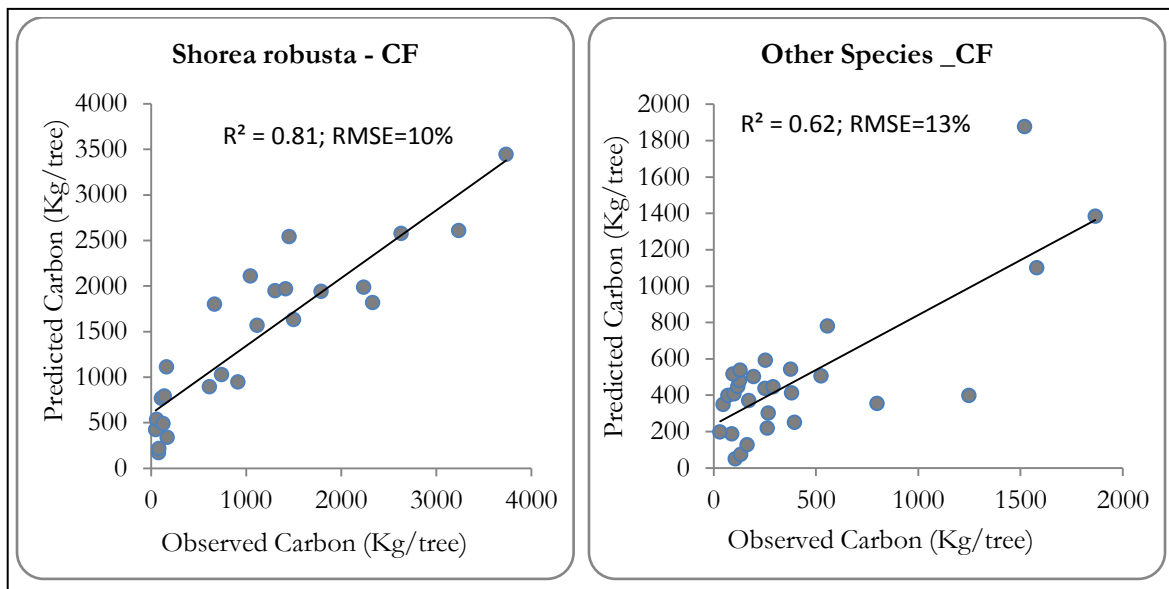


Figure 4-14: Scatter plots of model validation for *Shorea robusta* and other species in CF forests

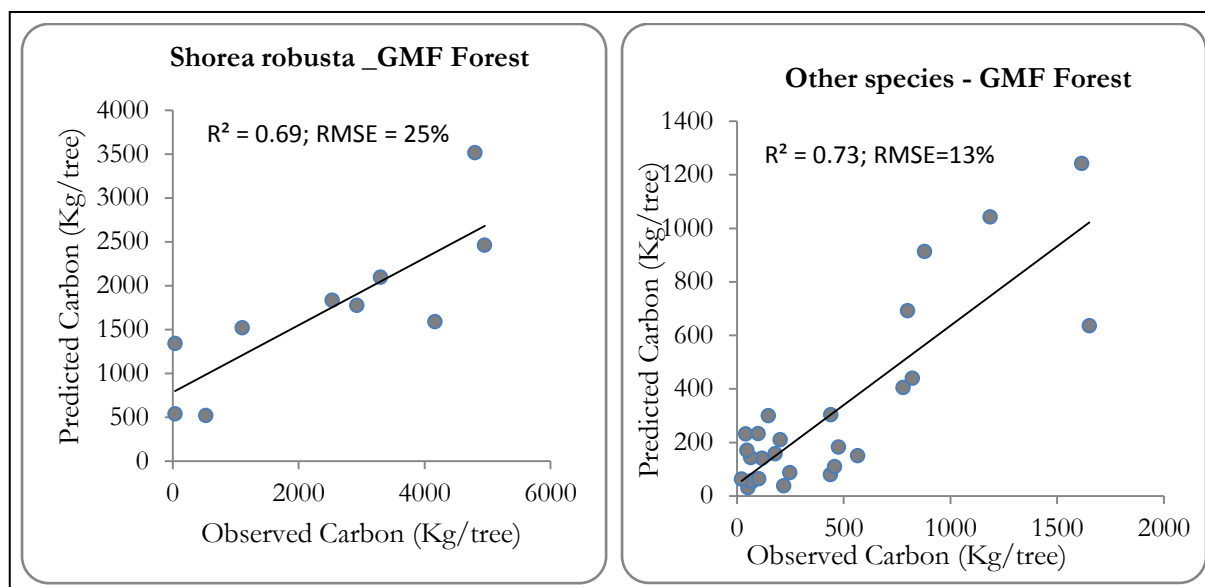


Figure 4-15: Scatter-plots of the model validation for *Shorea robusta* and other species for GMF forest

Table 4-16: Various accuracy measures for the models 1-4

Site Name	Model/Species	Sample size (Validation)	Coefficient of Determination (R^2)	RMSE
CF Forest	<i>Shorea robusta</i>	25	0.81	10%
	Other species	29	0.62	13%
GMF Forest	<i>Shorea robusta</i>	10	0.69	25%
	Other species	27	0.73	13%

From Table 4-16, *Shorea robusta* model for CF forest explained 81% of the observed carbon stock with an error of 10%, while 73% of the observed carbon stock was explained by the model for other species in government forest with an error of 13%.

4.7. Carbon stock mapping

The validated non-linear (Interactive) regression models were used to estimate AGB for the study sites based on the species classification (*Shorea robusta* and others species). AGB was further converted to carbon stock using a Conversion Factor of 0.5. A total of 187,025,846 kgs of carbon was estimated for CF forest which covers an area of 764 ha thus approximately 244 t C/ha. A total of 29,902,700 kgs of carbon was estimated for GMF forest which covers an area of 213 ha which is approximately 140 t C/ha. Figure 4-16 and Figure 4-17 show the carbon maps for the two forest management types. A t-test was performed to test the strength of the difference in the carbon stocks at 95% confidence level. Table 4-17 shows that there is a significant difference in carbon stocks in the two forest management types.

Table 4-17: T-test for Carbon stocks from the two forests.

t-Test: Two-Sample Assuming Equal Variances in carbon stocks		
	<i>CF</i>	<i>GMF</i>
Mean	1215.692921	1009.033
Variance	2636656.304	2232613
Observations	153843	29635
Pooled Variance	2571397.494	
Hypothesized Mean Difference	0	
df	183476	
t Stat	20.31517126	
P(T<=t) two-tail	1.19177E-91	
t Critical two-tail	1.959976858	

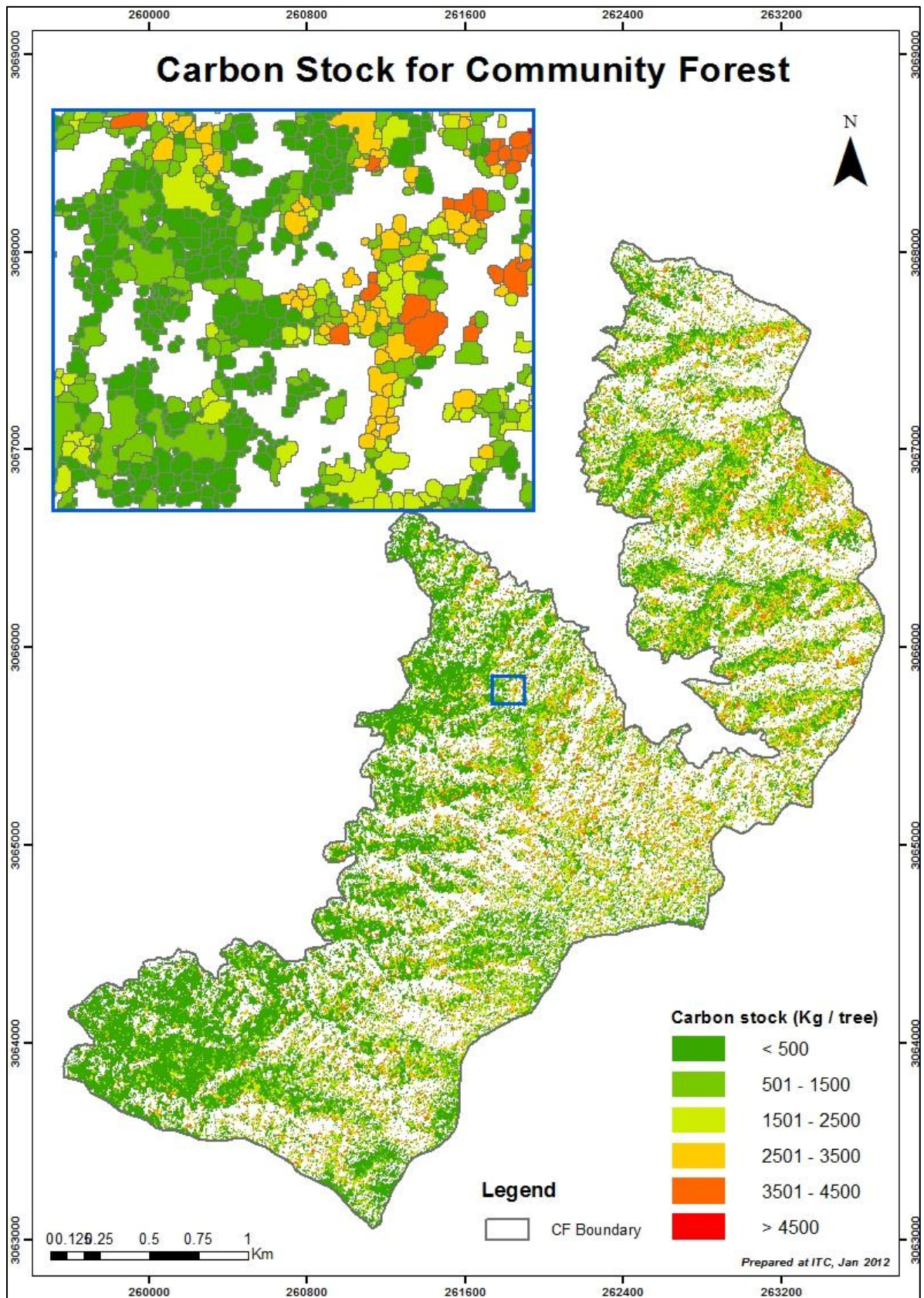


Figure 4-16: Carbon stock map for CF forest

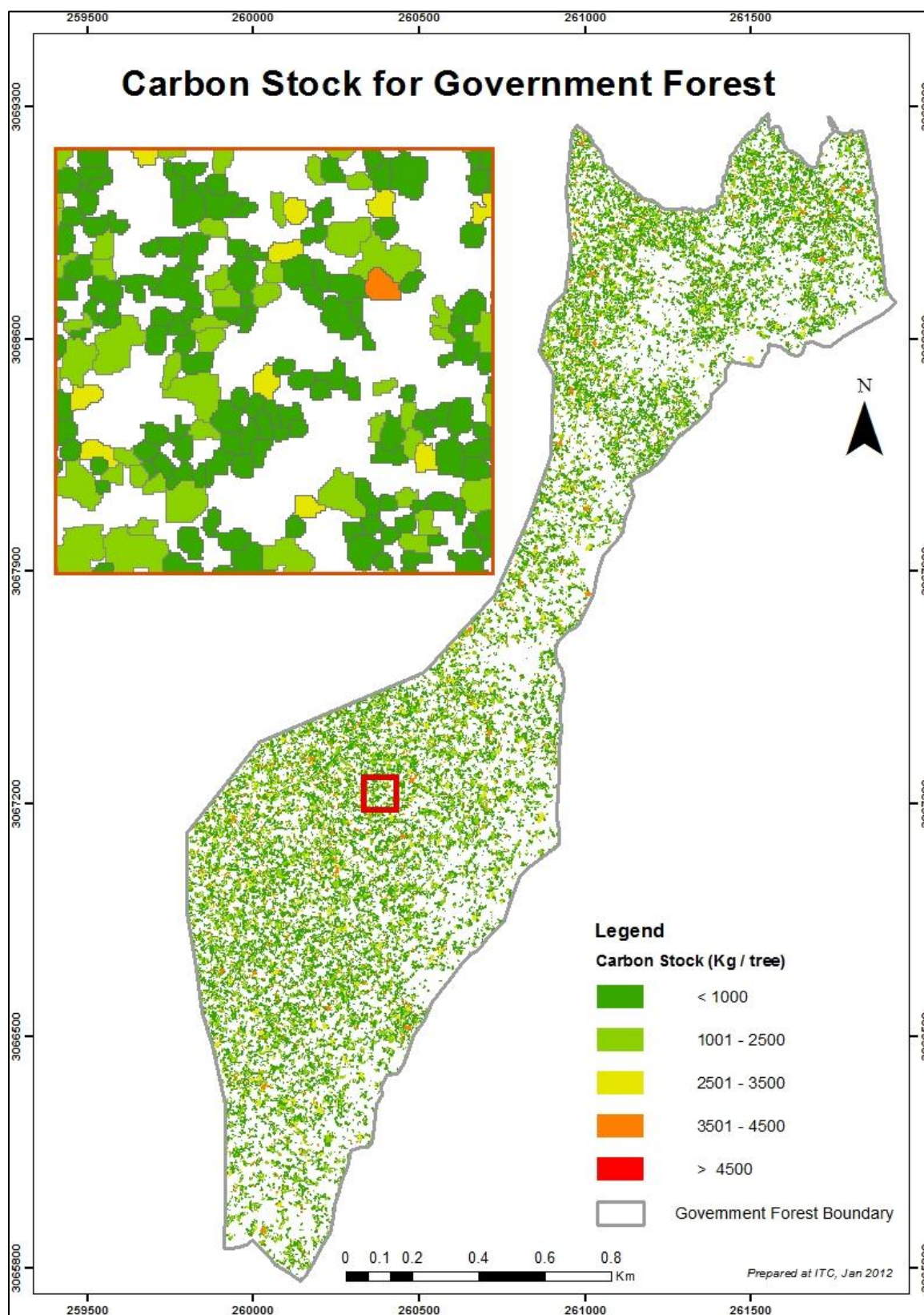


Figure 4-17: Carbon stock map for GMF forest

5. DISCUSSION

5.1. Forest Condition Assessment

5.1.1. Comparison of forest management activities in the two forest management types

In this study, AGB/carbon stock was estimated for two forest management types: government managed forest (GMF) and community forest (CF). AGB/carbon stock is directly impacted by the condition of the forest. These two forests have different management systems being implemented. This section compares the forest management activities undertaken in each of the sites.

Community Forests

The aim of CF in forest management and utilization is to achieve the following: 1) sustainable, active or intensive forest management that yields optimal production of forest products while conserving forest biodiversity, 2) feasible, economically viable business enterprises to market products and raise revenues at CFUGs and sub/interest group level and 3) re-investment of business revenues in other livelihood enhancing activities that meet the socio-economic priorities of all CFUG members equitably, especially the poor and socially excluded (Sapkota *et al.*, 2009).

Government forests

The aim of government in forest management is to achieve the following: 1) rehabilitate the degraded forests to restore flora and fauna, 2) coordination and cooperation with other sectors to evacuate illegal settlements, controlling encroachment and illegal trade of forest products and 3) management of habitat of endangered species of plant and wildlife. Table 5-1 is a summary of the activities that are carried out in the two forest management types.

Table 5-1: Summary of forest management activities in the two forest types

Activity	Community Forest	Government forest
1. Seedling production	x	x
2. Occasional planting of trees	x	x
3. Biodiversity conservation	x	
4. Regular silvicultural operations	x	x
5. Extraction of non-timber forest products	x	
6. Regeneration management	x	x
7. Timber harvesting	x	x
8. Encroachment management		x
9. Forest certification		x
10. IGA promotion		x

The activities marked with an (x) indicate that they are practiced in that particular forest type. Some activities only apply to one of the forests while others are carried out in both forests. From the table, activity 1,2,4,6 and 7 are practiced in both forests whereas 3 and 5 are only carried out in community

forests. These latter activities are guided by the objectives of community forest establishment in Nepal, which are conservation of biodiversity, REDD implementation programme and livelihood enhancement (World Bank, 2001; Sapkota *et al.*, 2009). Additionally, the improvement of the livelihoods of the people is directly related to activity number 5. For the government forest however, their general objective is income generation from timber harvesting and is concerned with income generating activities (IGA), forest certification and encroachment management. Activities 8, 9 and 10 are only practised in government forest where forest management objective is more oriented to market production. However, these are practised on a minimal scale in this government forest because it is within a watershed area (Kayerkhola), where large scale extraction of timber for market is restricted.

From the field observations, the implementation of these activities has not been very successful, especially in the government forest which has faced adverse deforestation over the years without any reforestation. This is evident from the stand density and basal area statistics reported in section 4.1 of this research. These activities therefore, are related to the differences in the condition of the two forest management regimes in the study as discussed below which eventually impact on the carbon stocks.

5.1.2. Site statistics

A statistical analysis of the field data was carried out for the two forest management types. From Figure 4-13, (boxplots) and Table 4-7 in section 4.6, average DBH and height was significantly higher both for *Shorea robusta* and other species in GMF than in the CF Figure 5-1. This was so because the GMF was an old forest with small number of trees which are remnants of the continuous logging while, the CF was a young regenerating forest with many small trees hence the small size of DBH and height. There are variations also amongst the species where *Shorea robusta* has both higher DBH and height on average than the other species in the two forest types (Figure 5-1).



Figure 5-1: Photographs showing sample trees from community (left) and government forest (right).

The species distribution in the sites was also varying. GMF had more than 22 species while CF had 17 species. *Shorea robusta* was dominating in both forests (Figure 4-11 and Figure 4-12). However, the proportion of *Shorea robusta* was significantly different in the two forests. In the CF, it constituted 64% of total trees species, while in the GMF, it constituted only 28% of the total tree species. GMF is highly degraded due to extraction of this particular species which is highly valued for its timber, hence the smaller numbers of *Shorea robusta* trees in the GMF. While in the CF, *Shorea robusta* and all other species are taken care of by the CFUG members because they manage the forest sustainably. Additionally, occasional replanting is hardly done in the GMF although it is proposed as one of the major activities in the management or operational plans. On the other hand, other species were fewer in CF 36% and higher in GMF (72%) because they are less valuable species in the timber market while climatic conditions also favour the growth of *Shorea robusta* hence its dominance. Therefore, commercial timber species were found dominating in CF, while the non-commercial timber species were dominating in the government forest.

Stand density

The mean stand density as well as the basal area was also calculated Table 4-1 section 4.1. The average stand density for the GMF was 120 trees/ha, while that of CF was 397 trees/ ha. This is because of the forest disturbance caused by anthropogenic influence on the GMF forest, majorly extracting *Shorea robusta* species for market and other trees for fuel wood. During the field visit, it was evident that the forest has been encroached due to the presence of small holder crop farms in the GMF. Unlike in the CF, there has been hardly any regeneration in the GMF due to the interference, hence over the years, the previously logged areas have been colonized by grasses and shrubs (Figure 5-1). The CF has a higher stand density and compact as seen on the canopy density model (Figure 4-1). It was formerly owned by the government, but was handed to the community in 1970 for management and utilization. Prior to the handing, these forests were deforested too, but due to the effort of the community members guided by the forest operational plans and the REDD implementation preparedness, the forest was left to regenerate and now it has assumed the structure of a natural forest with young trees as the majority. Generally, the GMF was characterized by patchy distribution of stems (Figure 5-1) while the CF had dense homogeneous distribution of tree stems hence the differences in stand density.

The estimates of stand density obtained in this study, are comparable to those of (Sagar and Singh, 2006) in a dry tropical forest in India which ranged from 35 to 419 trees/ha across the various sites sampled. However, the mean stand density in this study was much lower than that obtained by (Jha & Singh, 1990) of 315 to 559 trees/ha in Renukut and Obra forest sites in India.

Basal area

Basal area is a standard measure of tree size cross-sectional area near the base of the trunk (at breast height). It is a common unit of timber quantity or stocking within a landscape per land area, for example square meters per hectare (Fastie, 2010). The basal areas were derived from diameter at breast height (DBH). The basal area for GMF was 15 m²/ha while that of CF was 20 m²/ha (Table 4-1). Although the

basal areas are varying, they were not significantly different from each other. The basal area of individual trees from the two forest sites was also established (appendix 3). GMF trees had generally higher basal areas compared to trees from the CF because GMF trees were significantly large in terms of DBH (appendix 3). However, the overall basal area of the CF exceeded that of GMF because of the differences in stand density as shown in (Table 4-1 section 4.1.1).

Similar results of basal area have been found in other studies though different methods of estimation were used. Fastie, (2010) estimated stand basal area from forest panoramas for Bananza birch forest in Alaska and obtained basal areas of 29.96m²/ha from field measurements, 25.26m²/ha to 32.14m²/ha basal area was derived from image analysis and basal area estimated with the prism in the field ranged from 20.66 to 29.85m²/ha. The values of basal area obtained in this study were higher than those obtained from a similar dry tropical forest in India where the mean basal area was 13.78m²/ha (Sagar and Singh, 2006).

5.1.3. Canopy Density Modeling

In this research, canopy density models for the two forest sites were derived from LiDAR data as described in section 3.7.2 and results shown in section 4.1.1.

Canopy density model for government forest resulted in large areas with little or no vegetation (blue colour) as compared to the community forest as shown on the canopy density maps (Figure 4-1 and 4-2). This result is related to other statistical analysis such as the stand density and the basal areas estimated for the two forests. As discussed in section 5.1.2, government forest resulted in lower values of both mean stand density and basal area than the community forest which explains why the model indicates little or no vegetation. This difference in the two canopy models is also related to species distribution as discussed the same section above. Other species dominated in the GMF with over 72% occurrence and less of *Shorea robusta* while on the contrary, in the CF, *Shorea robusta* formed the majority of the trees with 64% occurrence. *Shorea robusta* was less in the government forest because it is highly valued species in the timber industry and often extracted by illegal loggers. Generally, the growth of *Shorea robusta* is better than other species in this region but unsustainable extraction of this species has led to degradation in the GMF. The difference in canopy density can also be attributed to leakage effects of REDD projects although it was not assessed in this study. Leakage refers to increase in greenhouse gas emissions outside of the project area but directly attributable to the REDD project activities implemented inside of the project area (ICIMOD, 2010). A distinction is made between primary leakage, when the emissions are directly attributable to the deforestation agents, and secondary leakage when the emissions are not directly attributable to the deforestation agents but rather to other actors through effects on prices and markets (Aukland *et al.*, 2003). This could have been the case in this study because community managed forests are REDD projects while government managed forest studied is not a REDD project but is adjacent to the REDD project area (CF).

The canopy density models developed were validated using the canopy density data obtained from the field. The agreement (correlation coefficient) between observed canopy density and estimated canopy density for GMF and CF was 89% ($r=0.89$) and 77% ($r=0.77$) respectively (Figure 4-3). The accuracy for CF was significantly lower than that of GMF.

Canopy density models have been applied in other studies for example for monitoring forest fragmentation in Indonesia in Mt. Simpang and Mt. Tilu Nature Reserves (Hadi *et al.*, 2004), assessing deforestation and degradation e.g. (Namaalwa *et al.*, 2006) in Uganda, monitoring changes in biomass stocks (DeFries *et al.*, 2006) and detecting the forest health (Hadi *et al.*, 2004).

The accuracies obtained in this study are similar to those in other researches. For example, (Huang *et al.*, 2001) estimated tree canopy density for three large areas in the USA (Virginia, Utah and Oregon) using Landsat 7 ETM+ and high resolution images. The study resulted in correlations (r) of 0.89, 0.85, 0.87 and 0.70 between the observed canopy density and the estimated canopy density which are similar to the results obtained in this research. Iverson *et al.*, (1989) also estimated forest cover density over large regions of Southern Illinois using Landsat Thematic Mapper (TM) and related them to Advanced Very High Resolution Radiometer (AVHRR) pixels for the same location and obtained a correlation coefficient ($r = 0.89$).

5.2. Canopy Height modeling and accuracy assessment

5.2.1. Canopy Height Modeling (CHM)

The LiDAR derived canopy height model (CHM) is shown for a part of the study area in Figure 4-5 section 4.2, where brightness is proportional to height. The brighter areas represent high height values while darker areas represent low height values. We can see individual tree crowns for most of the tall trees (top most part of the canopy) where interlocking of crowns is less than the lower parts of the canopy.

5.2.2. Validation of the CHM

The LiDAR derived canopy heights were validated using the tree height measurements from field data. The correlation coefficient (r) for community forest CHM was $r=0.88$ (Figure 4-6 section 4.2.1), while that for GMF forest was $r=0.90$. Despite the low density of LiDAR point clouds (0.8 points/m²), the mean error of height estimation was 2.4m for a height range of 7m to 36m; RMSE =12% (GMF forest) and 3.8m for a height range of 7m to 38m; RMSE = 19% (CF forest) Table 4-2 section 4.2.1. Notably also, the error was lower in GMF forest height estimation than CF forest. This is attributed to terrain and canopy density. The GMF site was relatively flat (0 to 15%) with fewer trees as discussed earlier in this chapter while the CF site was characterized by very steep slopes ranging from 25% to 95% and dense canopy structure. These issues reduce a bit the accuracy of canopy height measurements, since the visibility to treetop was obscured by other surrounding trees and introduced some errors.

These causes of such small reduction in the accuracy of height estimation have also been reported in other studies. For instance, according to Kraus *et al.*, (2004), terrain point density fundamentally influences the

DTM accuracy, therefore especially for the rough forest terrain, underestimation of the terrain heights appeared. Overestimation of the heights also occurs if trees lean towards the lower side of slopes as described by (Hirata, 2004). At higher altitudes, the probability that the trees are interlocked to each other increases, therefore, it is more difficult to extract single-tree heights (Hollaus *et al.*, 2006). Considering all these uncertainties, the derived correlations between the field-measured and the LiDAR derived canopy heights are considered reasonable and satisfactory.

The results obtained in this study are comparable to those of (Hollaus *et al.*, 2006) who estimated canopy heights for the Western Australian Alps using airborne laser scanning (ALS) data for summer and winter 0.9 and 2.7 points/m² average point density respectively. Their study resulted in coefficient of determination ($R^2=0.84$ to 0.87) between field-measured height and ALS canopy heights. While using the same accuracy measure for comparison purposes, the results obtained in this study, $R^2 = 0.78$ and 0.81 for CF and GMF respectively Figure 4-6 section 4.2.1, were slightly lower than those reported by Hollaus *et al.*, 2006 as already discussed, which was done in a pine and spruce forest. (Naesset, 1997a) also regressed Lidar derived canopy heights with ground reference stand heights and obtained a $R^2 = 0.91$. St-Onge (2000) used small-footprint LiDAR data acquired from an ALTM to study individual trees. A Laplacian of Gaussian (LoG), a combined spatial filter and edge detection operator was applied to a canopy height model to delineate individual tree crowns. A linear model was used to correlate the LiDAR heights with ground measurements which resulted in a ($R^2=0.90$). The accuracies realized in this study plus other studies as cited in this discussion, are evidence that tree heights can actually be extracted from LiDAR data just as accurately and close to ground measurements (Lim *et al.*, 2003) especially in areas of flat terrain coupled with moderately high density point clouds.

5.3. Image segmentation and accuracy Assessment

5.3.1. Delineation of tree crowns in eCognition

In this research, tree crown delineation was done using multi-resolution segmentation approach as described in section 3.7.1 and results shown in section 4.3.1

Several criteria have been used for quantitative evaluation of segmentation accuracy (Moller *et al.*, 2007; Radoux and Defourney, 2008; Zhang, 1996; Clinton *et al.*, 2010 and Zhan *et al.*, 2005). In this study, we adopted the methods presented by Zhan *et al.*, 2005 (1:1 matching) and Clinton *et al.*, 2010 (“D”value). Tree crown delineation for both forests resulted in accuracy of $D = 0.30$ or 70% accurate while it was 78% and 77% when using 1:1 correspondence with reference crowns for government and community forest respectively as displayed in Table 4-3 section 4.3.1. The delineation in government forest was slightly better than that of community forest. This is attributed to the canopy density where by government forest had most trees isolated from each other while the community forest was very dense with intermingled crowns Figure 5-1. This made it more difficult to explicitly segment crowns of individual trees more accurately. Examples of visually assessed well and poorly delineated crowns are shown in Figure 5-2 (a and b).

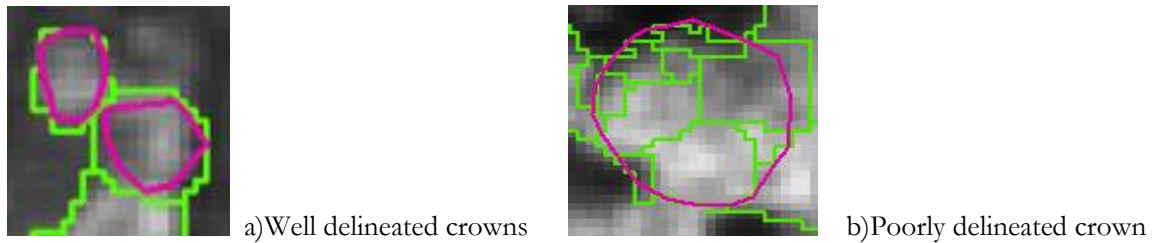


Figure 5-2: An example of well delineated crowns and poorly delineated crowns.

The purple represents the reference crown while the green represent the tree objects from Multi-resolution segmentation

Synergistic use of remotely sensed data has become the focus of present studies to maximize on the information extraction, reduce uncertainties and enhance the results in biomass estimation (Goetz *et al.*, 2009; Lu, 2006 and Koch, 2010). In this study, both Geoeye and airborne LiDAR data were loaded in eCognition and segmentation carried out basing on the two layers. From local maxima search, each of the segments is assigned a canopy height value. In this case, the highest canopy values were used for modelling biomass, unlike other studies that have utilized other canopy heights such as mean and percentiles of height or all the three categories of height. For instance, (Wulder & Seemann, 2003) utilised mean canopy height. During the segmentation process too, the tree heights were limited to a range of 5m to 40m as described in section 3.5.3. This ensured that small trees or shrubs as well as overly tall objects that are not likely to be trees are not included in the carbon stock mapping, because this could potentially introduce uncertainties in the final carbon estimate. Lefsky *et al.*, (1999a) segmented images and used canopy height ranges of 4m to 40m for deciduous forests of eastern Maryland, USA, using canopy height profiles made using the SLICER (Scanning LiDAR Imager of Canopies by Echo Recovery) instrument.

Multiresolution segmentation is a bottom -up region growing algorithm (Ke *et al.*, 2010) and the most widely used segmentation method (Baatz & Schape, 2000). It has been widely applied in other studies especially the image extraction from optical data. However, there are very few studies that have synergistically extracted image objects from multi-sensor data which is the case in this research. The segmentation accuracy results obtained in this study (78% and 77%) were much higher than those reported by Kim *et al.*, (2010). They estimated carbon storage of individual trees in Gwangneung forest of South Korea and obtained segmentation accuracy of 32% and 63% from fusion of Lidar data of 5 to 10 points/m² and aerial photographs (3bands and 0.25 m spatial resolution).

5.4. Object based Image classification and accuracy assessment

Delineated tree crowns were further used for species classification as described in section 3.8.1 and results shown in section 4.4.

An object-oriented image classification approach was applied using Definiens eCognition software. Image objects generated from segmentation were classified into two classes: *Shorea robusta* and other species. Other species included all other trees that were not *Shorea robusta*. The overall classification accuracy was

70% and 82%, for CF and GMF forest respectively (Table 4-4 and Table 4-5 section 4.4). Figure 4-10 and Figure 4-9, show the species classification maps for CF and GMF forests respectively.

The accuracy of GMF forest was higher than that of CF forest because it was a more open forest hence tree discrimination was much easier than in the dense canopy forest (CF). The accuracy of *Shorea robusta* species was higher (79%) in CF forest compared to that of GMF forest (78%), while on the other hand, the accuracy of other species was higher in GMF forest (82%) than in CF forest (54%). This can be attributed to species dominance. *Shorea robusta* formed the majority of trees in CF forest (64%) while other species formed the majority of trees in the GMF forest (72%). The reason for low user and producers' accuracy for *Shorea robusta* in GMF forest is because of the small sample size for training and validation (12 and 9) in comparison with the same class in the community forest (45 and 43). The lower accuracies for class "other" in the community forest too, are attributed to the fact that, different species with variation in spectral characteristics had to be grouped together to form a single class "other", which introduced confusion in the spectral response.

Tree species classification has been carried out by other researchers. For example, a study by (Persson *et al.*, no date) classified Scots pine, Norway spruce and deciduous trees in Sweden using high resolution Laser data (7 points/m²) and high resolution NIR digital images (0.1m resolution). They reported tree species classification accuracy of 90%. These results are not comparable to the output of our study because of the differences in point density and the digital image resolution. Their results are better and more accurate than our results. Consequently, we can say that the higher number of airborne LiDAR point cloud per square meter, the higher the classification accuracy. Also, the higher the spatial resolution of the classified image, the better the classification accuracy. Leckie *et al.*, (2003) classified seven species in a coniferous forest in Nahmint River of Port Alberni, British Columbia using a 8 band multispectral image acquired using a hyper-spectral CASI sensor. They reported an average species classification accuracy of 92.8%. A study by Brandtberg (2007), in West Virginia, USA, used airborne LiDAR data to classify individual tree species under leaf-off and leaf-on conditions and obtained an overall classification accuracy of 64%. The species classified were oaks, red maple and yellow poplar. Ke *et al.* (2010) also synergistically used QuickBird multispectral imagery (2.4m) and LiDAR data (0.16 points/m²) for tree species classification in Heiberg Memorial Forest and State Forest lands in central New York State. The overall accuracy reported was 91.6%. Considering their lower point density and lower multispectral image resolution than the data used in this study, their results are by far much better than what was obtained in our study, which utilized multispectral imagery of 0.5m and LiDAR data of 0.8 points/m². However, considering the species composition, the results are not comparable because their site had a mixture of confers and deciduous trees. Generally, coniferous trees are much easier to isolate than broadleaved trees as was the case in our study.

Some of the possible causes of lower accuracy in tree species classification especially those based solely on spectral metrics, have been reported in other studies. For instance, Ke *et al.*, (2010), used QuickBird multispectral image (2.4m) at a scale parameter of 20 and obtained an accuracy of 53% and 61% at a scale

parameter of 50. These low accuracies were attributed to large local spectral variation caused by crown textures, gaps and shadows.

5.5. Modeling Height, CPA and Carbon stock

5.5.1. Model development and validation

The relationship between height, CPA and AGB was established as described in section 3.10 and results are shown in section 4.6.

Nonlinear regression models (Interactive) were found to be best explaining this relationship, after testing with both linear and other types of non-linear regression models. These interactive models were found to have less error (RMSE) in prediction and resulted in a higher coefficient of determination (R^2) with all the dataset than the other models. The same model choice criterion was used by Frazer *et al.*, (2011). Most importantly also, the choice of non-linear model was influenced by considering the field process in the area of study. The distribution of data in scatter plots displayed in appendix 5, show for instance, that the relationship between tree parameter height and biomass is non-linear. This is because the site is a young regenerating forest where a tree at young stage would rapidly increase in height at a faster rate than increase in the biomass/carbon while at a median height, the rate of biomass accumulation tended to increase significantly or more rapidly.

Both CPA and height (predictor or independent variables) were considered for explaining the variations in AGB/carbon stock (response or dependent variable). Different tree species were modelled separately according to classification (*Shorea robusta* (Sal) and others). These models are shown in section 4.5.1. All models were validated using 30% of sampled data and resulted in RMSE displayed in table 4-16 in section 4.6.1. *Shorea robusta* (Sal) resulted in coefficient of determination ($R^2=0.81$) and ($R^2=0.69$) for CF and GMF forests respectively, while other species resulted in ($R^2=0.62$ and 0.73) for both sites respectively. Figure 4-14 and Figure 4-15 section 4.6.1). This means that height and CPA explained 81% and 69% of variance in AGB /Carbon stock for *Shorea robusta* in CF and GMF forests respectively.

The model with least error was that for *Shorea robusta* in (CF forest) with RMSE = 10% the model with highest error RMSE = 25% was *Shorea robusta* in GMF forest. Validation of *Shorea robusta* from GMF forest had highest error, which can be attributed to the small sample size (10) used for validation (Table 4-16). This happened because GMF samples had few trees of *Shorea robusta* species. The reasons behind these small numbers of *Shorea robusta* were earlier discussed in section 5.1.2. Generally, modelling of other species resulted in lower coefficient of determination than that of *Shorea robusta*. This is due to the aggregation of many species with variations into class 'other' of different spectral reflectance, different crown shape and different allometry, which cannot be explained by a single model, while *Shorea robusta* has homogenous characteristics.

Studies about the relationship between CPA, height and carbon stock or biomass of tree species, studied in this research have rarely been done. Nevertheless, Song *et al.*, (2010) used crown diameter from

QuickBird and IKONOS image with up to 18° of off-nadir view angle to predict DBH estimates and obtained $R^2 = 0.5$ to 0.6 for all species. In their study, DBH was taken as a surrogate of biomass as highlighted by Zhao *et al.*, (2008). Their results were lower than those obtained in this study. Similar to the case in our study, other studies have obtained good relationship with CPA and height. For example, Bartelink, (1996) studied the allometric relationships among stem, crown dimensions, leaf area, height with biomass using linear and non-linear models for beech forest in the Netherlands. The study reported a $R^2 = 0.924$ for CPA and biomass which improved to $R^2 = 0.982$ when height was included. Kuuluvainen (1989), also modelled the relationship between CPA and above ground biomass of various tree classes of Norwegian spruce in Switzerland and obtained (R^2 range of 0.22 to 0.79). Zhao *et al.*, 2008 modelled carbon stock using LiDAR derived heights and obtained R^2 range of 0.80 to 0.95 for pine plantation in eastern Texas, USA. These results are higher than the output from the models developed in our study (except for CF *Shorea robusta* $R^2 = 0.81$) although our research was done in a tropical hardwood forest. Drake *et al* (2002) carried out a study in a dense, neo-tropical forest and reported height and estimated biomass relationship range ($R^2 = 0.88$ to 0.94) which are comparable to the results obtained in this study.

5.5.2. Biomass and carbon stock estimation

The carbon stock estimated for the study areas in this research was approximately 244 t C/ha and 140 t C/ha for CF and GMF forests respectively. These results are lower than those reported by ICIMOD, 2010 that the mean carbon stocks were approximately 288 t C/ha for the same CF forest who estimated carbon using allometric equations on forest inventory data for 91 plots in the same community forest. A study by Tianxiang *et al.*, (1998) on estimation of total biomass in 115 counties Qinghai and Tibet provinces of China, reported maximum biomass of 196539 t C/ha for Motuo county and a range of 115 t C/ha to 140 t C/ha for other north west Tibetan Plateau regions. The results of the GMF site in our study can be compared to the results of most of these counties. However, our results are lower than those of the global terrestrial vegetation (782 t C/ha) (Tianxiang *et al.*, 1998).

5.5.3. Carbon stock comparison for the two forest types

One of the objectives of this study was to investigate if there is a difference in carbon stock between the two forest types under different management regimes. The results of a t-test on the carbon stock from the two sites have indeed shown that there is a significant difference in carbon stock as shown in Table 4-17 section 4.7. Some of the reasons for this difference include differences in stand density and basal area for the two areas as discussed earlier in this chapter. Despite the higher DBH values of trees in the government forest, the overall biomass of GMF is much lower than that of CF. To a large extent, this is influenced by basal area and stand density as revealed in the output of this research.

5.5.4. Relationship between forest management and AGB /carbon stock

Generally, from the management activities as discussed in section 5.1.1, there is considerable overlap in the activities from the forest management practices in the two forest types. The key parameters as revealed

in this study that explain the differences in carbon stock are canopy density which is a function of tree density and basal area. These are directly influenced by harvesting rates and replacement of trees in a forest. One of the highlighted activities of the government forest is to control encroachment and illegal trade of forest products. Most of GMF forests in Nepal are established for timber production and most of them are situated in the Terai region. However, there exist other GMF forests in other areas that serve other functions such as biodiversity conservation or watershed protection as deemed important by the Ministry of Forests. The GMF forest under this study is located in a watershed area and the priority is catchment protection. For this reason, extraction of wood is restricted. However, the site favours the growth of *Shorea robusta* species which is on high demand in the timber market. This has attracted the adjacent communities over the years to encroach in the forest and selectively extract this species while leaving behind other less valuable species, which has resulted in few numbers of *Shorea robusta* as compared to other species in the area as discussed in section 5.1.2. This was evident during the fieldwork due to presence of old and fresh tree cuts on a patchy pattern as well as the small holder farms and grazing activities in the site. The government has put measures to control this encroachment by fencing the site and digging trenches to prevent illegal entry by loggers as shown by primary data from the area (Figure 5-3 a and b). The extent of the success of these measures remains a subject for further research. From the findings of this study, we can conclude that indeed, forest management practices influence significantly the carbon stocks in the two forest management types. However, care should be taken when making generalizations based on these findings because not all government managed forests in Nepal are poorly managed and, on the other hand, not all community forests are well managed.

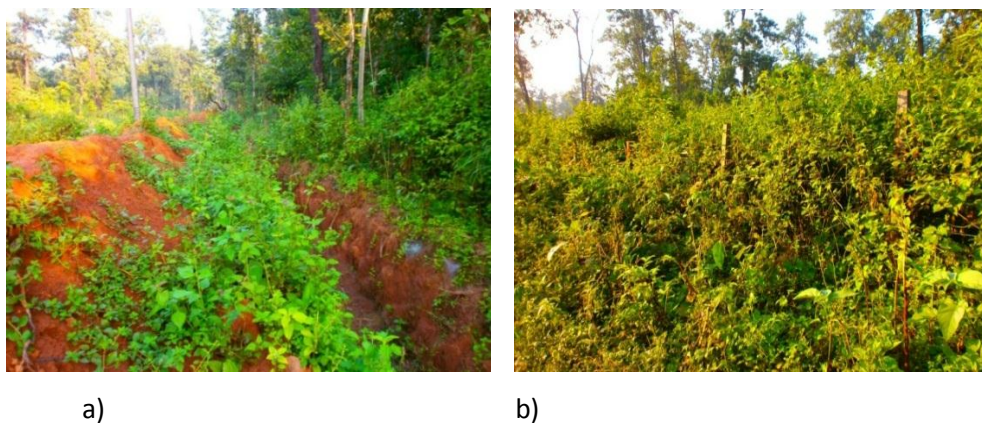


Figure 5-3: Photographs of trenches and fence in the Government forest

5.6. Sources of error in biomass estimation

5.6.1. Data characteristics

Image / data acquisition dates

Data integration was employed in this study. Both Geoeye satellite images and airborne LiDAR data were used. Geoeye was acquired on November 2009 while LiDAR data was acquired in March 2011. Fieldwork was carried out in September/October 2011. The analysis in this study was done with the assumption that all data was acquired on the same date or rather no significance changes have taken place within the time gaps. Considering that the geospatial space is dynamic, this can introduce errors in the estimation. For example, Song *et al.* (2010) noted that a tree crown during the field work may be slightly bigger than in the images because of the growth season in between, which was not an exception in this study.

Ortho-rectification and co-registration

For successful extraction of information from various datasets, image co-registration is a very key and essential process to obtain accurate information. In most cases, the co-registration process is accompanied by errors especially those influenced by terrain and topographic effects in the study area. In this study, Geoeye image acquired in 2009, was orthorectified based on Orthophoto image taken in March 2011. Although the RMSE was low, there were still slight mismatches of the Geoeye dataset with LiDAR data. This can introduce errors especially in the identification of smaller objects (trees). The field data collected was also affected by GPS error. The accuracy of GPS used in the field was on average 4m to 8m depending on the canopy density. Therefore, the actual location of the trees as marked on the ground and as appearing on the image was a challenge. Co-registration error is a common problem as reported by Frazer *et al.*, (2011) who simulated the impact of co-registration error and its interaction with plot size in estimation of LiDAR canopy height and density metrics in a young temperate coniferous coastal forest of western North America. The study found out that co-registration error (spatial overlap) between ground-reference and LiDAR samples negatively impacted the estimation of LiDAR metrics, regression model fit and the prediction accuracy of TAGB. The study also reported that larger plots maintained a higher degree of spatial overlap between ground-reference and LiDAR datasets for any given GPS error and that they are more resilient to the ill effects of co-registration error compared to small plots.

Shadow effect

The presence of shadow in the image often obscures the pattern of the trees which negatively affected the identification of tree tops as they sometimes confuse with branches especially in the dense tropical forest. In satellite images, shadows are considered a nuisance obscuring important object space detail. If the solar elevation is low at the time of image acquisition, then the presence of shadows will be unavoidable. The principal problem caused by shadows is either a reduction or total loss of information in an image (Dare, 2005). Reduction of information can potentially lead to corruption of biophysical parameters derived from pixel values, such as vegetation indices (Leblon *et al.*, 1996). Total loss of information means that areas of the image cannot be interpreted (Dare, 2005). In a study by Gonzalez (2010), shadows were cast up to 25m long, which hindered the ability of the automated crown detection algorithm not only to accurately locate tree tops, but also to locate trees with relatively smaller crowns. Based on how the tree crown appears on satellite images with different sun elevation and view angle, researchers have developed the template matching algorithm for detecting tree crowns (Olofsson, 2002; Pollock & Woodham, 1996)

(Figure 5-4). Template matching is an image processing technique where a library of 3-D model trees is cross-related against any potential tree position in the digital image.

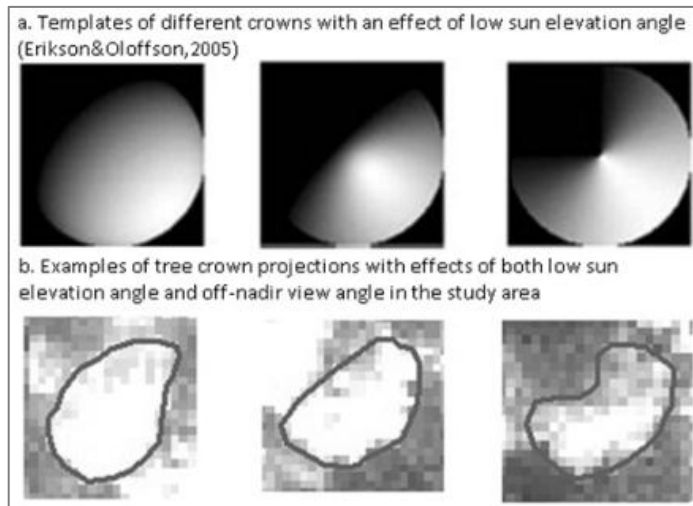


Figure 5-4: Examples of irregularly shaped crowns and templates

The Geoeye used in our study has shadows but most of them were masked out during segmentation. The problem of shadow and tree identification in this study was overcome by integration of LiDAR data in segmentation. In the case of using optical data alone for segmentation, only brightness is used to delineate the trees, while the use of LiDAR data provides additional criteria like height value. This ensures that trees in shadow areas are delineated

5.6.2. Processing and analysis

Image processing can also potentially introduce errors in biomass estimation. The major stages in image segmentation in this study were canopy height modelling, segmentation, classification and modelling of AGB or carbon stock. The possible errors at each of these stages are discussed below.

CHM modelling

The current focus of LiDAR application in forestry is the derivation of canopy height (Lim *et al.*, 2003). It has been however suspected that the laser response to a forest canopy is not solely a function of tree height, but also a function of canopy closure and density (Nelson *et al.*, 1984; Aldred and Bonner, 1985). The significance of this hypothesis is that if canopy closure and density significantly influence laser response, then inaccurate canopy profiles may be derived from LiDAR data resulting in poor estimates of forest attributes (Lim *et al.*, 2003). This phenomenon was verified by Nelson *et al.*, (1984) who found out that forest canopy profiles varied across an area exhibiting a gradient of canopy closures caused by gypsy moth damage using Airborne Oceanographic Laser (AOL). Effect of topography also plays an important role in LiDAR data acquisition. For very heterogeneous terrain, (Nelson, 1997) demonstrates that spherical crown shapes in closed canopy situations lead to increased canopy height. This explains why in this study, the error of estimating height in the CF forest was much higher than the GMF forest (3.8m against 2.6m). Furthermore, the CF forest was characterized by very steep terrain (25% to 95%) slope

unlike the government forest which was relatively flat (0 to 15%) slope. Some of the reasons for such differences in Lidar derived height verses field observed height are explained below.

To some extent, the differences between LIDAR derived height and field height found in this study should be expected. The effects of modeling stem heights and crown dimensions as well as the assumptions that the crowns are cylindrical or circular are simplifications. Drake *et al.*, (2002) points out that in reality, crowns are highly irregular in shape and crown materials are often clumped. These certainly contribute to differences between field and LiDAR derived profiles (Drake *et al.*, 2002). In addition, the LiDAR signal is affected by the decreasing total amount of energy as the LiDAR pulse travels lower into the canopy. An example of this situation is illustrated in a study by Drake *et al.* (2002).

Segmentation and classification

Image segmentation was a major and crucial process in this study. The scale parameter usually determines the size of the objects generated (Benz *et al.*, 2004). In addition to scale parameter, object size and shape are also influenced by characteristics of layers used during segmentation. In this study, large crowns representing big trees particularly *Shorea robusta* in both forests were over-segmented. This conclusion is based on visual assessment of the automatically delineated crowns in comparison to the manually delineated crowns. Also the “D” value measures for over-segmentation were much higher than under-segmentation. Figure 5-2 b, gives a visual impression of the over-segmentation problem which resulted in multiple segments overlapping with a single reference object. Chen *et al.*, 2007 illustrated three possible cases that tree crowns are mis-segmented which include: (a) 1-to-m (over-segmentation), (b) n-to-1 (under-segmentation), and (c) n-to-m as seen in Figure 5-5.

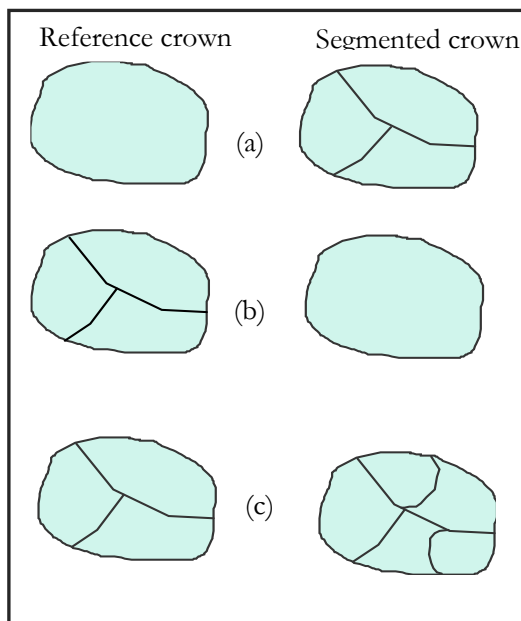


Figure 5-5: Three possible cases that tree crowns are mis-segmented.

The same problem was also reported in a study by Ke *et al.*, (2010) who segmented image objects based on LiDAR data and QuickBird image at scale parameter range of 20 to 800. In their study, they also obtained

multiple objects (e.g. Figure 5-2b) at the smallest scale (20) which compares to the scale of 18 that was used in this study.

In this study, species classification was undertaken with acceptable accuracy. However, this does not rule out the possibility of error in the process. Generally, a good segmentation output leads to a good classification of the objects (Ke *et al.*, 2010), while poor matches between segmented and reference objects produce lower classification accuracies. Some of the causes of the lower accuracy especially in the CF forest can be attributed to large local spectral variation caused by crown texture, gaps and shadows.

Modelling of carbon stock - Allometric equations, wood specific gravity and plot size

The most common methods to determine aboveground biomass (AGB) of forests include the combination of forest inventories with allometric tree biomass regression models and airborne or satellite-based remote sensing techniques (Houghton *et al.*, 2001; Brown, 2002 and Houghton, 2005). Recent remote sensing techniques such as LiDAR enable increasingly detailed assessment of spatial variation in AGB over large spatial scales, but ultimately their accuracy depends on calibration with field data (Lefsky *et al.*, 2002; Asner *et al.*, 2010). Thus, allometric models are a crucial link in the estimation of forest AGB stocks (Asner *et al.*, 2010).

Allometric equations are normally classified into two types; species specific and general equations which can further be split into site specific models. Owing to lack of species-wise allometric equations for most regions, multispecies allometric regression models are commonly used for the estimation of tree AGB. These are a major source of uncertainty in the estimation of plot and landscape level carbon stocks (Breugel *et al.*, 2011). In this study, generalized allometric equations were used that also incorporated wood specific gravity. According to Breugel *et al.*, (2011), the use general allometric equation in biomass estimation is biased due to the fact that they are made by aggregating many species in multispecies allometric models. For this reason, they might have introduced errors in this study although the amount of this specific error has not been assessed in the present study.

Besides choosing an appropriate allometric model, Clark and Clark (2000); Chave *et al.*, (2004) have proposed the use of simple plots of >0.25 ha for carbon stock estimates. They highlight that, many small plots rather than a few large plots best reflect the spatial variability of AGB stocks and may reduce the uncertainty in the estimation at landscape-level (Sierra *et al.*, 2007; Kauffman *et al.*, 2009). The inclusion of wood specific gravity in the allometric equations reduces the error in carbon estimation (Chave *et al.*, 2004). In this study, the sample size for fitting and validating the models for *Shorea robusta* was below the required minimum of n=30 (Table 4-12 and Table 4-16), which could have an effect on the accuracy of AGB estimates, as was concluded by Breugel *et al.*, (2011).

Other errors

Field measurement

Apart from the images used in this study, other primary plots and tree measurements data collected from the field were also used. The location of individual trees and sample plot centres were recorded using a GPS which introduced some positional error. Field height measurements were coupled with error from the Laser Range Finder or the Haga Altimeter as well as inaccuracies arising from dense canopy that obscured the view of tree tops for the targeted trees.

Missing data (Airborne LiDAR points)

The LiDAR data used in this study was of low point density although it was adequate for the intended purpose. This dataset however had gaps (no data) which hindered the extraction of information on those locations. Moreover, despite the fact that certain areas that were visible enough were masked out as described and illustrated earlier in Figure 3-2 section 3.4.4, some of the gaps were still present and that affected the derivation of the CHM more accurately from this data.

5.7. Magnitude of errors

Various studies have reported that biomass estimations are coupled with uncertainties (Chave *et al.*, 2004, Breugel *et al.*, 2011 and Gonzalez *et al.*, 2010). This has necessitated the search for more robust methods for biomass estimation in current researches. Despite this scenario, the process still is vulnerable to error which was not an exception in our study. This section revisits the aforementioned errors and the level at which they influenced the accuracy of the final biomass output (Table 5-2).

Sources of errors	Canopy Height Modeling	Tree crown delineation	Object based classification	Modeling Height, CPA, Biomass
Ortho-rectification		*	*	
Shadow effect		*		*
Acquisition dates		*	*	
Data gaps	*	*	*	*
Over-segmentation				*
Low point density	*	*		
Allometric equations				*
Field measurement			*	*
Interlocking of trees		*	*	*

Table 5-2: Source of errors and their influence on different steps in this research

The quantification of the exact magnitude of these errors is beyond the scope of this study. However, from the result and discussion sections, it is worth noting that, some errors such as over-segmentation in the tree crown delineation were more influential particularly in the modelling of biomass. Nevertheless, considering all the uncertainties in this research, the results can be considered satisfactory.

5.8. Strengths and Limitations of this study

Strengths

- Integration of LiDAR data reduced the effect relief displacement and shadow effects which are common in high resolution multispectral imagery based-segmentations, hence resulting in higher segmentation and classification accuracies unlike in previous studies that have utilized optical data alone.
- Shadow problems such as elongated or very large crowns or errors were minimized in the segmentation process by including the CHM.
- Wood specific gravities for trees in the study area were included in the allometric equation used. This reduced the errors by improving the fit of height, CPA and AGB regression models (Chave *et al.*, 2004).

Limitations

- Due to data integration from various sources, inadequate ortho-rectification may have caused mismatches in the two layers hence bringing a confusion in the type of information (spectral and canopy attribute) extracted for individual trees from the two images.
- The estimation of scale parameter in eCognition software that was used is a trial and error process. This is a limitation in this study which could have greatly influenced the segmentation output that particularly affected the large trees in the study area.

6. CONCLUSIONS AND RECOMMENDATIONS

6.1. Conclusions

In this research, we evaluated the synergistic use of VHR Geoeye satellite images and airborne LiDAR data for AGB/carbon stock estimation and comparison for two forest management regimes, as a case study in tropical forest area of Chitwan, Nepal. With regards to the results obtained, the following conclusions were made on the research objectives and questions formulated for this study.

Question 1. What is the accuracy of biomass estimation for the two forests management types?

AGB/carbon in this study was estimated using interactive regression models, specifically one for *Shorea robusta* and one for other species for each of the forests. The accuracy of estimation for community forest (CF) was $R^2=0.81$ with RMSE = 10%, for *Shorea robusta* and $R^2=0.62$ with RMSE=13% for other species. The accuracy for the government managed forest (GMF) was $R^2=0.69$ with RMSE=25% for *Shorea robusta* and $R^2=0.73$ with RMSE=13% for other species. This means that the prediction accuracy for *Shorea robusta* in CF (90%), was much better than that for the same species in GMF (75%). On the other hand, the prediction accuracy for other species in both forests was the same (87%).

Question 2. What is the above ground Biomass/carbon stock in the two forests?

The average carbon stock for CF was approximately 244 t C/ha while that for GMF was approximately 140 t C/ha.

Question 3. Is there a significant difference in Biomass/carbon stock from the two forests?

Yes. The results of the average carbon stock and t-test revealed that there is a significant difference in carbon stocks from the two forest management types.

Question 4. Is there a relationship between the management practices and above ground biomass /carbon?

AGB/carbon stock is a function of stand density, basal area, species composition and canopy density among other factors that have not been dealt with in this study. These are influenced by the forest management practices. The results of this study show that there are significant differences in these variables from the two forests, which in turn lead to the difference in their respective average carbon stocks. Therefore, I conclude that there is a strong relationship between forest management practices and AGB/carbon stock.

Question 6. Is there evidence of deforestation in the two forest management types?

Although much focus was not given in assessing deforestation in this study, from the primary data, basically observation during fieldwork as well as site statistics analysis (stand density, canopy density models), I conclude that there is some level of deforestation in the GMF.

Question 7. What is the stand density in each management unit? Is there a significant difference in tree density between the two units?

The tree density for CF was 397 trees/ha while that for GMF was 120 trees/ha. I therefore conclude that there is a significant difference in stand density from the two forest types.

6.2. Recommendations

This research has shown that data integration improves carbon stock estimation. However, in order to optimize the information from multi-data or multiple sensors, effective matching or co-registration is indispensable.

Despite the low density airborne LiDAR data used in this study, the results were satisfactory hence, the methods used are transferable to other areas. However, for more accurate estimation, I recommend the use of higher point density LiDAR data than what was used in this study.

Modelling of AGB from CPA and LiDAR-derived canopy height for *Shorea robusta* for GMF was relatively poor (RMSE=25%) compared to the same species model in CF (RMSE=10%). This was attributed to the small sample size both for model calibration and validation. I therefore, recommend the use of sufficient observations for carbon modelling at species / tree level.

Leakage analysis and monitoring after implementation of REDD projects

Despite the fact that REDD projects advocate for reduction of emissions from deforestation and forest degradation, conservation of a forest for REDD may significantly reduce the forest resource that was available to its dependants. If the source for needed resource is not substituted, it can potentially cause deforestation in other areas outside the REDD project. I therefore recommend that this type of assessment be carried out.

REFERENCES

- Acharya, K. P. (2002). Twenty-four years of community forestry in Nepal. *International Forestry Review*, 4(2), 149-156.
- Ahmad, R., & Singh, R. P. (2002). Comparison of various data fusion for surface features extraction using IRS PAN and LISS-III data. In R. K. Gupta, R. P. Singh & Y. Menard (Eds.), *Land Surface Characterization and Remote Sensing of Ocean Processes* (Vol. 29, pp. 73-78).
- Aldred, A., & Bonner, M. (1985). *Application of airborne lasers to forest surveys*. Canadian Forestry Service. Petawawa National Forestry Centre, Information Report
- Ali, S. S., Dare, P., & Jones, S. D. (2008). Fusion of Remotely Sensed Multispectral Imagery and LiDAR Data for Forest Structure Assessment at the Tree Level. *The International Archives of the Photogrammetry, Remote Sensing and Spatial Information Sciences.*, XXXVII.
- Amolins, K., Zhang, Y., & Dare, P. (2007). Wavelet based image fusion techniques - An introduction, review and comparison. *Isprs Journal of Photogrammetry and Remote Sensing*, 62(4), 249-263.
- Amro, I., & Mateos, J. (2010). Multispectral image pansharpening based on the contourlet transform. In B. Javidi, A. MohammadDjafari & T. Fournel (Eds.), *2009 International Workshop on Information Optics* (Vol. 206).
- Anderson, G. L., Hanson, J. D., & Haas, R. H. (1993). Evaluating Landsat Thematic Mapper derived vegetation indices for estimating above-ground biomass on semiarid rangelands. *Remote Sensing of Environment*, 45, 165-175.
- ANSAB. (2010). *Forest Carbon Stock Measurement* (1st ed.). Kathmandu, Nepal: ANSAB, FECOFUN, ICIMOD.
- Arbonaut. (2011). *Monitoring Change in Carbon stocks and Achieving REDD+ Targets*. Helsinki, Finland. Retrieved from www.arbonaut.com
- Asner, G. P. (2001). Cloud cover in Landsat observations of the Brazilian Amazon. *International Journal of Remote Sensing* .(22), 3855-3862.
- Aukland, L., Coasta, PM., Brown, S (2003). A Conceptual framework and its application for addressing leakage; the case of avoided deforestation. *Climate Policy* 3, 123-136
- Baatz, M., & Schape, A. (2000). Multiresolution Segmentation - an optimization approach for high quality multi-scale image segmentaion. In J. Strobl, T. Blaschke & G. G (Eds.), (pp. 12-23). Wichmann, Heidelberg, Germany.: Angewandte Geographic Informationsverarbeitung XII.
- Baccini, A., Friedl, M. A., Woodcock, C. E., & Warbington, R. (2004). Forest biomass estimation over regional scales using multisource data. *Geophys. Research*, 31.
- Baishya, R., & Barik, S. K. (2011). Estimation of tree biomass, carbon pool and net primary production of an old-growth Pinus kesiya Royle ex. Gordon forest in north-eastern India. *Annals of Forest Science*, 68(4), 727-736.
- Bartelink, H. H. (1996). Allometric relationships for biomass and leaf area of beech (*Fagus sylvatica* L).
- Benz, U., Hofmann, P., Willhauck, G., Lingenfelder, I., & Heynen, M. (2004). Multiresolution, object-oriented fuzzy analysis of remote sensing data for GIS-ready information. *ISPRS Journal of photogrammetry and Remote Sensing*, 58, 239-258.
- Blaschke, T. (2010). Object based image analysis for remote sensing. *ISPRS Journal of Photogrammetry and Remote Sensing*, 65(1), 2-16.
- Bombelli, A., Henry, M., Castaldi, S., Adu-Bredu, S., Arneth, A., Grandcourt, A.Valentini, R. (2009). An outlook on the Sub-Saharan Africa carbon balance. *Biogeosciences*, 6, 2193–2205.
- Brantberg, T. (2007). Classifying individual tree species under leaf-off and leaf-on conditions using airborne LiDAR. *ISPRS Journal of Photogrammetry and Remote Sensing*, 61(3), 290-303.
- Bravo, F., Bravo-Oviedo, A., & Diaz-Balteiro, L. (2008). Carbon sequestration in Spanish Mediterranean forests under two management alternatives: a modeling approach. *European Journal of Forest Research*, 127(3), 225-234.
- Breugel, M., Johannes, R., Dylan, C., Frans, B., & Jefferson, S. H. (2011). Estimating carbon stock in secondary forests: Decisions and uncertainties associated with allometric biomass models. *Forest Ecology and Management*, 262(8), 1648-1657.
- Brown, S. (1997). Estimating biomass and biomass change of tropical forests. *a primer*.
- Brown, S. (2002). Measuring carbon in forests: current status and future challenges. *Environmental Pollution*, 116(3), 363-372.

- Brown, S., Gillespie, A. R., & Lugo, A. E. (1989). Biomass estimation methods for tropical forests with application to forest inventory data. *Forest Science*, 35, 881-902.
- Chave, J., Andalo, C., Brown, S., Cairns, M. A., Chambers, J. Q., Eamus, D., Yamakur, T. (2005). Tree allometry and improved estimation of carbon stocks and balance in tropical forest. *Ecosystem Ecology*, 145, 87-99.
- Chave, J., Condit, R., Aguilar, S., Hernandez, A., Lao, S., & Perez, R. (2004). Error propagation and scaling for tropical forest biomass estimates. *Philosophical Transactions of the Royal Society of London Series B-Biological Sciences*, 359(1443), 409-420. doi: 10.1098/rstb.2003.1425
- Chen, Q., Gong, P., Baldocchi, D., & Tian, Y. Q. (2007). Estimating Basal Area and Stem Volume for Individual Trees from LiDAR Data. *Photogrammetric Engineering and Remote Sensing*, 73(12), 1355-1365.
- Clark, D. B., & Clark, D. A. (2000). Landscape-scale variation in forest structure and biomass in a tropical rain forest. *Forest Ecology and Management*, 137, 185-198.
- Clinton, N., Holt, A., Scarborough, J., Yan, L., & Gong, P. (2010). Accuracy Assessment Measures for Object-based Image Segmentation Goodness. *Photogrammetric Engineering and Remote Sensing*, 76(3), 289-299.
- Dare, P. M. (2005). Shadow Analysis in High-Resolution Satellite Imagery of Urban Areas. *Photogrammetric Engineering and Remote Sensing*, 71(2), 169-177.
- Davis, S. C., Hessler, A. E., Scott, C. J., Adams, M. B., & Thomas, R. B. (2009). Forest carbon sequestration changes in response to timber harvest. *Forest Ecology and Management*, 258(9), 2101-2109. doi: 10.1016/j.foreco.2009.08.009
- Definiens. (2011). User Guide. Germany: Trimble Germany GmbH, Trappentreustr. 1, D-80339 Munchen, Germany.
- DeFries, R., Archard, F., Brown, S., Herold, M., Murdiyarso, D., Schlamadinger, B., & deSouza, C. (2007). Earth observation for estimating greenhouse gas emissions from deforestation in developing countries. *Environmental Science & Policy*, 10, 385-394.
- Dixon, R. K., Brown, S., Houghton, R. A., Solomon, A. M., Trexler, M. C., & Wisniewski, J. (1994). Carbon pools and flux of global forest ecosystems. *Science* 263, 185-190.
- Dragut, L., Tiede, D., & Levick, S. R. (2010). ESP: a tool to estimate scale parameter for multiresolution image segmentation of remotely sensed data. *International Journal of Geographical Information Science*, 24(6), 859-871.
- Drake, J. B., Dubayah, R. O., Knox, R. G., Clark, D. B., & Blair, J. B. (2002). Sensitivity of large-footprint lidar to canopy structure and biomass in a neotropical rainforest. *Remote Sensing of Environment*, 81(2-3), 378-392.
- Drake, J. B., Knox, R. G., Dubayah, R. O., Clark, D. B., Condit, R., Blair, J. B., & Hofton, M. (2003). Above-ground biomass estimation in closed canopy Neotropical forests using lidar remote sensing: factors affecting the generality of relationships. *Global Ecology and Biogeography*, 12(2), 147-159. doi: 10.1046/j.1466-822X.2003.00010.x
- Dubayah, R. O., & Drake, J. B. (2000). Lidar remote sensing for forestry. *Journal of Forestry*, 98(6), 44-46.
- EPA. (2011). US Greenhouse Gas Inventory Report.
- Erdas. (2010). Online documentation:HPF Resolution Merge. C:\Program Files\ERDAS\ERDAS Desktop 2011\help\html\wwhelp\wwhimpl\js\html\wwhelp.htm
- Erikson, M., & Olofsson, K. (2005). Comparison of three individual tree crown detection methods. *Machine Vision and Applications*, 16(4), 258-265. doi: 10.1007/s00138-0005-0180-y
- Fagan, M., & DeFries, R. (2009). Measurement and Monitoring of World's Forests *A Review and Summary of Remote Sensing Technical Capability, 2009–2015*.
- Falkowski, M. J., Gessler, P. E., Morgan, P., Hudak, A. T., & Smith, A. M. S. (2005). Characterizing and mapping forest fire fuels using ASTER imagery and gradient modeling. *Forest Ecology and Management*, 217(2–3), 129-146.
- FAO. (2005). Global Forest Resources Assessment, 2005. FAO Forestry Paper 147, Food and Agriculture Organization of the United Nations. *FAO Forestry Paper 147*. Rome, Italy.
- FAO. (2010). Impact of the global forest industry on atmospheric greenhouse gases. *Forestry paper*(159).
- Fastie, C. L. (2010). *Estimating stand basal area from forest panoramas*. Paper presented at the Fine International Conference on Gigapixel Imaging for Science, Middlebury College.

- Fennerschool. (1996). Stocking, Density and competition, from <http://fennerschool-associated.anu.edu.au/mensuration/BrackandWood1998/DENSITY.HTM>
- Fennerschool.(1997).StandBasalArea,fromhttp://fennerschoolassociated.anu.edu.au/mensuration/BrackandWood1998/S_BA.HTM
- Flanders, D., Hall-Beyer, M., & Pereverzoff, J. (2003). Preliminary evaluation of eCognition object-based software for cut block delineation and feature extraction. *Canadian Journal of Remote Sensing*, 29(4), 441-452.
- Foody, G. M., Boyd, D. S., & Cutler, M. E. J. (2003). Predictive relations of tropical forest biomass from Landsat TM data and their transferability between regions. *Remote Sensing of Environment*, 85 (4), 463-474.
- ForestMonitor.(2006).TheTerai Forests, from <http://www.forestsmonitor.org/fr/reports/549391/549398>
- Frazer, G. W., Magnussen, S., Wulder, M. A., & Niemann, K. O. (2011). Simulated impact of sample plot size and co-registration error on the accuracy and uncertainty of LiDAR-derived estimates of forest stand biomass. *Remote Sensing of Environment*, 115(2), 636-649.
- Gautam, B. R., & Kandel, P. N. (2010). Working paper on LiDAR mapping in Nepal.
- GeoEye.(2010).ImageryCollection,from<http://www.geoeye.com/CorpSite/products-and-services/imagery-collection/Default.aspx>
- Gibbs, H. K., Brown, S., Niles, J. O., & Foley, J. A. (2007). Monitoring and estimating tropical forest carbon stocks: making REDD a reality. *Environmental Research Letters*, 2(4).
- Goetz, Baccini, A., Laporte, N., Johns, T., Walker, W., Kellndorfer, J., Sun, M. (2009). Mapping and monitoring carbon stocks with satellite observations: a comparison of methods. *Carbon Balance and Management*, 4(1), 1-7.
- Gonzalez, P., Asner, G. P., Battles, J. J., Lefsky, M. A., Waring, K. M., & Palace, M. (2010). Forest carbon densities and uncertainties from Lidar, QuickBird, and field measurements in California. *Remote Sensing of Environment*, 114(7), 1561-1575.
- Gonzalo, G. J., Peltola, H., Briceno-Elizondo, E., & Kellomaki, S. (2007). Changed thinning regimes may increase carbon stock under climate change: A case study from a Finnish boreal forest. *Climatic Change*, 81(3-4), 431-454.
- Gougeon, F. A., & Leckie, D. G. (2006). The individual tree crown approach applied to Ikonos images of a coniferous plantation area. *Photogrammetric Engineering Remote Sensing* 72(11), 1287-1297.
- Gough, C. M., Vogel, C. S., Schmid, H. P., & Curtis, P. S. (2008). Controls on Annual Forest Carbon Storage: Lessons from the Past and Predictions for theFuture. *Bioscience*, 58(7), 609-622.
- Hadi, F., Wikantika, K., & Sumarto, I. (2004). *Implementation of Forest Canopy Density Model to Monitor Forest Fragmentation in Mt. Simpang and Mt. Tilu Nature Reserves, West Java, Indonesia*. Paper presented at the 3rd FIG Regional Conference Jakarta, Indonesia.
- Hajnsek, I., Jagdhuber, T., Schon, H., & Papathanassiou, K. P. (2009). Potential of estimating soil moisture under vegetation cover by means of PolSAR, IEEE T. *Geosci. Remote.* 47, 442-454.
- Hay, G. J., Castilla, G., Wulder, M. A., & Ruiz, J. R. (2005). An automated object-based approach for the multiscale image segmentation of forest scenes. *International Journal of Applied Earth Observation and Geoinformation*, 7(4), 339-359.
- Heath, L. S., Smith, J. E., Woodall, C. W., Azuma, D. L., & Waddell, K. L. (2010). Carbon stocks on forestland of the United States, with emphasis on USDA Forest Service ownership. *ECOSPHERE*.
- Hedl, R., Svatek, M., Dancak, M., Rodzay, A. W., Salleh, A. B. M., & Kamariah, A. S. (2009). A new technique for inventory of permanent plots in tropical forests: a case study from lowland dipterocarp forest in Kuala Belalong, Brunei Darussalam. *Blumea*, 54(1-3), 124-130.
- Herold, M., & Johns, T. (2007). Linking requirements with capabilities for deforestation monitoring in the context of the UNFCCC-REDD process. *Environmental Research Letters*, 2 in press.
- Hese, S., Lucht, W., & Sachmullius, C. (2005). Global biomass mapping for an improved understanding of the CO2 balance-the Earth observation mission carbon-3D. *Remote Sensing of Environment*, 94, 94-104.
- Hirata, Y. (2004). Three-Dimensional forest measurement with airborne laser. *Japanese Society of Civil Engineering*(89), 28-30.

- Hollaus, M., Wagner, W., Eberhöfer, C., & Karel, W. (2006). Accuracy of large-scale canopy heights derived from LiDAR data under operational constraints in a complex alpine environment. *ISPRS Journal of Photogrammetry and Remote Sensing*, 60(5), 323-338.
- Houghton, R. A. (2005). Tropical deforestation as a source of greenhouse gas emissions. In P. M. a. S. Schwartzman (Ed.), *Tropical Deforestation and Climate Change* (pp. 13-21). Belém, Pará, Brazil. : Amazon Institute for Environmental Research.
- Houghton, R. A., Lawrence, K. T., Hackler, J. L., & Brown, S. (2001). The spatial distribution of forest biomass in the Brazilian Amazon: a comparison of estimates. *Global Change Biology*, 7, 731-746.
- Huang, C., Yang, L., Wylie, B., & Homer, C. (2001). *A Strategy for Estimating Tree Canopy Density Using Landsat 7 Etm+ And High Resolution Images Over Large Areas*. Paper presented at the Third International Conference on Geospatial Information in Agriculture and Forestry, Denver, Colorado.
- Hurt, G., C., Dubayah, R., Drake, J. B., Moorcroft, P. R., Pacala, S. W., Blair, J. B., & Fearon, M. G. (2004). Beyond Potential Vegetation: Combining LiDAR Data and a Height Structured Model for Carbon Studies. *Ecological Applications*, 14(3), 873-883.
- Husch, B., Beers, T. W., & Kershaw, J. A. (2003). Forest mensuration *Hoboken*(Wiley & Sons.), 261
- Husch, B., Miller, C. I., & Beers, T. W. (1982). *Forest Mensuration* (Ronald Press Co, Trans. third ed. ed.). New York NY.
- Hyde, P., Nelson, R., Kimes, D., & Levine, E. (2007). Exploring LIDAR-RaDAR synergy - predicting aboveground biomass in a southwestern ponderosa pine forest using LiDAR, SAR and InSAR. [Article]. *Remote Sensing of Environment*, 106(1), 28-38.
- ICIMOD. (2010). Forest Carbon stock in three Watersheds (Ludikhola, Kayerkhola and Charnawati). In ANSAB (Ed.). Kathmandu.
- Imhoff, M. L. (1995). Radar Backscatter and Biomass Saturation: Ramifications for Global Biomass Inventory. *IEEE Transactions on Geoscience and Remote Sensing*, 33(2), 511.
- IPCC. (2007b). Summary for Policymakers. *Climate Change: The Physical Science Basis. Contribution of Working Group I to the Fourth Assessment Report of the Intergovernmental Panel on Climate Change*.
- Iverson, L. R., Cook, E. A., & Graham, R. L. (1989). A Technique for Extrapolating and Validating Forest Cover Across Large Regions - Calibrating AVHRR Data with TM Data. *International Journal of Remote Sensing*, 10(11), 1805-1812.
- Jamalabad, M. S., & Abkar, A. A. (No date). Forest Canopy Density Monitoring, Using Satellite Images. 1-4.
- Jandl, G., Lindner, M., Vesterdal, L., Bauwens, B., Baritz, R., Hagedorn, F., B., K. A. (2007). How strongly can forest management influence soil carbon sequestration? *Geoderma* 137, 253 –268.
- Janssens, I., Sampson, D. A., Cermák, J., Meiresonne, L., Riguzzi, F., & Ceulemans, R. (1999). Above- and below-ground phytomass and carbon storage in a Belgian Scots pine stand. *Annals of Forest Sciences*, 56, p. 81-90.
- Jennings, S. B., Brown, N. D., & Sheil, D. (1999). Assessing forest canopies and understory illumination: Canopy closure, canopy cover and other measures. *Forestry*, 72, 59-73.
- Jha, C. S., & Singh, J. S. (1990). Composition and Dynamics of Dry Tropical Forest in Relation to Soil Texture. *Journal of Vegetation Science*, 1(5), 609-614.
- Joshi, C., Leeuw, J., & Duren, C. I. (2006). Remote Sensing and GIS Applications for mapping and spatial modelling of invasive species.
- Kale, P. M., Ravan, A. S., Roy, P. S., & Singh, S. (2009). Patterns of Carbon Sequestration in Forests of Western Ghats and Study of Applicability of Remote Sensing in Generating Carbon Credits through Afforestation/Reforestation. *Indian Society of Remote Sensing*, 37, 457-471.
- Karjalainen, T., Pussinen, A., Liski, J., Nabuurs, G. J., Eggers, T., Lapveteläinen, T., & Kaipainen, T. (2003). Scenario analysis of the impacts of forest management and climate change on the European forest sector carbon budget. *Forest Policy and Economics*, 5(2), 141-155.
- Kauffman, J., Hughes, F. R., & Heider, C. (2009). Carbon pool and biomass dynamics associated with deforestation, land use, and agricultural abandonment in the neotropics. *Ecological Applications*, 19, 1211-1222.
- Ke. Y., Quackenbush, L. J., & Jungho, I. M. (2010). Synergistic use of QuickBird multispectral imagery and LIDAR data for object-based forest species classification.

- Ketterings, Q. M., Coe, R., Van Noordwijk, M., Ambagau, Y., & Palm, C. A. (2001). Reducing uncertainty in the use of allometric biomass equations for predicting above-ground tree biomass in mixed secondary forests. *Forest Ecology and Management* 146 (1-3), 199-209.
- Kim, M., Madden, M., & Warner, T. (2009). Forest type mapping using object specific texture measures from multispectral IKONOS imagery: segmentation quality and image classification issues. *Photogrammetric Engineering and Remote Sensing*, 75(7), 819-830.
- Kim So-Ra, Kwak, D. A., Olee, W. K., Son, Y., Bae, S. W., Kim C., & Yoo, S. (2010). Estimation of carbon storage based on individual tree detection in *Pinus densiflora* stands using a fusion of aerial photography and LiDAR data.
- Klaus, S. L., Grimes, P., & Ziock, H. J. (2010). *Capturing Carbon Dioxide From Air*. Columbia University. New York.
- Koch, B. (2010). Status and future of laser scanning, synthetic aperture radar and hyperspectral remote sensing data for forest biomass assessment. *ISPRS Journal of Photogrammetry and Remote Sensing*, 65(6), 581-590.
- Krankina, O. N., Bergen, K. M., Sun, G., Masek, J. G., Shugart, H. H., & Kharuk, V. (2004). Remote sensing of Boreal Forest in selected regions. In e. a. Gutman G. (Ed.), *Land change science: Observing, monitoring, and understanding trajectories of change on the Earth's surface* (Vol. vol. 6.). Northern Eurasia: Springer E-book.
- Kraus, K., Wagner, W., Ullrich, A., & Melzer, T. (2004). From Single-pulse to full-waveform Airborne Laser Scanners: Potential and Practical Challenges. from Institute of Photogrammetry and Remote Sensing, Vienna University of Technology, Austria
- Kuuluvainen, T. (1989). Relationship between crown projected area and components of above ground biomass in Norway spruce trees in even-aged stands: Empirical results and their interpretation. *Forest Ecology and Management*, 40(3-4), 243-260.
- Kuuluvainen, T. (1991). Relationships between crown projected area and components of above-ground biomass in Norway spruce trees in even-aged stands: Empirical results and their interpretation. *Forest Ecology and Management*, 40(3-4), 243-260.
- Le Toan, T., S. Quegan, I. Woodward, M. Lomas, N. Delbart, & Picard, G. (2004). Relating Radar remote sensing of biomass to modelling of forest carbon budgets. *Climate Change*, 67(2), 379-402.
- Leblon, B., Granberg, H., & Gallant, L. (1996). Effects of shadowing types on ground-measured visible and near-infrared shadow reflectances. *Remote Sensing of Environment*, 58(3), 322-328.
- Lefsky, M. A., Cohen, W. B., Parker, G. G., & Harding, D. J. (2002). LiDAR Remote Sensing for ecosystem studies. *Biogeosciences*, 52(1), 19-30.
- Lefsky, M. A., Harding, D., Cohen, W. B., Parker, G., & Shugart, H. H. (1999a). Surface Lidar Remote Sensing of Basal Area and Biomass in Deciduous Forests of Eastern Maryland, USA. *Remote Sensing of Environment*, 67(1), 83-98.
- Leighty, W. W., Hamburg, S. P., & Caouette, J. (2006). Effects of management on carbon sequestration in forest biomass in southeast Alaska. *Ecosystems*, 9(7), 1051-1065.
- Li, R., & Weiskittel, A. (2010). Development and evaluation of regional taper and volume equations for the primary conifer species in the Acadian Region. *Ann For Science*, 67(302).
- Lim, K., Treitz, P., Wulder, M. A., St-Onge, B., & Flood, M. (2003). LiDAR remote sensing of forest structure. *Progress in Physical Geography*, 27(88).
- Lu, D. (2005). Aboveground biomass estimation using Landsat TM data in the Brazilian Amazon. . *International Journal of Remote Sensing* (26), 2509-2525.
- Lu, D. S. (2006). The potential and challenge of remote sensing-based biomass estimation. *International Journal of Remote Sensing*, 27(7), 1297-1328.
- Malhi, Y., & Grace, J. (2000). Tropical forests and atmospheric carbon dioxide (pp. 332 - 337). Edinburgh.
- Miner, R., & Perez-Garcia, J. (2007). The greenhouse gas and carbon profile of the global forest products industry. *Forest Products Journal*(57), 80-90.
- Möller, M., Lymburner, L., & Volk, M. (2007). The comparison index: A tool for assessing the accuracy of image segmentation. *International Journal of Applied Earth Observation and Geoinformation*, 9(3), 311-321.
- Mora, B., Wulder, M. A., & White, J. C. (2010). Segment-constrained regression tree estimation of forest stand height from very high spatial resolution panchromatic imagery over a boreal environment. *Remote Sensing of Environment*, 114(11), 2474 - 2484.

- Muukkonen, P., & Heiskanen, J. (2005). Biomass estimation based on simultaneous use of standwise forest inventory data, ASTER and MODIS satellite data.
- Myneni, R. B., Keeling, C. D., Tucker, C. J., Asrar, G., & Nemani, R. R. (1997). Increased plant growth in the northern high latitudes from 1981-1991. *Nature Geoscience*(386), 698-702.
- Naesset, E. (1997a). Determination of tree height of forest stands using airborne laser scanner data. *ISPRS Journal of Photogrammetry and Remote Sensing*, 52, 49-56.
- Namaalwa, J., Sankhayan, P. L., & Hofstad, O. (2007). A dynamic bio-economic model for analyzing deforestation and degradation: An application to woodlands in Uganda. *Forest Policy and Economics*, 9(5), 479-495.
- Natural Resources Canada. (2010). Forest Carbon Accounting: The Need For Forest Carbon Accounting, from http://carbon.cfs.nrcan.gc.ca/index_e.html
- Nelson, R. (1997). Modeling forest canopy heights: The effects of canopy shape. *Remote Sensing of Environment*(60), 327-334.
- Nelson, R., Krabill, W., & Maclean, G. (1984). Determining Forest Canopy Characteristics Using Airborne Laser Data. *Remote Sensing of Environment*, 15(3), 201-212.
- Neteler, M., & Mitasova, H. (2004). Satellite Image Processing Open Source GIS: A Grass Approach *Springer, US*, 773, 201-252.
- Neteler, M., & Mitasova, H. (2008). Open Source GIS: a GRASS GIS approach. The international series in engineering and computer science. *Springer*, 773.
- Olofsson, K. (2002). *Detection of Single trees in aerial images using template matching*. Paper presented at the ForestSAT Symposium Heriot Watt University, Edinburgh, UK.
- Panta, M. (2003). *Analysis of forest Canopy density and factors affecting it using RS and GIS techniques: A case study of Chitwan District of Nepal*. ITC (University of Twente), Enschede.
- Patenaude, G., Milne, R., & Dawson, T. P. (2005). Synthesis of remote sensing approaches for forest carbon estimation: reporting to the Kyoto Protocol. *Environmental Science & Policy*, 8(2), 161-178.
- Persson, A., Holmgren, J., Solderman, U., & Olsson, H. (No date). Tree Species Classification of Individual Trees in Sweden by combining High Resolution Laser Data with High Resolution Near-Infrared Digital Images. *International Archives of Photogrammetry, Remote Sensing and Spatial Information Sciences*, XXXVI(8).
- Petrovic, V. (2003). Multi-level image fusion. In B. V. Dasarathy (Ed.), *Multisensor, Multisource Information Fusion: Architectures, Algorithms, and Applications 2003* (Vol. 5099, pp. 87-96).
- Platt, R. V., & Schoennagel, T. (2009). An object-oriented approach to assessing changes in tree cover in the Colorado Front Range 1938-1999. *Forest Ecology and Management*, 258(7), 1342-1349.
- Pollock, R., & Woodham, R. (1996). *The automatic recognition of individual trees in aerial images of forests based on a synthetic tree crown image model*. National Library of Canada.
- Radoux, J., & Defourny, P. (2008). Quality assessment of segmentation results devoted to object-based classification.
- Object-Based Image Analysis. In T. Blaschke, S. Lang & G. J. Hay (Eds.), (pp. 257-271): Springer Berlin Heidelberg.
- Ryan, M. G., M.E. Harmon, R.A. Birdsey, C.P. Giardina, L.S. Heath, R.A. Houghton, Skog., K. E. (2010). A Synthesis of the Science on Forests and Carbon for U.S. Forests. *Issues in Ecology*.
- Sagar, R., & Singh, J. S. (2006). Tree density, basal area and species diversity in a disturbed dry tropical forest of northern India: implications for conservation. *Environmental Conservation*, 33(3), 256-262.
- Sapkota, I. P., Tigabu, M., & Oden, P. C. (2009). Tree diversity and regression of community-managed Bhabar lowland and Hill Sal forests in central region of Nepal. *Southern Swedish Forest Research Centre*.
- Scheller, R. M., & Mladenoff, D. J. (2005). A spatially interactive simulation of climate change, harvesting, wind, and tree species migration and projected changes to forest composition and biomass in northern Wisconsin, USA. *Global Change Biology*, 11(2), 307-321.
- Schmitt, C. B., Burgess, N. D., Coad, L., Belokurov, A., Besançon, C., Boisrobert, L., Winkel, G. (2009). Global analysis of the protection status of the world's forests. *Biological Conservation*, 142(10), 2122-2130.
- Sierra, C. A., del Valle, J. I., Orrego, S. A., Moreno, F. H., Harmon, M. E., Zapata, M., Benjumea, J. F. (2007). Total carbon stocks in a tropical forest landscape of the Porcè region, Colombia. *Forest Ecology and Management*, 243(2-3), 299-309.

- Smith, W. B., & Brand, G. J. (1983.). Allometric biomass equations for 96 species of herb, shrubs and small trees. *Research Note NC-299*. USDA Forest Service.
- Somogyi, Z., Teobaldelli, M., Federici, S., Matteucci, G., Pagliari, V., Grassi, G., & Seufert, G. (2008). Allometric biomass and carbon factors database. *Iforest-Biogeosciences and Forestry*, 1, 107-113.
- Song, C., Dickinson, M. B., Su, B., Zhang, L., & Yaussey, D. (2010). Estimating average tree crown size using spatial information from IKONOS and QuickBird images: Across-sensor and across-site comparisons. *Remote Sensing of Environment*, 114(5), 1099-1107.
- St-Onge, B. A. (2000). Estimating Individual Tree Heights of the Boreal Forest Using Airborne Laser Altimetry and Digital Videography. from Department of Geography, Universite du Quebec Montreal, Canada
- Swanson, M. E. (2009). Modeling the effects of alternative management strategies on forest carbon in the Nothofagus forests of Tierra del Fuego, Chile. *Forest Ecology and Management*, 257(8), 1740-1750.
- Thenkabail, P. S., Enclona, E. A., Ashton, M. S., Legg, C., & Jean De Dieu, M. (2004.). Hyperion, IKONOS, ALI, and ETM+ sensors in the study of African rainforests. *Remote Sensing of Environment*, 90, 23–43.
- Tianxiang, L., Wenhua, L., & Yunfa, L. Y. (1998). Estimation of Total Biomass and Potential Distribution of Net Primary Productivity in the Tibetan Plateau *Chinese Academy of Sciences*(4).
- Treuhaft, R. N., Gonçalves, F. G., Drake, J. B., Chapman, B. D., dos Santos, J. R., Dutra, L. V., Purcell, G. H. (2010). Biomass estimation in a tropical wet forest using Fourier transforms of profiles from lidar or interferometric SAR. *Geophys. Res. Lett.*, 37(23), L23403.
- UN - REDD. (2009). The United Nations Collaborative Programme on Reducing Emissions from Deforestation and Forest Degradation in Developing Countries
UNREDDProgramme Retrieved May 28, 2011, from <http://www.unredd.org/AboutREDD/tabid/582/Default.aspx>
- USAID (Writer). (2009). Forests and Climate Change Toolbox.
- Waring, R. H., Way, J., Hunt, E. R. J., Morrissey, L., Ranson, K., Weishampel, J. F., Franklin, S. E. (1995.). Imaging radar for ecosystem studies. *BioScience* (45), 715–723
- Worldbank. (2001). Community Forestry in Nepal. In B. World (Ed.).
- Wu, H., Liu, C., & Zhou, X. (2008). Data Fusion with Integration of Airborne Laser Scanning Data and Ortho-Aerial Photos. *The International Archives of the Photogrammetry, Remote Sensing and Spatial Information Sciences.*, XXXVII.
- Wulder, M. A., & Seemann, D. (2003). Forest Inventory Height update through the integration of LiDAR data with segmented Landsat Imagery. *Canadian Journal of Remote Sensing*(29), 536-543.
- Zhan, Q. M., Molenaar, M., Tempfli, K., & Shi, W. Z. (2005). Quality Assessment for geo-spatial objects derived from remotely sensed data *International Journal of Remote Sensing*, 26(14), 2953-2974.
- Zhang, Y. J. (1996). A survey on evaluation methods for image segmentation. *Pattern Recognition*, 29(8), 1335-1346.
- Zhao, K. G., Popescu, S., & Nelson, R. (2008). Lidar remote sensing of forest biomass: A scale-invariant estimation approach using airborne lasers. *Remote Sensing of Environment*, 113(1), 182-196.

APPENDICES

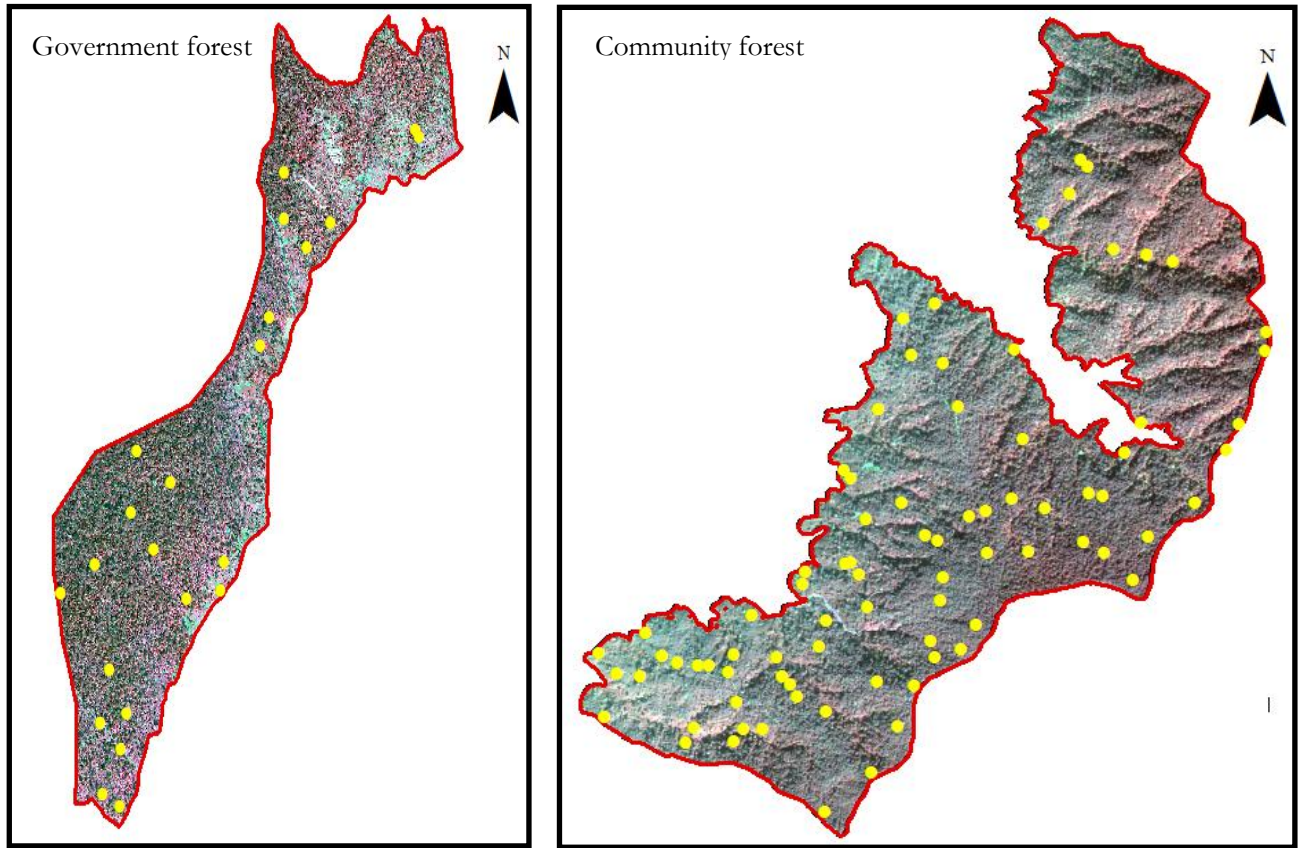
Appendix 1: Data collection Sheet

Name of Recorder..... Date..... Canopy Cover (%).....
 Slope (%) Aspect..... Elevation (m).....

Management Type		Coordinates
Strata Name		X
Sampling Plot No.		Y

Tree No.	Species	DBH (cm)	Height (m)	Crown Diameter (m)	Remark
1					
2					
3					
4					
5					
6					
7					
8					
9					
10					
11					
12					
13					
14					
15					
16					
17					
18					
19					
20					
21					
22					
23					
24					
25					

Appendix 2: Sample plot location for community and government managed forests



Appendix 3: An example of sample individual tree basal area from CF and GMF forests

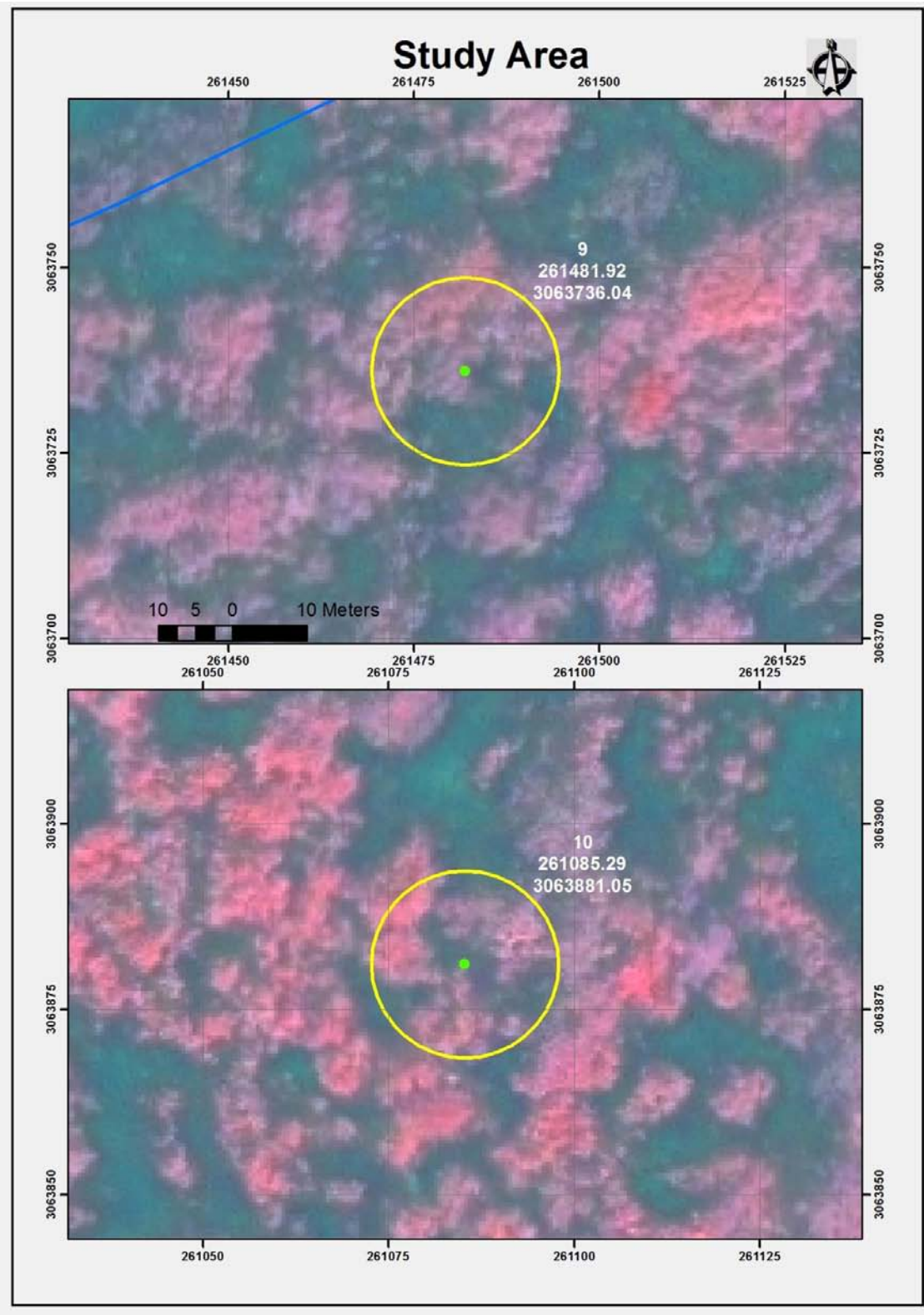
Government managed forest

Tree No	Species name	DBH cm	Basal area (m ²)
1	<i>Lagerstromia parviflora</i>	62	0.30
2	<i>Shorea robusta</i>	81.5	0.52
3	<i>Shorea robusta</i>	94.5	0.70
4	<i>Lagerstromia parviflora</i>	49.7	0.19
5	<i>Albizzia julibrissin</i>	40	0.13
6	<i>Lagerstromia parviflora</i>	51	0.20
7	<i>Lagerstromia parviflora</i>	43.3	0.15
8	<i>Shorea robusta</i>	88.6	0.62
9	<i>Shorea robusta</i>	79.5	0.50
10	<i>Shorea robusta</i>	69.5	0.38
11	<i>Shorea robusta</i>	67.9	0.36
12	<i>Semicarpous anacardium</i>	21	0.03
13	<i>Terminalia belerica</i>	45	0.16
14	<i>Lagerstromia parviflora</i>	44.5	0.16

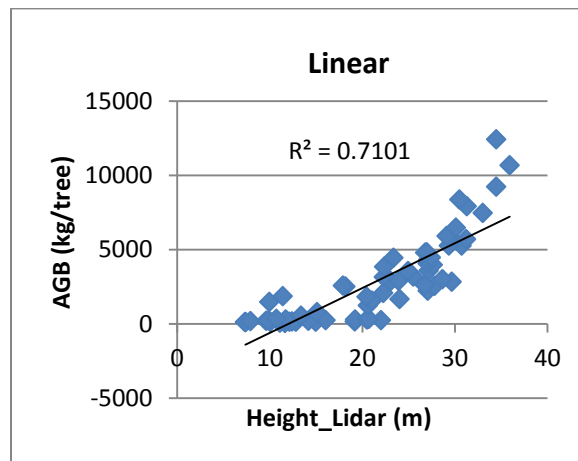
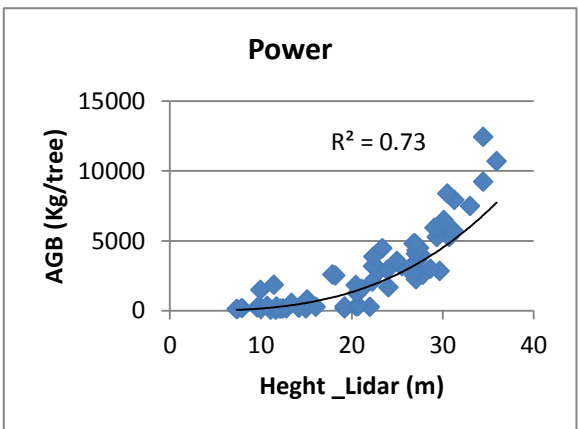
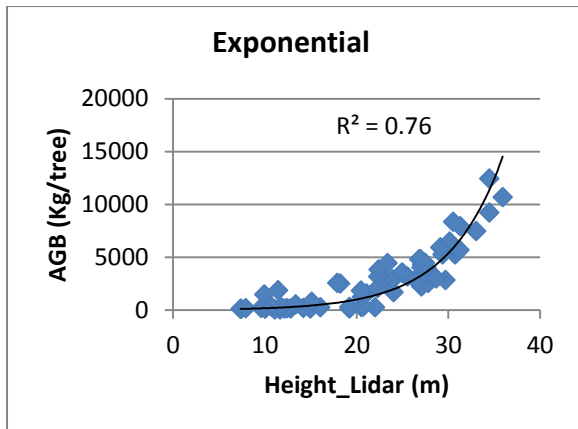
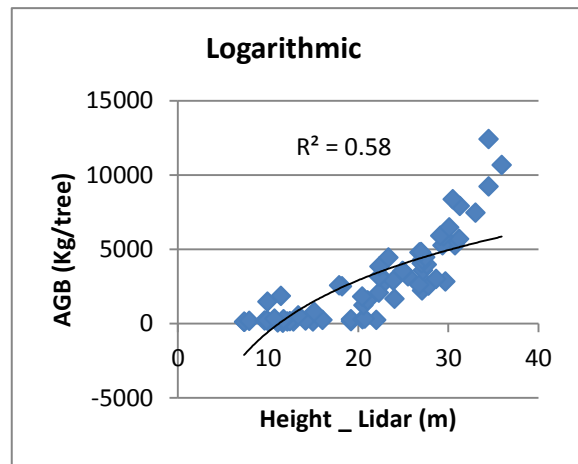
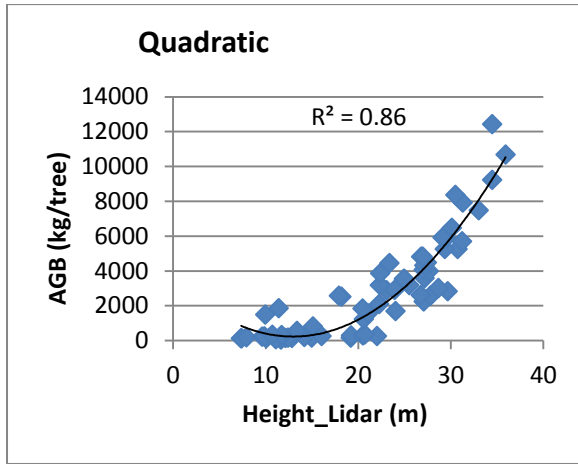
Community managed forest

Tree no.	Species Name	DBH (cm)	Basal area (m ²)
1	<i>Shorea robusta</i>	12.7	0.01
2	<i>Caeseriagraveolens</i>	13.3	0.01
3	<i>Cassia fistula</i>	24.2	0.05
4	<i>Cassia fistula</i>	11.7	0.01
5	<i>Shorea robusta</i>	20.4	0.03
6	<i>Holarrbena pubescens</i>	17	0.02
7	<i>Shorea robusta</i>	10.4	0.01
8	<i>Cassia fistula</i>	21	0.03
9	<i>Shorea robusta</i>	11.2	0.01
10	<i>Caeseriagraveolens</i>	10.5	0.01
11	<i>Shorea robusta</i>	11.5	0.01
12	<i>Cassia fistula</i>	10.5	0.01
13	<i>Holarrbena pubescens</i>	10.1	0.01
14	<i>Shorea robusta</i>	12.7	0.01

Appendix 4: Map of sample plot used for tree identification in the field



Appendix 5: Data distribution and Models comparison



Appendix 6: Slope correction table for the radius of the plot (Plot size = 500m²)

Slope%	Radius(m)	Slope%	Radius(m)	Slope%	Radius(m)
0	12.62				
1	12.62	36	13.01	71	13.97
2	12.62	37	13.03	72	14.00
3	12.62	38	13.05	73	14.04
4	12.62	39	13.07	74	14.07
5	12.62	40	13.09	75	14.10
6	12.63	41	13.12	76	14.14
7	12.63	42	13.14	77	14.17
8	12.64	43	13.16	78	14.21
9	12.64	44	13.19	79	14.24
10	12.65	45	13.21	80	14.28
11	12.65	46	13.24	81	14.31
12	12.66	47	13.26	82	14.35
13	12.67	48	13.29	83	14.38
14	12.68	49	13.31	84	14.42
15	12.69	50	13.34	85	14.45
16	12.70	51	13.37	86	14.49
17	12.71	52	13.39	87	14.52
18	12.72	53	13.42	88	14.56
19	12.73	54	13.45	89	14.60
20	12.74	55	13.48	90	14.63
21	12.75	56	13.51	91	14.67
22	12.77	57	13.53	92	14.71
23	12.78	58	13.56	93	14.74
24	12.79	59	13.59	94	14.78
25	12.81	60	13.62	95	14.82
26	12.82	61	13.65	96	14.85
27	12.84	62	13.68	97	14.89
28	12.86	63	13.72	98	14.93
29	12.87	64	13.75	99	14.97
30	12.89	65	13.78	100	15.00
31	12.91	66	13.81	101	15.04
32	12.93	67	13.84	102	15.08
33	12.95	68	13.87	103	15.12
34	12.97	69	13.91	104	15.15
35	12.99	70	13.94	105	15.19